CRYSTALLOGRAPHIC STUDIES OF TWO POLYMORPHS OF

HYDRIDODICARBONYLBIS(TRIPHENYLPHOSPHINE)IRIDIUM(I)

AND OF TWO NITRIDO-BRIDGED TRANSITION METAL COMPLEXES.

A thesis submitted for the

degree of Doctor of Philosophy

in the University of London

by

MARIA CIECHANOWICZ

Magister chemii
Jagiellonian University,Cracow.

Department of Chemistry

Imperial College

London, S.W.7.   June 1971

SUMMARY

The principles and techniques of crystal-structure analysis are discussed and a brief description of the computer programs which have been used is given. The crystal structures of four metal complexes have been determined from diffractometer or photographic data.

The first two are structures of the two polymorphic forms of hydridodicarbonylbis(triphenylphosphine)iridium(I).

(i) The orthorhombic form of $IrH(CO)_2(PPh_3)_2$.

(ii) The monoclinic (I) form of $IrH(CO)_2(PPh_3)_2$.

The second two are stuctures of polynuclear nitrido-bridged transition metal anionic complexes. They are:

(iii) Potassium μ-nitrido-bis $\left[\text{tetrachloroaquoruthenate(IV)}\right]$, $K_3Ru_2NCl_8(H_2O)_2$.

(iv) The μ-nitrido-hexasulphatotriaquotri-iridate (IV,IV,III) ion, $\left[Ir_3N(SO_4)_6(H_2O)_3\right]^{-4}$.

(i,ii) The iridium complex is a homologue of $RhH(CO)_2(PPh_3)_2$, which is believed to be the active species in the hydroformylation of alkenes using $RhH(CO)(PPh_3)_3$ as catalyst. In organic solvents the iridium complex is known to exist as two isomeric forms under-going rapid intermolecular inter-conversion. It was interesting to find out what the molecular geometry is in the solid state. Examination of the crystals showed the presence of

three polymorphic forms. The structures of two of
those have so far been determined.

Both structure determinations were from diffracto-
meter data and their main features are as follows:

	(i)	(ii)
Space group	$Pna2_1$	$P2_1/a$
Unit-cell dimensions	a=17.759	a=18.036
	b=10.001	b=10.075
	c=18.389	c=19.474
		β =113.365°
Z	4	4
Final R factor	0.0187	0.028
Number of reflections	2518	3248
Some distances:		
Ir – P	2.372;2.377	2.357;2.359
Ir – C	1.868;1.834	uncertain (CO groups disordered)
Ir – O	3.023;3.029	2.902-3.076
Ir – H	1.64	

In the case of the orthorhombic form the hydride
hydrogen atom was successfully located and the co-
ordination about the iridium atom can be best
described as a distorted trigonal bipyramid. In the
case of the monoclinic (I) form both carbonyl groups
were found to be disordered and locating the hydride
hydrogen atom proved to be impossible. The results
are compared with the well defined geometry of the
orthorhombic form.

(iii) The structure has been determined from the 697 three-dimensional visually estimated intensity data and refined to R=0.088. The crystals are monoclinic with unit-cell dimensions a=15.89, b=7.34, c=8.16Å, β=120.4°. The space group is C2/m and Z=2. The main features of the $\left[Ru_2NCl_8(H_2O)_2\right]^{3-}$ ion are:

a) a linear O-Ru-N-Ru-O system with very short Ru-N distances of 1.720Å, indicating multiple bonding, and fairly long Ru-O (water) distances of 2.18Å.

b) an eclipsed configuration of chlorine atoms co-ordinated to ruthenium (four to each one). The two independent Ru-Cl distances of 2.364 and 2.367Å are normal.

The potassium ions are co-ordinated to eight chlorines at distances in the range 3.20-3.36Å.

(iv) This is believed to be the first trinuclear nitrido-bridged complex structure to be determined. The final R factor is 0.032 for 565 reflections measured on an automatic diffractometer. The compound crystallises in the cubic space group I$\bar{4}$3d with 16 molecules in a unit cell for which a=22.805Å. The complex anion has C_3 point group symmetry with the nitrogen atom being co-planar with and at the centre of an equilateral triangle formed by the iridium atoms. The six sulphate groups link adjacent iridium atoms which have an octahedral coordination with the nitrogen and water

molecules trans to each other.

Some of the more interesting distances are:
Ir-N 1.918Å, Ir-O(water) 2.058Å, Ir-O(sulphate)
2.006-2.059Å.

ACKNOWLEDGEMENTS

DEDICATED

to

my parents

Leibniz held that man, every
man, was a "microcosm", the
cosmos in miniature, and that
we could penetrate to the
meaning of the world if we
could fathom the mystery of
ourselves.

CONTENTS

Chapter III: The crystal structure of potassium

μ-nitrido-bis[tetrachloroaquoruthenate(IV)],

$K_3[Ru_2N\ Cl_8\ (H_2O)_2]$

Chapter IV : The structure of the μ-Nitrido-hexasulpha-

totriaquotri-iridate(IV,IV,III) ion,

$[Ir_3N(SO_4)_6(H_2O)_3]^{-4}$

SECTION A.

A short introduction to the theoretical and experimental basis of X-ray structure determination.

CHAPTER I

THEORETICAL PRINCIPLES OF STRUCTURE DETERMINATION

INTRODUCTION

The principles used in the determination of crystal structure are essentially those of physical optics. However, to get diffraction phenomena from crystals having interplanar spacings (which correspond to the repetition distances in an optical grating) of the order of a few Angstrom units, a radiation of similar wavelength has to be used, such as the characteristic X-radiations of Cu, Mo, Cr or Fe.

Crystals are composed of groups of atoms repeated at regular intervals in three dimensions, each group having an identical and parallel environment. For the purpose of diffraction theory it is sufficient to regard each group of atoms as replaced by a representative point, and the collection of points so formed is the lattice of the crystal. The lattice repetition distances along each of the three noncoplanar directions are called the lattice constants, which with the interaxial angles are called the lattice parameters. When considered as a set of three vectors they define a unit cell.

The X-rays used in studying the arrangement of atoms have a range of wavelengths from about 0.5 to 3.0 $\overset{o}{A}$ and therefore are capable of resolving separate atoms, but they cannot be bent sufficiently by any kind of lens to give a direct image of the atomic arrangements. They can only be scattered by the crystal matter so as to give

various kinds of diffraction patterns.

The following first chapter will deal briefly with the phenomena of X-ray scattering and its use in crystal-structure determination, while the second chapter concerns itself with two basic experimental methods of recording diffraction patterns and determining the intensities of the individual reflections.

An outline will be given of the theoretical and practical basis of only those procedures which have been used in the determination of the four structures described in this thesis.

I.1   THE DIFFRACTION OF X-RAYS

An electron in the path of an unpolarised X-ray beam is set into forced vibrations of the same frequency as the X-radiation and acts as a source of secondary X-rays unmodified in wavelength but radiated in all directions. By this interaction the electron is said to scatter or to diffract X-rays. All electrons in the path of an X-ray beam scatter synchronously and scattered waves will interfere either destroying one another or combining to form new wave fronts. This cooperative scattering produces a diffraction pattern. The directions of possible diffracted beams depend only on the size and shape of the unit cell and the X-ray wavelength. Their intensities vary considerably and depend on the arrangement of atoms within the unit cell; some symmetrical arrangements produce recognisable patterns of systematic absences among the reflections.

The geometry of diffraction

Consider a parallel beam of X-rays of wavelength λ falling on the lattice in a direction defined by the vector s_0 and scattered in the direction defined by the vector s, both vectors having modulus $1/\lambda$. Let P_1 and P_2 (Fig.I.1) be two lattice points separated by a vector distance $\vec{r} = u\vec{a} + v\vec{b} + w\vec{c}$, where $\vec{a}$, $\vec{b}$, $\vec{c}$ are the lattice parameters and u, v, w are integers. The path difference between the two scattered waves is $P_1L - P_2K$ (see the same figure).

$$P_1 L = |r| \cos \gamma$$

and $\quad \cos \gamma = \dfrac{\vec{r}.\vec{s}}{|r|\,|s|}$

since $\quad |s| = \dfrac{1}{\lambda}$

$$\cos \gamma = \dfrac{(\vec{r}.\vec{s})\lambda}{|r|}$$

Therefore $\quad P_1 L = (\vec{r}.\vec{s})\lambda$

Similarly $\quad P_2 K = (\vec{r}.\vec{s}_0)\lambda$

and $\quad P_1 L - P_2 K = \lambda\,(\vec{r}.\vec{s} - \vec{r}.\vec{s}_0) \qquad\qquad (I.1)$

$$= \lambda\,\vec{r}.\vec{S}$$

where $\quad \vec{S} = \vec{s} - \vec{s}_0$ is called the scattering vector.

In order that the waves scattered by P_1 and P_2 shall be in phase, this path difference should be equal to a whole number of wavelengths. Thus $(u\vec{a} + v\vec{b} + w\vec{c}).\vec{S} = $ integer, and u,v,w are also integers. If now all lattice points must fulfil this condition simultaneously, i.e. it must be true for any integer values of u,v, or w, then

$$\vec{a}\,\vec{S} = n_1$$
$$\vec{b}\,\vec{S} = n_2 \qquad\qquad \text{i.e. three integers} \qquad\qquad (I.2)$$
$$\vec{c}\,\vec{S} = n_3$$

These equations are known as Laue's equations. When Laue's equations are simultaneously satisfied, a diffracted beam of maximum intensity will be produced.

Bragg showed that the incident and diffracted beams were equally inclined to (and therefore apparently reflected by) the family lattice planes whose Miller indices*are h k l if $n_1 = nh$, $n_2 = nk$, $n_3 = nl$, where the common factor, n, is known as the order of reflection.

* Miller indices can be regarded as showing the number of cuts made by the set of planes in each axis during one unit translation.

The Laue equations can be rewritten in the following form:

$$\frac{\vec{a}}{h} \cdot \vec{S} = n$$

$$\frac{\vec{b}}{k} \cdot \vec{S} = n$$

$$\frac{\vec{c}}{l} \cdot \vec{S} = n$$

(I.3)

Subtraction of the first two equations gives

$$\left(\frac{\vec{a}}{h} - \frac{\vec{b}}{k}\right) \cdot \vec{S} = 0$$

which means that the vector $\vec{S}$ is perpendicular to the vector $\vec{a}/h - \vec{b}/k$. Similarly $\vec{S}$ is perpendicular to $\vec{a}/h - \vec{c}/l$. Since both vector differences are in the plane hkl (see Fig. I.2a) the vector $\vec{S}$ is perpendicular to this plane. But $\vec{S}$ is a vector in the direction of the bisector of the incident and diffracted beam, since the moduli of $\vec{s}$ and $\vec{s}_0$ are equal (Fig.I.3); thus this bisector is identical with the normal to the h k l plane and therefore each diffraction can be regarded as "reflexion" of the rays from lattice planes. It is convenient to introduce the spacing $\underline{d}$ of the planes h k l; this is the perpendicular distance from the origin to the plane shown in Fig.(I.2a), and can be calculated as the projection of, for example $\vec{a}/h$ on the vector $\vec{S}$ (Fig.I.2b).

$$d = \left|\frac{\vec{a}}{h}\right| \cos a$$

but

$$\cos a = \frac{\frac{\vec{a}}{h} \cdot \vec{S}}{\left|\frac{\vec{a}}{h}\right| |\vec{S}|}$$

therefore

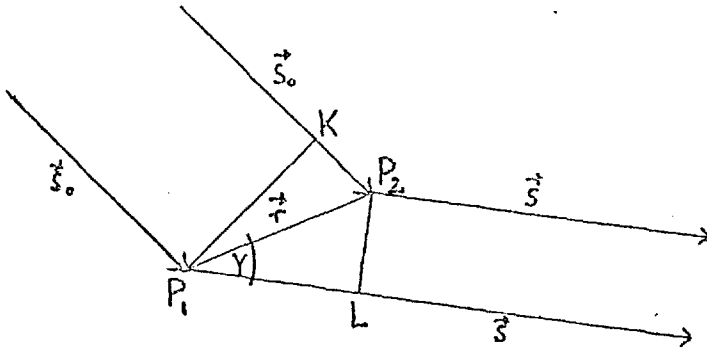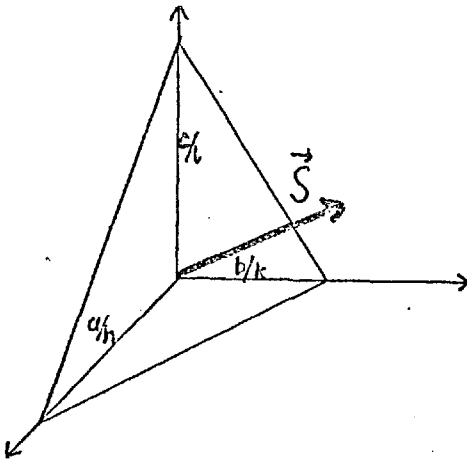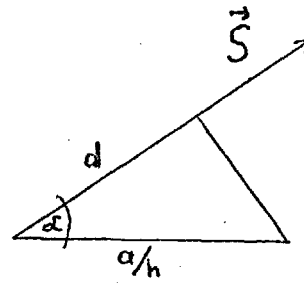$$d = \frac{\frac{\vec{a}}{h} \cdot \vec{S}}{|\vec{S}|}$$
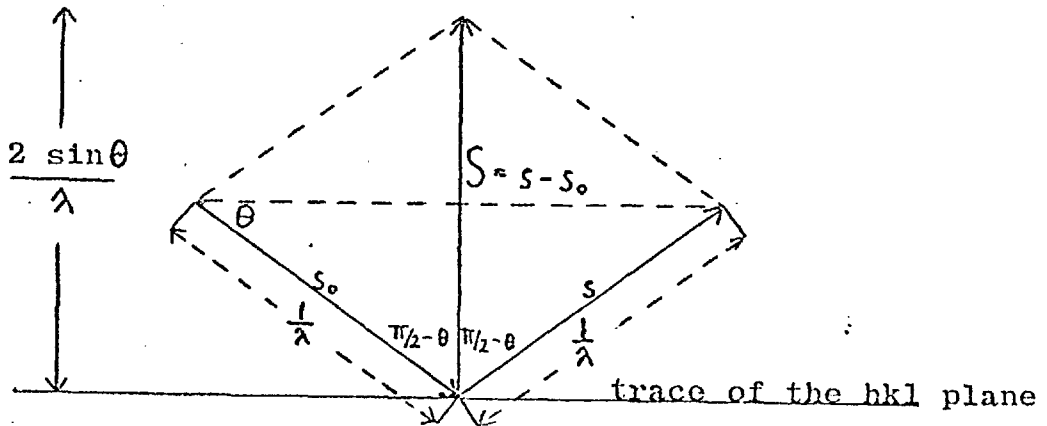
Fig. I.1.

Fig.I.2a.

Fig.I.2b.

Fig.I.3.

But $\dfrac{\vec{a}}{h} \cdot \vec{S} = n$ (Eq.I.3) and as is apparent from Fig.(I.3)

$$|\vec{S}| = \frac{2 \sin\theta}{\lambda}$$

Thus $d = \dfrac{n\lambda}{2 \sin\theta}$

and $n\lambda = 2d \sin\theta$

This is <u>Bragg's Law</u>.

In practice the order of reflection, <u>n</u>, is "absorbed" in the spacing <u>d</u> of the hkl planes: $\sin\theta$ for the n-th order of reflection from planes with spacing <u>d</u> is the same as that for the first-order reflection from planes with spacing <u>d/n</u> .

If we rearrange Bragg's equation such that

$$\sin\theta = \frac{\lambda}{2} \frac{1}{d} \ : -$$

The interpretation of X-ray diffraction patterns would be facilitated if the reciprocal relation between $\sin\theta$ and $1/d$ could be replaced by a direct one. The reciprocal lattice concept gives the solution to this problem. The <u>reciprocal lattice</u> (r.l.) can be defined as follows. Consider the normals to all possible direct lattice planes radiating from some point taken as origin. Mark the point P_{hkl} on the normal to the planes hkl, and at a distance of p/d_{hkl} from the origin. The value of <u>p</u> is usually taken as 1 in theoretical considerations and as λ in practical work. $1/d$ is designated d* and from the derivation of Bragg's Law it is evidently identical to $|\vec{S}|$. To show that the array of points P_{hkl} gives a lattice we can consider equations (I.3). The first one is equivalent to the statement that the

projection of $\vec{S}$ on $\vec{a}$ is constant for a fixed value of h,
namely h/a;   that is, the ends of all vectors $\vec{S}$ having
the same value of h lie on a plane perpendicular to $\vec{a}$.
If h = 0, the plane passes through the origin;   if h = 1,
the plane has an intercept on $\vec{a}$ of 1/a; if h = 2, it makes
double the intercept; and so on.   In other words, the ends
of the vectors $\vec{S}$ fall on a set of equispaced planes
perpendicular to the $\vec{a}$ axis, each plane corresponding to
a particular value of h.   In a similar way, sets of
equidistant planes perpendicular to the $\vec{b}$ and $\vec{c}$ axes will
be set up, with planes corresponding to a particular value
of k and l respectively.   The intersections of these three
sets of planes represent the end points of vectors that
satisfy the three Laue equations simultaneously, and so
give the solution of Bragg's equation .   The set of
points obtained by intersections of planes equally spaced
in each of the three directions gives a lattice of points
in reciprocal space and, therefore, known as the reciprocal
lattice.   The unit cell of this lattice is defined by three
vectors a*, b*, c*, and each r.l. point is defined by three
integers h,k,l and the corresponding vector $\vec{S}=h\vec{a}*+k\vec{b}*+l\vec{c}*$.
Figure (I.4) shows a two-dimensional projection of two sets
of lattice planes in direct space with their corresponding
points in reciprocal space.

We can show how useful the concept of the r.l. is in
the interpretation of diffraction by the following
considerations.

Imagine the crystal oriented   to the X-ray beam of
wavelength λ in such a way that its reciprocal lattice plane
a*b* is parallel to the beam.   Draw a line XO in the
direction of the X-ray beam passing through the r.l.

origin O and along this line choose the point B at a
distance of $1/\lambda$ from point O. From the point B describe
a circle of radius $1/\lambda$, having on its circumference
r.l. origin O and r.l. point P. (Fig.I.5). Since the
angle OPA is a right angle

$$\sin \theta = \frac{OP}{OA} ,$$

and since OA = $2/\lambda$ and OP = $1/d_{hkl}$ (by definition),

$$\sin \theta = \frac{\lambda}{2d_{hkl}}$$

which is just Bragg's Law.

It follows that a reflection occurs whenever a r.l.
point coincides with a circle constructed as described.
By rotating this circle around its diameter AO, a sphere
called the sphere of reflection is generated. When the
r.l. is rotated about its origin, r.l. points are brought
into coincidence with the surface of the fixed sphere of
reflection and Bragg's Law is fulfilled. Since the
diameter of this sphere is $2/\lambda$, every r.l. point within
that distance of the origin can be brought into a reflecting
position. Thus every r.l. point within a sphere of radius
$2/\lambda$, the limiting sphere, is a potential reflection.
(Fig.I.6).

It is worth noticing that when the r.l. is defined in
terms of d* = 1/d, the radius of the sphere of reflection
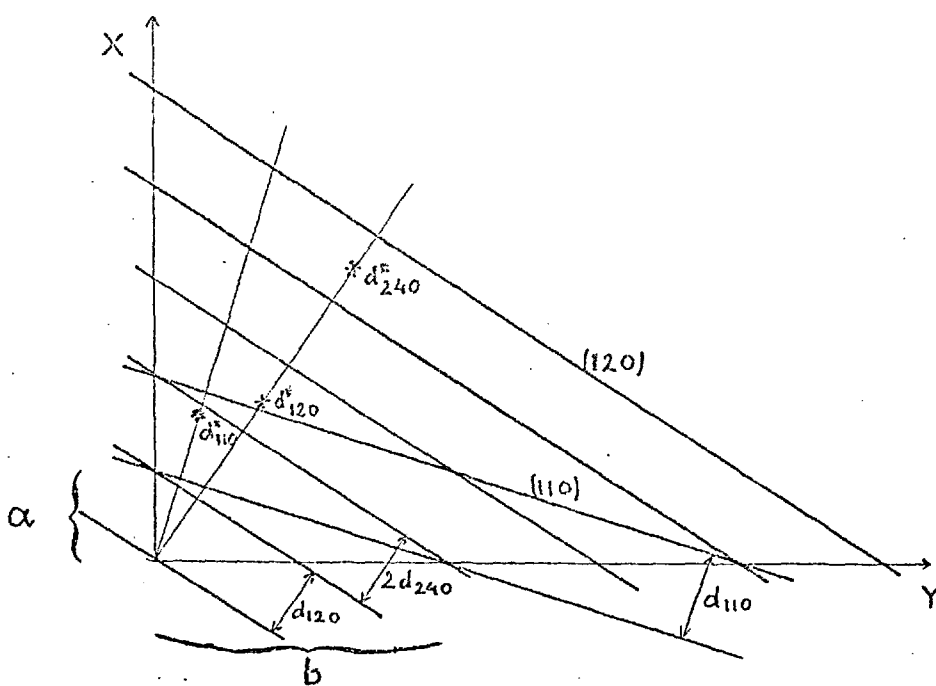is $1/\lambda$, but when d* = λ/d the radius is 1 r.l. unit.

Fig.I.4. Projection of direct lattice planes and the corresponding reciprocal lattice points.
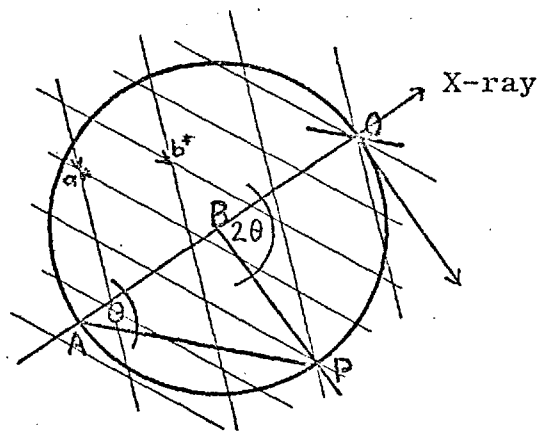

Fig.I.5. Section through the reciprocal lattice and the sphere of reflection.
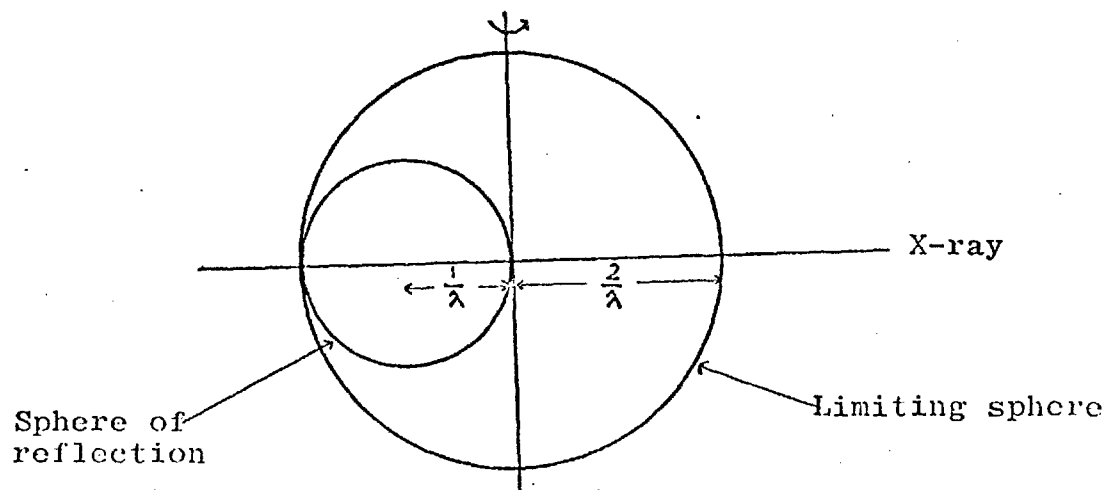

Fig.I.6. Section through the sphere of reflection and the limiting sphere.

The intensity of diffraction

Hitherto the scattering units have been assumed to be electrons whose linear dimensions could be neglected in comparison with the X-ray wave-length, and therefore scattering by a single electron was independent of angle, apart from the effects of polarisation.

In atoms, however, the electrons occupy a finite volume and only the waves scattered in the direction of the incident beam are in phase. For other directions electrons scatter out of phase, and the amplitude of the wave scattered by the whole atom decreases as the scattering angle increases. If one assumes spherical atoms the amplitude is a function only of the type of atom and $\sin \theta / \lambda$ (Fig. I.7). The scattering power of a given atom for a given reflection is known as its <u>scattering factor</u> f_o and is expressed by the ratio

$$f_o = A_a / A_e$$

where A_a is the amplitude of the wave from the whole atom and A_e from a free electron located at the position of the atomic nucleus, both being measured in the same direction of the scattered wave. For angle $\theta = 0$ this ratio is equal to the atomic number Z.

The normal scattering-factor curves are calculated on the basis of the electron distribution in a stationary atom, but in reality the atoms in crystals are vibrating about their mean lattice positions. The effect of such thermal motion produce transient modulation of the periodicity $\underline{d}$ of the lattice planes over a large volume and thus the apparent scattering power of the real atom

falls off more rapidly than that of the stationary model
(see Fig.I.7). Debye and Waller showed that the X-ray
intensity of reflection at temperature T is given by

$$I_T = I_o \exp \left[-2B(\sin^2\theta / \lambda^2) \right] \tag{I.5}$$

where I_o = intensity corresponding to the atom at rest and

$$B = 8\pi^2 \overline{u^2}$$

$\overline{u^2}$ is the mean-square displacement of the atom along the
normal to the reflecting planes and depends on the
temperature, the mass of the atom, and the elastic constants
of the crystal. Thus the scattering factor for a real atom
vibrating isotropically can be given by the expression

$$f = f_o \exp \left[-B(\sin^2\theta / \lambda^2) \right] \tag{I.6}$$

The exponential part of this equation can be rearranged to
underline the fact that the effect of the thermal vibration
of an atom for any set of lattice planes(hkl) depends on the
interplanar spacing $\underline{d}$.

$$\exp \left[-\frac{B}{4} \left(\frac{2\sin\theta_{hkl}}{\lambda} \right)^2 \right] = \exp \left[-\frac{B}{4} \left(\frac{1}{d_{hkl}} \right)^2 \right] \tag{I.7}$$

Since $\dfrac{1}{d^2_{hkl}} = (h^2 a^{*2} + k^2 b^{*2} + l^2 c^{*2} + 2hka^* b^* \cos\gamma^*$

$$+2hla^* c^* \cos\beta^* + 2klb^* c^* \cos\alpha^*) \tag{I.8}$$

and since the temperature factor must have a parameter for
every term in this expression, as each represents a
component perpendicular to the set of planes(hkl), the
general temperature factor expression for an anisotropically
vibrating atom is

$$\exp \left[-1/4 (B_{11} h^2 a^{*2} + B_{22} k^2 b^{*2} + B_{33} l^2 c^{*2} + 2B_{12} hka^* b^* \cos\gamma^* \right.$$

$$\left. +2B_{13} hla^* c^* \cos\beta^* + 2B_{23} klb^* c^* \cos\alpha^*) \right] \tag{I.9}$$
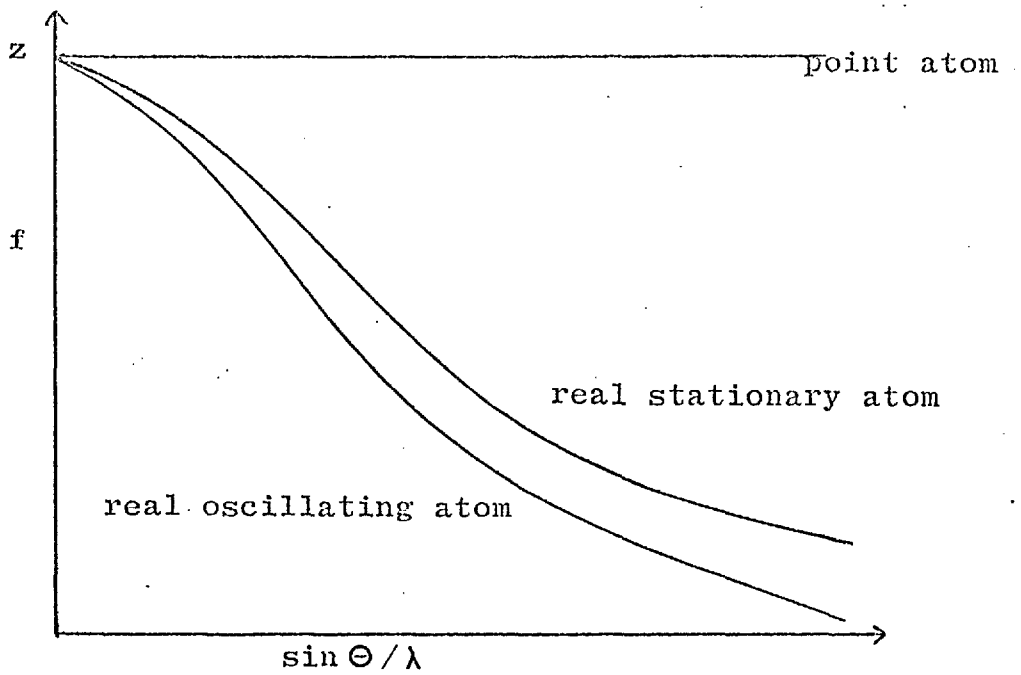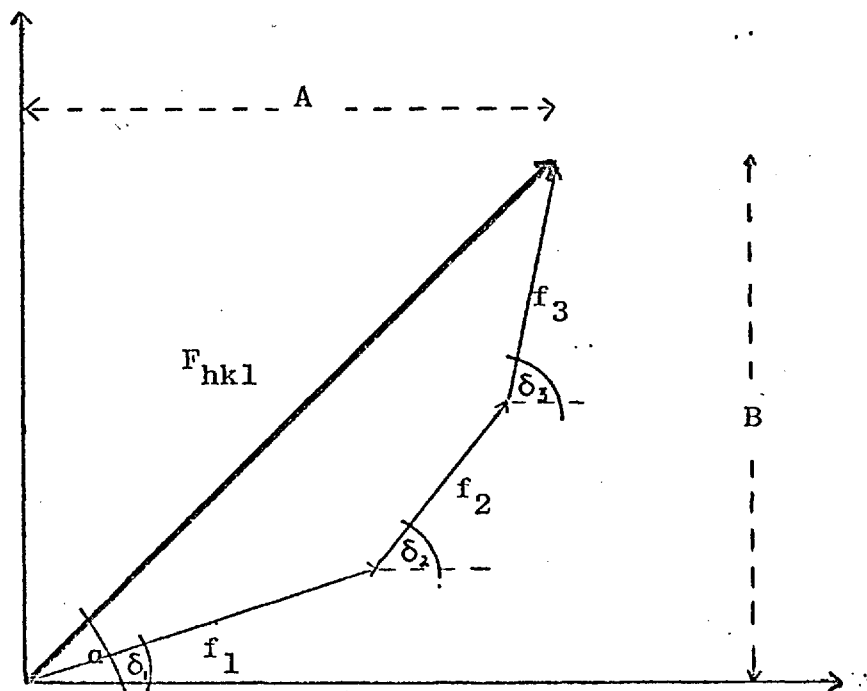
Fig.I.7.

Fig.I.8.
Vector representation of waves with
different amplitudes and phases.

The six B_{ij} thermal parameters serve to describe the
ellipsoidal electron distribution, and for an atom in a
general position they are independent. For an atom in a
position of special symmetry, however, certain restrictions,
discussed by H.A. Levy (1), are imposed on them by the
symmetry of the site.

Whereas the scattering from an atom depends on the
distribution of its electrons, the scattering from a unit
cell depends on the atomic arrangements. Suppose that
the unit cell of a crystal contains three atoms, each of a
different kind. The amplitudes of the hkl waves scattered
by those atoms and their phase relation is shown on a
vector diagram (Fig.I.8). Each wave is represented by a
vector whose length and inclination to the horizontal are
proportional to the atom's scattering factor and the phase
angle δ with respect to the wave scattered by hypothetical
electrons at the origin of the cell. The length of the
resultant gives the amplitude F_{hkl}, and its inclination
the phase angle a_{hkl} of the composite wave due to all
three atoms. F_{hkl} is called the structure factor. In
general for the unit cell containing j atoms the structure
factor is the resultant of j waves scattered in the direction
of the reflection hkl by all the atoms in the unit cell.

The only observable quantities are X-ray intensities
which, being proportional to amplitude squared, give only
the modulus of the structure factor, $\left| F_{hkl} \right|$, called the
structure amplitude, and leave the phase angle unknown.

To calculate the structure factor the knowledge of atomic scattering factors and their phases is required. The first are tabulated as a function of $\sin\theta/\lambda$, the latter can be calculated in terms of the positions of the atoms and the indices of the reflection. Thus, from the definition of the indices, the set of planes h̲ k̲ l̲ cuts a,b and c into h̲,k̲ and l̲ divisions respectively. According to Bragg's Law the phase difference between reflections from successive planes of any given set h̲ k̲ l̲ is 2π radians. Hence, the phase differences for unit translations along any of the three axial directions are $2\pi h$, $2\pi k$ and $2\pi l$ radians. If an atom A has fractional coordinates x,y,z the phase difference between this atom and the origin O(0,0,0) for the set of planes hkl is

$$\delta = 2\pi\,(\vec{r}.\vec{S}) = 2\pi\,(x\vec{a}+y\vec{b}+z\vec{c}).(h\vec{a}^*+k\vec{b}^*+l\vec{c}^*) = 2\pi\,(hx+ky+lz)$$

From (Fig. I.8)

$$|F_{hkl}| = (A^2_{hkl}+B^2_{hkl})^{\frac{1}{2}} \qquad (I.10)$$

where A_{hkl} and B_{hkl} for a unit cell with j atoms are:

$$A_{hkl} = \sum_{j=1}^{N} f_j \cos 2\pi\,(hx_j+ky_j+lz_j) \qquad (I.11)$$

$$B_{hkl} = \sum_{j=1}^{N} f_j \sin 2\pi\,(hx_j+ky_j+lz_j) \qquad (I.12)$$

The phase of the resultant wave is

$$\alpha_{hkl} = \tan^{-1}\left(\frac{B_{hkl}}{A_{hkl}}\right) \qquad (I.13)$$

These last equations are normally used for computing structure factors.

Other useful ways of representing the structure factor are writing it down as a complex number,

$$F_{hkl} = A_{hkl} + iB_{hkl} \qquad (I.14)$$

and

$$F_{hkl} = \sum_{j=1}^{N} f_j e^{2\pi i(hx_j + ky_j + lz_j)} \qquad (I.15)$$

So far the structure factor has been considered in terms of the waves scattered from the N atoms in a unit cell. A more general approach treats the structure factor as the sum of the wavelets scattered from all the infinitesimally small elements of a unit cell with electron density changing continuously throughout. Thus, if $\rho(x,y,z)$ is the electron density at the point (x,y,z) the amount of scattering matter in the volume element dx dy dz is ρ dx dy dz and the structure factor equation is

$$F_{hkl} = V \int_0^1 \int_0^1 \int_0^1 \rho(x,y,z) \exp\left[2\pi i(hx+ky+lz)\right] dx \; dy \; dz$$

$$(I.16)$$

This form of equation provides a means of calculating structure factors for a given electron distribution. In practice, however. in the process of determining a crystal structure the inverse operation has to be performed – an electron-density distribution has to be obtained from the structure factors which are calculated in turn from the measured intensities. The next section will deal with this problem.

I.2   STRUCTURE DETERMINATION IN OUTLINE

The density of scattering matter in a crystal is triply periodic, and can therefore be expressed by a three-dimensional Fourier series

$$\rho(x,y,z) = \sum_h \sum_k \sum_l A_{hkl} \exp\left[-2\pi i(hx+ky+lz)\right] \quad (I.17)$$

(where h,k,l are integers between $-\infty$ and $+\infty$)

and if this is substituted into Eq.(I.16), it follows that

$$A_{hkl} = \frac{F_{hkl}}{V} \quad (I.18)$$

i.e. there is one term in the Fourier series for each observed reflection.

As we can only measure $\left|F_{hkl}\right|$ and have to deduce its phase a_{hkl} separately, it is convenient to write

$$F_{hkl} = \left|F_{hkl}\right| \exp(2\pi i \, a_{hkl})$$

Hence Eq.(I.17) becomes

$$\rho(x,y,z) = \frac{1}{V} \sum_h \sum_k \sum_l \left|F_{hkl}\right| \exp\left[-2\pi i(hx+ky+lz - a_{hkl})\right]$$
$$(I.19)$$

This form of equation will raise the question how the electron density, which is a real quantity, can be expressed in a form containing imaginary components. The following consideration answers this question. When Friedel's law holds

$$F_{hkl} = A_{hkl} + i \, B_{hkl}$$

and $F_{\overline{hkl}} = A_{hkl} - i \, B_{hkl}$

Using the contraction

$$\delta = hx+ky+lz$$

and combining the terms for hkl and $\overline{hkl}$

$$\rho = \frac{1}{V} \sum_{-\infty}^{\infty} h \sum_{-\infty}^{\infty} k \sum_{0}^{\infty} l(A+iB)\exp(-2\pi i\delta)+(A-iB)\exp(+2\pi i\delta)$$

hence

$$\rho = \frac{2}{V} \sum_{-\infty}^{\infty} h \sum_{-\infty}^{\infty} k \sum_{0}^{\infty} l(A \cos 2\pi\delta + B \sin 2\pi\delta),$$

$$= \frac{2}{V} \sum_{-\infty}^{\infty} \sum_{-\infty}^{\infty} \sum_{0}^{\infty} \left| F_{hkl} \right| \cos(2\pi\delta - \alpha_{hkl}) \qquad (I.20)$$

which is real.

The fundamental difficulty in using these formulae is the determination of the phase angles α_{hkl}. A simplification occurs if the crystal is centrosymmetric and the origin is taken at a symmetry centre. In such a crystal there is an atom at $\overline{x},\overline{y},\overline{z}$ for each atom at x,y,z. As a result the sine terms in expression (I.12) cancel each other, so that the only possible values of α are 0 or π. Then the phase problem reduces to the determination of the sign, + or -, of the structure factor.

For structures containing a heavy atom whose scattering dominates the intensities and controls a large number of the phases, the Patterson function provides a means of solving the so-called "Phase problem" in crystallography. This approach is known as the "heavy-atom" method and has been used throughout the work in this thesis.

Patterson showed that a Fourier summation using $\left| F_{hkl} \right|^2$ values

$$P_{u,v,w} = \frac{1}{V} \sum h \sum_{-\infty}^{\infty} k \sum l \left| F_{hkl} \right|^2 \cos 2\pi (hu+kv+lw)$$

$$(I.21)$$

gives a vectorial pattern of the distances between the atoms in the structure. Vectors between atoms with scattering factors f_i, f_j and positions (x_i, y_i, z_i) and (x_j, y_j, z_j) give rise to peaks in a Patterson map at positions $\pm (x_i - x_j, \; y_i - y_j, \; z_i - z_j)$ with heights approximately proportional to $Z_i Z_j$. It follows therefore that a Patterson map is always centrosymmetric regardless of whether there is a centre of symmetry in the real structure. For a structure containing N atoms in a unit cell, the map will show (apart from a large origin peak) $N^2 - N$ other peaks per unit cell; the heavy atom – heavy atom peaks being the most prominent. Hence the positions of the heavy atoms may be obtained, which allows one to calculate their contribution to the structure factor and this gives an approximate phase angle for each reflection.

Then a preliminary Fourier synthesis carried out with observed moduli and calculated α_{hkl}'s leads to a first electron-density map which is a rough approximation to the crystal structure. The map may suggest minor adjustments to the heavy-atom positions, and may reveal the positions of several of the lighter atoms. This longer list of atomic coordinates is now used for calculating improved phases which in turn are used in the second Fourier synthesis which gives a still more accurate electron-density map.

The Patterson approach can be conveniently used in determining the phases for structures where $\sum Z^2_{heavy} / \sum Z^2_{light} \sim 1$. On one side, the heavier an atom, the easier it is to locate it and the more it tends to

determine the phases of all the reflections. On the other
hand, when the atom is very heavy compared with the others
in the structure, its dominance becomes too great and the
comparison of $|F_o|$ and $|F_c|$ becomes relatively insensitive
to the positions of the light atoms. If F_H is the
contribution of the heavy atoms to F_c, when the ratio
$|F_H| / |F_o|$ diverges too much from unity, the phase angle
a_c calculated for heavy atom contribution becomes a less
reliable first approximation to the true phase of a
reflection. We can then discard the terms with less
reliable phases by using a rejection test by which only
those reflections with $|F_H| > p|F_o|$ are used in the
Fourier summation. Values of $\underline{p}$ in the range 0.25 $\rightarrow$ 0.33
have been found useful.

When part of the structure is known, a difference
Fourier synthesis is very useful in revealing the remaining
details of the structure.

$$\Delta \rho = \frac{1}{V} \sum_h \sum_k \sum_l (|F_o| - |F_c|)e^{i\,a_c}e^{-2\pi i\,(hx+ky+lz)}$$

$$(I.22)$$

This largely eliminates series-termination errors, which
appear as concentric peaks and ripples surrounding the
heavy atoms if the Fourier summation is done on data which
is truncated by the limiting sphere.

I.3   CORRECTIONS TO INTENSITY DATA

To solve a structure on the basis of measured intensities several corrections must be applied to convert these measurements into the squares of the structure amplitudes. The necessary corrections are:

1. Scaling

2. Polarisation

3. Lorentz factor

4. Absorption

5. Anomalous scattering - dispersion

6. Extinction

The above mentioned factors can be considered as systematic errors in the measurement of intensities and their physical significance will now be examined for each factor in turn.

The polarisation correction allows for the fact that the incident beam, which is usually unpolarised, is partially polarised in the process of scattering by electrons. The degree of polarisation depends on the angle of scattering and is expressed as

$$p = \frac{1 + \cos^2 2\theta}{2} \qquad\qquad (I.23)$$

The Lorentz factor is dependent on the method of collection of the data, and represents the rate at which the r.l. point is swept through the reflecting sphere. For the equi-inclination Weissenberg technique the Lorentz factor is given by

$$L = \frac{\sin\theta}{\sin 2\theta \ (\sin^2\theta - \sin^2\mu)^{\frac{1}{2}}} \qquad\qquad (I.24)$$

where μ is the equi-inclination setting angle.

For a four-circle diffractometer it is given by

$$L = \frac{1}{\sin 2\theta}$$

as every reciprocal lattice point is brought into the horizontal plane for measurement.

As both L and p are functions of θ only, it is usual to combine them in a single correction factor (Lp) as follows:

$$I = k \left| F_o \right|^2 Lp \qquad (I.25)$$

where $\underline{I}$ is the intensity measured on an arbitrary scale, $\underline{k}$ is the corresponding scale factor. In the early stages of an investigation an approximate value of $\underline{k}$ can be estimated by Wilson's method (2), but in the latter stages it is derived from $\sum F_c / \sum F_o$ or equivalent least-squares operations.

T h e   a b s o r p t i o n   c o r r e c t i o n

The incident and reflected beams are partially absorbed in passing through a crystal, and consequently the intensity of a reflection is less than it would be from a perfectly non-absorbing substance. If a narrow beam of monochromatic radiation passes through a thickness $\underline{t}$ of a crystal, the emergent intensity $\underline{I}$ is related to the intensity $\underline{I}_o$ by

$$I = I_o e^{-\mu t} \qquad (I.26)$$

In this expression μ is the linear absorption coefficient of the crystal for the particular type of incident radiation used, and can be evaluated from the relation

$$\mu = \rho \sum_i p_i \mu_{m_i} \qquad (I.27)$$

where ρ is the density of the crystal, $\underline{p}_i$ is the relative weight of element $\underline{i}$, and μ_{m_i} is the mass absorption coefficient of element $\underline{i}$. The absorption effect depends on the shape of the crystal and in general decreases with increasing Bragg angle. So it must be calculated separately for each reflection and is dependent on the path lengths of the individual incident and diffracted beams through the crystal. The amount by which the intensity of the $\underline{h}$ $\underline{k}$ $\underline{l}$ reflection is reduced by absorption i.e. the transmission factor, is denoted by A_{hkl}. The reciprocal of A_{hkl} is the absorption factor $A^*_{hkl} = 1/A_{hkl}$: A^* is the factor by which the observed intensity must be multiplied to obtain the corrected intensity.

Consider a crystal volume element δV scattering the incident beam for the $\underline{h}$ $\underline{k}$ $\underline{l}$ reflection: r_i and r_d are respectively the path lengths of the incident and diffracted beams from δV. Then the transmission factor for the $\underline{h}$ $\underline{k}$ $\underline{l}$ reflection for the whole crystal is given by

$$A_{hkl} = \int_o^V (1/V) \exp\left[-\mu(r_i+r_d)\right] dV \qquad (I.28)$$

where V is the volume of the crystal, and μ the linear absorption coefficient. Several different methods have been published for evaluating this integral. The one used in this work is based on that proposed by Busing and Levy (3) i.e. the volume of the crystal is filled with a regularly spaced array of sampling points. For each reflection the path lengths of the incident and diffracted rays for all grid points are evaluated and used in a three-dimensional Gauss integration to give A_{hkl}.

The degree of accuracy of the correction depends on the accuracy with which the shape and size of the crystal has been determined and on the number of grid points used in a summation.

Dispersion   correction

The diffraction patterns from all crystals are normally centrosymmetric. This was first pointed out by Friedel and stated in his law:

$$I_{hkl} = I_{\overline{hkl}} \tag{I.29}$$

Hence it follows that

$$\left|F_{hkl}\right| = \left|F_{\overline{hkl}}\right| \tag{I.30}$$

and as Fig. I.9 shows for the centrosymmetric case

$$F_{hkl} = F_{\overline{hkl}} \qquad \text{(as equal simply to } A_{hkl})$$

and for a noncentrosymmetric structure

$$F_{hkl} = \left|F_{hkl}\right| e^{i\alpha} \tag{I.31}$$

$$F_{\overline{hkl}} = \left|F_{hkl}\right| e^{-i\alpha} \tag{I.32}$$

Friedel's law holds as long as no atoms in the crystal exhibit anomalous dispersion.

If an atom in the crystal has an absorption edge just on the long-wavelength side of the radiation used, scattering factors are no longer real numbers and can be represented by

$$f_0{}^{anom} = f_0 + \Delta f' + i\,\Delta f'' = f' + i\,\Delta f''$$

where f_0 is the normal scattering factor, $\Delta f'$ is the real component to be added to f_0, and $\Delta f''$ is the imaginary

component which has the function of advancing the phase
slightly. The effects of anomalous dispersion are
different for the centrosymmetric structure from those
for the noncentrosymmetric one. It can be illustrated
by the diagrams (I.10 - I.12). Thus for:

a) centric reflections - Friedel's law holds and

$$F_{hkl} = F_{\overline{hkl}}$$
(Fig. I.10)

b) acentric reflections - Friedel's law does not
hold and

$$F_{hkl} \neq F_{\overline{hkl}}$$
(Fig.I.11, I.12)

In Fig.(I.10 - I.12)
F_W is the resultant of scattering from atoms without
dispersion. In Fig.(I.12) $F_{\overline{hkl}}$ has been reflected across
the real axis to show more clearly the difference between
the structure factor amplitudes and phase angles.

When a dispersion correction is applied in practice the
effects are relatively greater at high $\sin\theta$ than at low,
because both terms $\Delta f'$ and $\Delta f''$ are almost independent of
$\sin\theta$.

Extinction

The internal texture of the real crystals with which
we are dealing lies between two extremes. On the one hand
the regularity of the crystal is perfect throughout its
volume. On the other small regions exist (mosaic blocks)
in each of which there is strict regularity, but the blocks
are randomly and slightly misaligned. These give different
resultant
intensities for diffracted beams, and most crystals give
absolute intensity values somewhere between the two extremes,
but more nearly of the mosaic type. The differences in
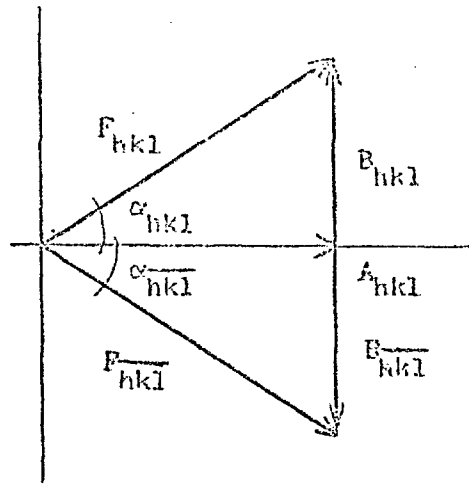
Fig. I. 9.
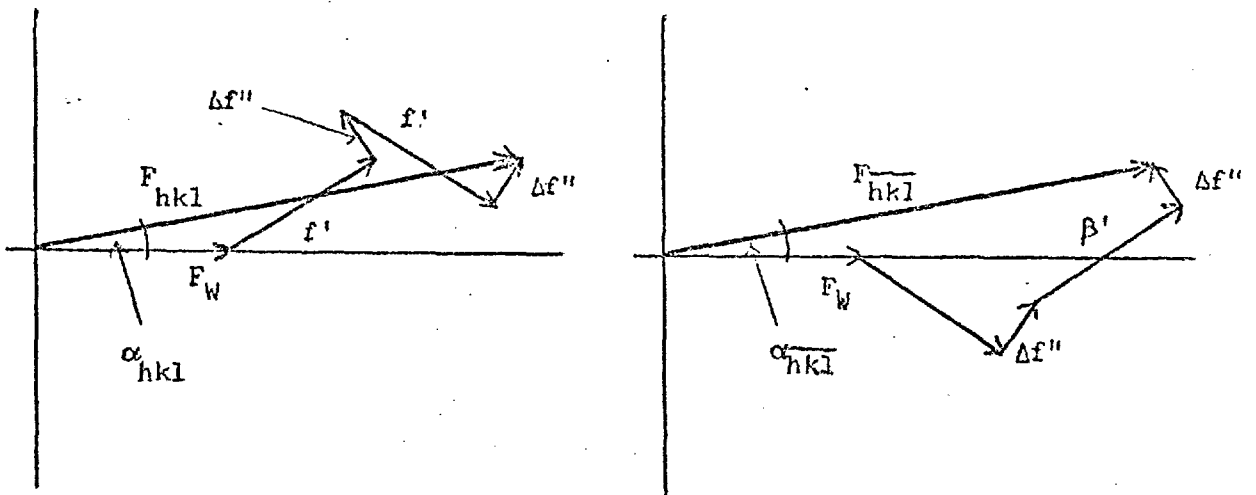
Fig. I. 10.
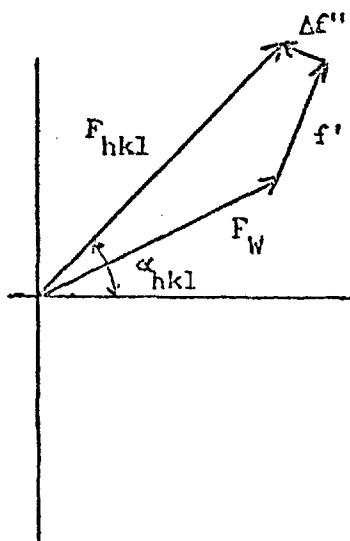
Fig. I. 11.
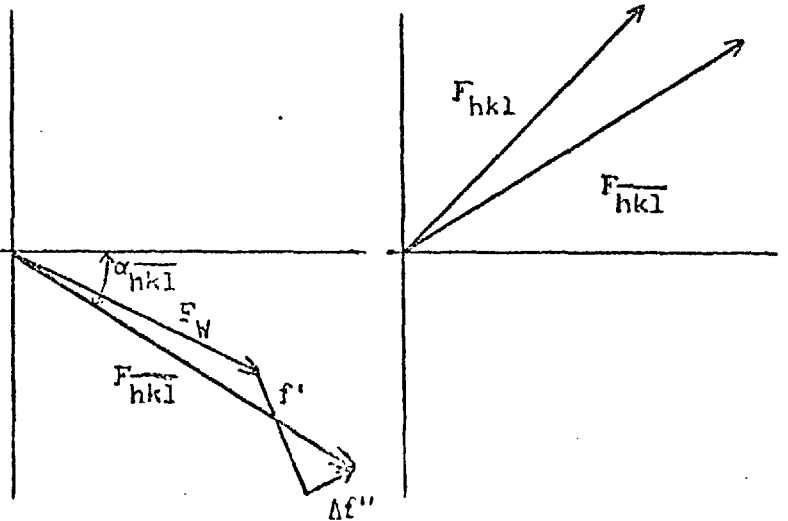
Fig. I. 12.

intensity are due to effects known as primary and secondary extinction.

Primary extinction

The incident beam penetrating through the layers of a perfect crystal is multiply reflected, and the transmitted beams mutually interfere. Since there is a phase change of $\pi/2$ on reflection the twice-reflected rays are parallel to the incident rays but are opposite in phase. This causes a progressive reduction in the intensity of the primary beam as it passes through the crystal, the energy having been diverted into the diffracted beam. The inner parts of the crystal, therefore, cannot make a full contribution to the diffracted intensity. This leads to the integrated intensity being proportional to $|F|$ for the ideally perfect crystal. Most crystals, however, are broken into mosaic blocks so small that the primary extinction in each can be neglected and the intensity is therefore proportional to $|F|^2$. If there is neglible primary extinction of the beam passing through a single mosaic block the crystal is "ideally mosaic".

Secondary extinction

When the incident beam penetrates into a mosaic crystal, blocks which are not correctly inclined at the Bragg angle do not reflect and are effectively "transparent". Those blocks near the surface, which do reflect, "screen" blocks further in. The total intensity of the reflection is therefore less that it would be if each block was bathed in a primary beam of the original strength. The effect is

equivalent to an increase of ordinary absorption over the range of angle in which reflection occurs. However, the beam penetrates to greater depth in a mosaic crystal than in an ideally perfect one, and a larger volume of the crystal takes part in the over-all reflection. The angular width of a reflection is largely determined by the range of misalignment of the mosaic blocks.

Both primary and secondary extinction are dependent on the strength of the reflection, on the wavelength of the primary beam and on the dimensions of the crystal. The effect is most pronounced for reflection at low $\sin \theta / \lambda$, where the general level of the intensity is highest. It results in a systematic tendency for the observed structure factors (F_o) to be lower that the calculated ones (F_c) for strong reflections only. The normal procedure for dealing with extinction is to remove the reflections for which extinction is suspected from the least-squares refinement. However, if possible it is desirable to apply a systematic correction for extinction. At present there is no established treatment for primary extinction, but a theoretical correction, to a first approximation, exists for secondary extinction. Zachariasen (4) has shown that the effect may be accounted for by modifying the absorption coefficient

$$\mu_{eff} = \mu + 2gQ(1+\cos^4 2\theta)/(1+\cos^2 2\theta)^2$$

where Q is the absolute integrated intensity per unit volume, and g is the secondary extinction coefficient.

This gives an expression for the corrected structure factor

$$F_{corr} = F_{obs} (1+c \, \beta_{2\theta} I_o) \tag{I.33}$$

where $\underline{I}_o$ is the observed intensity on an arbitrary scale, $\underline{c}$ is a parameter related to $\underline{g}$, to be adjusted, and $\beta_{2\theta}$ is given by

$$\beta_{2\theta} = \frac{2(1+\cos^4 2\theta).A'(2\theta)}{(1+\cos^2 2\theta)^2}$$

where

$$A'(2\theta) = \frac{\int (t_1+t_2) V . \exp(-\mu (t_1+t_2) dV}{\left(\int \frac{1}{V} \exp(-\mu (t_1+t_2) dV \right)^2}$$

and may be calculated for a crystal of an arbitrary shape during the calculation of the transmission factor A_{hkl}. The value of $\underline{c}$ may be found by a least squares procedure, substituting F_{calc} for F_{corr} (5) for the reflections suffering most strongly from extinction.

I.4. REFINEMENT OF THE STRUCTURE

The process of refinement is systematically to improve the agreement between F_o and F_c for all the observed reflections. This is done in two ways:

1) all necessary corrections are made to F_o to allow for known systematic errors — absorption, extinction, dispersion.

2) adjustments are made to the atomic model (by varying the atom coordinates and thermal parameters) and to the scale factor(s) used for converting the observed structure factors from an arbitrary scale to an absolute one.

The latter process of refinement is usually carried out by least-squares methods, minimizing the function

$$D = \sum w_{hkl} \left(\left| F_o \right| - \left| F_c \right| \right)^2 \qquad (I.34)$$

where the sum is taken over all independent observed structure amplitudes and $\underline{w}$ is the weight allotted to an observation.

The extent of disagreement is expressed by the $\underline{R}$ factor which is computed as

$$R = \frac{\sum \left| F_o \right| - \left| F_c \right|}{\sum \left| F_o \right|} \qquad (I.35)$$

It should be emphasized that it is the $\underline{D}$ function and not the $\underline{R}$ factor which is minimized during the least-squares procedure, although in general both decrease when the refinement proceeds.

The method of least squares

If $|F_c| = |F_c(p_1, p_2 \ldots p_n)|$ where p_j are parameters to be refined, minimization of (I.34) is achieved by taking the derivative with respect to each of the parameters and equating to zero. This leads to $\underline{n}$ normal equations[*].

$$\sum_{hkl} w_{hkl}\left(|F_o| - |F_c(p_1, p_2 \ldots p_n)|\right)\frac{\partial|F_c(p_1 \ldots p_n)|}{\partial p_j} = 0$$

$$j = 1, 2 \ldots n \qquad (I.36)$$

Since $|F_c|$ is not a linear function of the p's, equations (I.36) become intractable. They may be made linear, however, by approximating the function as a Taylor series and neglecting second and higher powers so that

$$|F_c(p_1 \ldots p_n)| = |F_c(a_1 \ldots a_n)| + \frac{\partial|F_c|}{\partial p_1}\Delta p_1 + \ldots \frac{\partial|F_c|}{\partial p_n}\Delta p_n$$

$$(I.37)$$

where a_j are approximate values of p_j (representing the structure at the particular moment of the refinement) and $\Delta p_j = p_j - a_j$. Substituting (I.37) in (I.36) gives

$$\sum_{hkl} w_{hkl}\left(\underbrace{|F_o| - |F_c(a_1 \ldots a_n)|}_{\Delta F} - \frac{\partial|F_c|}{\partial p_1}\Delta p_1 - \ldots \frac{\partial|F_c|}{\partial p_n}\Delta p_n\right)\frac{\partial|F_c|}{\partial p_j} = 0$$

$$j = 1, 2 \ldots n \qquad (I.38)$$

where ΔF now plays the role of the known observational quantity.

*The set of $\underline{n}$ equations in $\underline{n}$ unknowns is called the normal equations.

Expansion and rearrangement of Eq.(I.38) leads to the following set of $\underline{n}$ equations in $\underline{n}$ unknowns, the Δp_j's.

$$\sum_{r=1}^{m} w_r \left(\frac{\partial |F_{c_r}|}{\partial p_1} \right)^2 \Delta p_1 + \sum_{r=1}^{m} w_r \frac{\partial |F_{c_r}|}{\partial p_1} \frac{\partial |F_{c_r}|}{\partial p_2} \Delta p_2 + \ldots$$

$$\sum_{r=1}^{m} w_r \frac{\partial |F_{c_r}|}{\partial p_1} \frac{\partial |F_{c_r}|}{\partial p_n} \Delta p_n = \sum_{r=1}^{m} w_r \Delta F_r \frac{\partial |F_{c_r}|}{\partial p_1}$$

$$\sum_{r=1}^{m} w_r \frac{\partial |F_{c_r}|}{\partial p_2} \frac{\partial |F_{c_r}|}{\partial p_1} \Delta p_1 + \sum_{r=1}^{m} w_r \left(\frac{\partial |F_{c_r}|}{\partial p_2} \right)^2 \Delta p_2 + \ldots$$

$$\sum_{r=1}^{m} w_r \frac{\partial |F_{c_r}|}{\partial p_2} \frac{\partial |F_{c_r}|}{\partial p_n} \Delta p_n = \sum_{r=1}^{m} w_r \Delta F_r \frac{\partial |F_{c_r}|}{\partial p_2}$$

$$\sum_{r=1}^{m} w_r \frac{\partial |F_{c_r}|}{\partial p_n} \frac{\partial |F_{c_r}|}{\partial p_1} \Delta p_1 + \sum_{r=1}^{m} w_r \frac{\partial |F_{c_r}|}{\partial p_n} \frac{\partial |F_{c_r}|}{\partial p_2} \Delta p_2 + \ldots$$

$$\sum_{r=1}^{m} w_r \left(\frac{\partial |F_{c_r}|}{\partial p_n} \right)^2 \Delta p_n = \sum_{r=1}^{m} w_r \Delta F_r \frac{\partial |F_{c_r}|}{\partial p_n}$$

$$(I.39)$$

where m is the number of observations.

Because the Taylor series has been truncated by neglecting second and higher powers in the Δp_j's, the calculations

must be repeated using as approximate values for each repetition the results derived from the preceding calculation. The new values $a_j = a_j + \Delta p_j$. The process is repeated until convergence is obtained and successive cycles produce no further changes.

The set of equations (I.39) may be written in a matrix form

$$
\begin{pmatrix}
a_{11} & a_{12} & \cdots\cdots & a_{1n} \\
a_{21} & a_{22} & \cdots\cdots & a_{2n} \\
\cdot & & & \\
\cdot & & & \\
\cdot & & & \\
\cdot & & & \\
a_{n1} & a_{n2} & \cdots\cdots & a_{nn}
\end{pmatrix}
\begin{pmatrix}
x_1 \\
x_2 \\
\cdot \\
\cdot \\
\cdot \\
\cdot \\
x_n
\end{pmatrix}
=
\begin{pmatrix}
v_1 \\
v_2 \\
\cdot \\
\cdot \\
\cdot \\
\cdot \\
v_n
\end{pmatrix}
\qquad \text{(I.40)}
$$

where $a_{ij} = \displaystyle\sum_{r=1}^{m} w_r \dfrac{\partial |F_{cr}|}{\partial p_i} \dfrac{\partial |F_{cr}|}{\partial p_j}$, $x_j = \Delta p_j$

$$
v_i = \sum_{r=1}^{m} w_r (\Delta F_r) \frac{\partial |F_{cr}|}{\partial p_i}
$$

or more compactly as

$$
Ax = v \qquad\qquad \text{(I.41)}
$$

It can be shown that if equations (I.39) have a solution, an inverse matrix, A^{-1}, exists such that $A^{-1} A$ equals the matrix equivalent of 1. Then

$$
A^{-1} Ax = A^{-1} v
$$

$$
x = A^{-1} v
$$

Thus the least-squares computation can be divided into four parts: (i) calculation of F_c and derivatives (ii) building the matrix of derivative products (iii) inverting the matrix, and (iv) calculating the parameter shifts.

It should be noticed that the matrix A is a symmetric one and that its elements on the principal diagonal are sums of squares and therefore considerably larger than the off-diagonal elements, which are sums of products which may be either (+) or (-).

An anisotropic refinement of the structure requires that there are three positional and six temperature parameters for each of $\underline{n}$ atoms, and at least one scale factor. Altogether $9n+1=q$ parameters which give a q^2 matrix to be inverted. To reduce the time and computer-storage requirements the block-diagonal matrix approximation is commonly used, in which all off-diagonal terms except for those between x,y, and z and those between β_{ij} of the same atom are omitted. In this way a 3 x 3 and 6 x 6 matrix are all that are computed for each atom. However, the results do not converge nearly as rapidly as those from the full matrix, and there is sometimes a tendency to overcorrect, resulting in oscillation from one cycle to the next. To eliminate it damping factors may be applied, i.e. the shifts in parameters are multiplied by a factor less than 1.0.

Random errors

Any measured value can be affected by random and/or systematic errors. They must be considered separately and the chief systematic errors common in X-ray structure analysis were examined in a previous chapter. Different, because statistical in their character, are random errors.

Repeated measurements, provided they are affected only by random errors, follow the Gaussian error distribution. The curve is given by the equation

$$N = \frac{1}{(2\pi)^{\frac{1}{2}}\sigma} e^{-(\frac{1}{2}\sigma^2)(x-x_0)^2}$$

where $\underline{N}$ is the relative frequency with which the value $\underline{x}$ is obtained, $\underline{x}_0$ is the true value of the parameter $\underline{x}$, and $\underline{\sigma}$ is the standard deviation defined for the set of $\underline{m}$ measurements as

$$\sigma = \left(\sum_m \frac{(x_m-x_0)^2}{m}\right)^{\frac{1}{2}}$$ (I.42)

The least squares refinement gives the new values of the parameters and their $\underline{\sigma}$'s calculated for any parameter $\underline{p}_i$ from equation

$$\sigma_{p_i} = \left[b_{ii}\left(\sum_{r=1}^{m} w_r \Delta F_r^2\right)\Big/(m-n)\right]^{\frac{1}{2}}$$ (I.43)

where $\underline{b}_{ii}$ is the i'th diagonal element of the inverse matrix, $\underline{w}_r$ the weight of the r'th ΔF, $\underline{m}$ the number of observations, and $\underline{n}$ the number of parameters.

Refinement may be considered complete for a given structure, when the changes in the parameters are small

compared with corresponding σ's. It has been suggested
(6) that ratio

$$\frac{\text{parameter change}}{\sigma \text{ parameter}} < 0.3 \text{ for full-matrix least squares}$$

and ~ 0.01 for block-diagonal matrix least squares, is
satisfactory for the last cycle of the refinement.

Weighting functions

From statistical considerations, it can be shown that
the weighting factor occurring in Eq.(I.34) is proportional
to the square of the reciprocal of the standard deviation
of the observation: $w \propto 1/\sigma^2$. However, for data collected
on the Siemens diffractometer (approximately "constant
count" conditions) unit weights are found to be reasonably
satisfactory in the early stages of refinement. It follows
from the fact that σ_{F_O} is approximately constant throughout
the data and that non-random errors, which predominate for
diffractometer measurements, are distributed uniformly
throughout the reflection data. Nevertheless, the use of
proper weighting functions can produce a real, if small,
improvement in the results from a given set of data.

Hughes (7) suggested the following weighting scheme:

$$w^{\frac{1}{2}} = 1 \text{ for } |F_O| \leq |F^*|$$

$$\text{and } w^{\frac{1}{2}} = \frac{|F^*|}{|F_O|} \text{ for } |F_O| > |F^*|$$

The value of $|F^*|$ is chosen from an analysis of $|F_O|$ and
$|F_c|$ such that $\sum w \Delta F^2$ will be approximately constant for
all ranges of $|F_O|$.

When a weighting function is properly applied, standard
deviations of parameters should reach more realistic
values, whereas the R factor does not necessarily have to
decrease.

CHAPTER II

EXPERIMENTAL TECHNIQUES OF INTENSITY DATA COLLECTION

INTRODUCTION

Two general methods are available for measuring the
intensities of diffracted beams. Either the beams may be
detected by some sort of quantum counting device which
measures the number of photons directly - diffractometer
method, or else the degree of blackening of spots on
diffraction photographs may be measured and taken as
proportional to the beam intensity - photographic methods.
For many years only the latter methods were used with
visual or sometimes photometric estimation of the
intensities, but the accuracy was rarely better than 10%.
However since 1945 when the first powder diffractometer
was marketed, a rapid development of the new measuring
technique has been observed. Automatic diffractometers are
in general faster than visual measurements and far more
precise.

Since data for one of the structures comprising this
work were collected photographically, and for three others
on a diffractometer, both techniques will be described in
this chapter.

II.1.   PHOTOGRAPHIC DATA COLLECTION

The equi-inclination Weissenberg technique was
adopted when intensity data were collected photographically.
Cu-K_α radiation filtered through nickel foil was used
throughout.   A pack of four Ilford Industrial "G" films
was used for recording reflections for each layer and an
appropriate exposure time was chosen in order to record a
useful intensity range.

Having collected all the film packs, the next step
was to prepare a scale for estimating the intensities of
the spots.   This scale, or "wedge", was prepared by
selecting an intense reflection from the crystal studied
and then arranging that the crystal oscillates approximately
$\pm 2^{\circ}$ through the reflecting position.   A series of
exposures of this reflection of increasing length was made,
moving the film pot along between exposures.   The result
was a series of spots of varying intensity with limits being
on either side of the optimum intensity range.

With the aid of this "wedge" the intensities of all
spots (from the "contracted" side of the film) were
measured and values obtained for each reflection in the
pack were scaled up to those on the top film and a
subjectively estimated mean value was calculated for each
reflection.

The spot selected for preparing the "wedge" was
typical of the majority of spots on all layers and no
correction for spot shape was applied.

II.2. DIFFRACTOMETER DATA COLLECTION

Basis of diffractometer design
and control.

A general view of the Siemens Automatische Eine-
kristalle Diffraktometer, hereafter referred to as the
A.E.D., is shown in Fig.II.1. It consists of the X-ray
generator, goniometer for measuring diffraction angles and a
number of electronic circuits for controlling the A.E.D.
during its work and determining the intensity of diffraction.

X-ray generator.

High stability and intensity of the X-ray source are
essential requirements of the X-ray generator, because
they determine the rate of data collection and its
reliability. A high-stability source is required since
reflections are being recorded one at a time. On the A.E.D.
the high-voltage stabilizer specifies voltage to ± 0.1%
for ± 10% mains voltage fluctuations. The X-radiation from
a Cu target was passed through an appropriate β-filter and
collimator to give an almost parallel beam homogeneous in
intensity, which should bathe the crystal completely
without being excessively wide so as to avoid high signal-
to-noise ratio in the detector.

Goniometer.

The A.E.D. four-circle goniometer allows one to bring
each reciprocal lattice point into the equatorial plane,
since this is the only plane in which the counter rotates.
The three circles which determine the orientation of the
crystal are:

1) ω-circle, in the horizontal plane;

   range: $-4° < \omega < 7.5°$.

2) χ-circle, in the vertical plane and carried on the
   ω circle;

   range: $-5° < \chi < 91°$.

3) ϕ-circle, whose axis lies in the χ circle plane
   and can be moved to become any radius of the
   χ-circle over a range of $-5°$ to $+91°$;

   range $0 < \phi < \infty$.

The fourth circle, designated 2θ, carries the counter and
is coaxial with the ω-circle. The ω - and 2θ -circles are
usually coupled in a $\theta:2\theta$ ratio and the ω-circle is then
referred to as the θ-circle, Fig.II.2.

There are various technical solutions of the gonio-
meter construction all governed by the need for high
rigidity and stability and ensuring at the same time that
no collisions or obscurations can arise during exploring
the accessible part of reciprocal space. One normally
needs to examine no more than a hemisphere of reciprocal
space and the ranges of movement of the circles on the
A.E.D. allow for access to $\sim 58\%$ of the sphere. An
additional and very convenient provision is that the zero
of the ϕ-circle can be altered arbitrarily to coincide with
a reciprocal vector of the crystal.

The circles are driven by impulse motors, giving an
increment of $0.01°$ with each pulse. ($0.02°$ for 2θ).
When controlled from the steering tape, they can be moved
to the required position simultaneously (3 circles by the
smallest increment, two circles by the next increment, and

the remaining circle by the final increment). Their destinations can be checked automatically, and any error in the range $\pm$ 0.2° can be automatically corrected. If an error exceeds $\pm$ 0.2°, the instrument stops and has to be reset manually, which can be done with an accuracy of 0.01°.

X-ray detector and accompanying circuits.

Throughout the present work a Na(Tl) I scintillation counter was used in preference to the proportional counter. It has poorer energy resolution than the latter, but its quantum efficiency is $\sim$ 85%, i.e. 5 times better. The light flashes are converted to pulses in a photomultiplier and these are passed to a pulse-height analyser which has a voltage acceptance range preset so that about 90% of the main peak signal is accepted, but with suppression of harmonics, and most of the white and fluorescent radiation.

To ensure a statistical, Gaussian distribution of the pulse-height for a given photon energy, the extra-high tension supplied to the photomultiplier must be stable to about 0.01% and we usually cool the counter with water.

Diffractometer control.

The A.E.D. is an automatic, off-line instrument, which uses five-track punched paper tape, called a "steering tape", which bears all the instructions to guide the diffracto-meter during the intensity data collection. The tape has no timing instructions; optimum values of these are decided automatically by hardware. Thus a given steering tape can be used on any crystal of a given material. All control functions of the A.E.D., like the circles, digitizer checks,

half-shutters (their function will be mentioned later),
$\theta:2\theta$ couple/decouple, measurement commands, can be
operated either by the paper tape or from the manual control
desk.

Principles of data collection
on the A.E.D.

Preliminary to the intensity measurements are
alignment of the goniometer and setting up the crystal.

The examined crystal is mounted on a quartz fibre
with "Araldite" and the fibre was attached to the eucentric
goniometer head with dental wax. To obtain thermal
equilibrium, the crystal should be left in the air-
conditioned A.E.D. room for about 2 days.

After that the goniometer head is placed on the A.E.D.
and the slit collimator is placed in front of the detector
to increase the resolution in θ while setting up the
crystal and determining its lattice parameters. The crystal
is centred first by eye and then set and centered accurately
with the help of the half-shutters.

At this place it is perhaps worth mentioning how the
half-shutters work. A chosen reflection is scanned three
times: the first normally, the second with a horizontal half
-shutter in the counter collimator, and the third using a
vertical half-shutter in the same way. These are actuated
from paper tape signals. When the setting of the crystal
is completed, the half-shutter counts will be approximately
half those with no shutter.

The crystal is mounted with one of its crystallographic

axes parallel to the ϕ-axis by adjustment of the goniometer arc and the help of the horizontal half-shutter. A series of $\phi - \theta$ scans is carried out around several reciprocal lattice points on each of the principal axes, from which accurate θ values can be obtained.& hence accurate cell parameters $\llcorner$ Also the ϕ axis zero position can be brought calculated. to coincide with a chosen r.l. vector. When satisfactory lattice parameters have been obtained, all the necessary information for generating accurate setting angles is known.

Thus assume that the crystal is to be set with the c axis parallel to ϕ . Then $\chi = 0.0^o$ for the a*,b* axes and their orientation must be chosen such that a right-handed system of axes is used. (This is important if absorption and dispersion corrections are to be applied correctly). If the crystal is to be mounted in an arbitrary orientation it is necessary to know approximately what this orientation is so that three non-coplanar reflections can be indexed and their corresponding θ , χ and ϕ values found. Using those reflections and their setting angles a list of reflections and approximate setting angles can be generated by program.

There are three methods of integration over the reflection peak: the moving-crystal/fixed-counter scan, fixed-crystal/fixed-counter scan, and moving-crystal/ moving-counter ($\omega/2\theta$) scan. The last method was employed throughout this work as giving a more realistic inter-polation of the background with an intensity collection collimator greater in aperture size than the slit one used during preliminary work.

Before the actual intensity measurements are commenced

the scanning limits $\Delta\theta_1$ and $\Delta\theta_2$ have to be obtained by θ-scans of some representative peaks over the θ-range to be covered, and the "reference" and "control" reflections have to be chosen.

The reference reflection monitors the stability of the X-ray tube and counting equipment and reveals whether the crystal is suffering X-ray damage. This reflection is also used during processing of the output data for scaling the intensities by the average intensity of the reference reflections which precede and follow the block of reflections (usually 20).

The control reflections are usually specified after about every 250 reflections and each of them is measured three times with and without the half-shutters (as described previously) to check the crystal orientation.

At this stage all the information for generating the steering tape is in hand. The approximate number of generated reflections is given by the formula

$$N = \frac{4}{3}\pi \left(\frac{2\,\sin\theta_{max}}{\lambda} \right)^3 V.f$$

where θ_{max} is the maximum value of θ to which data is to be collected, λ is the radiation wavelength, V is the volume of the unit cell, and f is the fraction of the sphere to be collected. This formula applies to primitive unit cells and thus for a (e.g.) face-centered cell the number of reflections is further reduced by a factor of 2.

The special principle of intensity measurement on the A.E.D. is that all measurements start at the reflection peak, which enables the machine to test the maximum counting -rate of the reflection and either to insert automatically

one of five attenuators in the primary beam (for strong reflections), or to reduce the counting rate (for weak reflections), such that the counts fall within the range of maximum counter accuracy. A five-value measuring technique is employed to obtain the integrated intensity of each peak above the local background (Fig.II.3). The instrument first measures the low-θ half of the intensity peak ($\Delta\theta_1$), then the low-θ background, the counts being I_1 and I_2 respectively. The complete peak ($\Delta\theta_1 + \Delta\theta_2$) is then scanned giving count I_3 which is followed by measuring the high-θ and then scanning the other half ($\Delta\theta_2$) of the peak with counts I_4 and I_5 respectively.

The output is in the form of a five-track punched paper tape which gives for each reflection its serial number, indices, setting angles, the limits of scan in θ, five values of counts and the time measuring constant and the number of the attenuator used (if any).

Figure II.I. The Siemens diffractometer.

  Top plate: Four-circle goniometer.

  Bottom plate : The measuring and control

                    cabinets.

Figure II. 2.

The basic design of the Siemens A.E.D. goniometer.

$$(\mathsf{I}_1 + \mathsf{I}_5) = \mathsf{I}_3 = \mathsf{I}_2 = \mathsf{I}_4$$

$$\mathsf{I}_{net} = \frac{1}{2}\left[(\mathsf{I}_1 + \mathsf{I}_3 + \mathsf{I}_5) - (\mathsf{I}_2 + \mathsf{I}_4)\right]$$
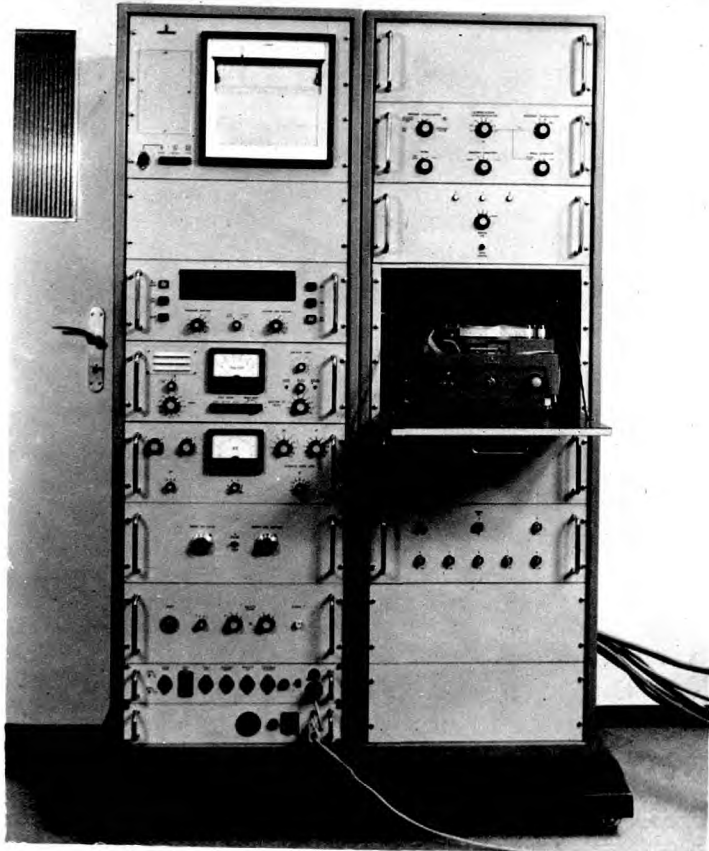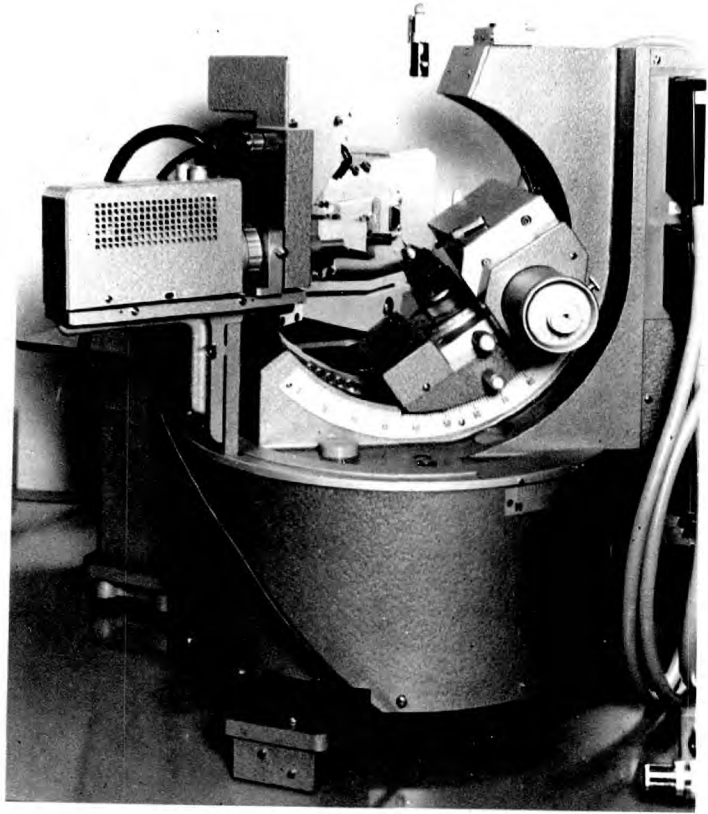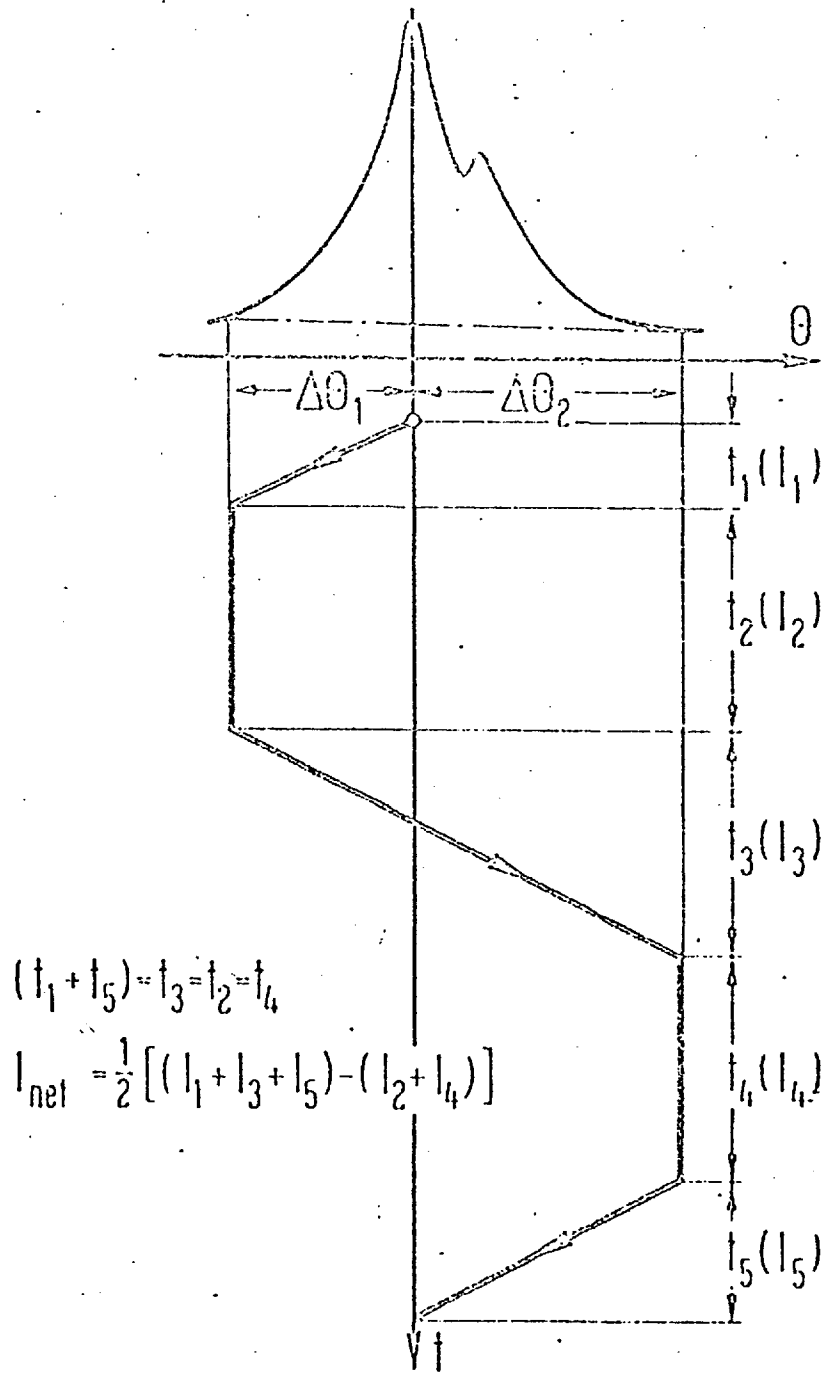
Figure II. 3.

The five-value measurement

REFERENCES

1. H.A. LEVY,

    Acta Cryst., 9, 679, (1956)

2. A.J.C. WILSON,

    Nature, 150, 152, (1942)

3. W.R. BUSING and H.A. LEVY,

    Acta Cryst., 10, 180, (1957)

4. W.H. ZACHARIASEN,

    Acta Cryst., 16, 1139, (1963)

5. S. ÅSBRINK and P.E. WERNER,

    Acta Cryst., 20, 407, (1966)

6. R.A. SPARKS in "Computing Methods and the Phase
    Problem in X-ray Crystal Analysis," R. Pepinsky,
    J.M. Robertson and J.C. Speakman, eds., Pergamon
    Press, Oxford, 1961, p.170 ff.

7. E.W. HUGHES,

    J.Am.Chem.Soc., 63, 1737, (1941)

Appendix : Computer programs used

COMPUTER PROGRAMS USED

Two distinct sets of crystallographic computer programs were used in this work:

1. Diffractometer programs

2. X-ray-63 system

The programs in both systems will be conventionally referred to by their names, and brief description will indicate their functions.

Diffractometer Programs

These are written in EXCHLF and form a part of a locally-written system of separate programs for the University of London ATLAS computer (all written by P.G.H. Troughton).

They are stored at the Centre on magnetic tape, from which they can be called by a short input paper tape containing the call to the required program, necessary data, and option instructions.

SEKO – Calculates setting angles and generates Five-value-measurement steering tape for the Siemens automatic diffractometer.

SODI – Processes the data tapes output from the A.E.D. It tests the circle digitizer checks and evaluates the net intensities. Each intensity measurement is scaled up by the time-constant (M) and attenuation factors (A_t), then by the reference reflection (K). $(LP)^{-1}$ corrections are applied and the value of the standard deviation for each observation evaluated.

On the basis of counting statistics, the

standard deviation of the net count, (I_{net}),

is given by

$$\sigma(I_{net}) = \tfrac{1}{2}(I_1+I_2+I_3+I_4+I_5)^{\frac{1}{2}}$$

$$\sigma(F_o^2) = K.(Lp)^{-1}M.A_t.\ \sigma(I_{net})$$

and $\sigma(F_o) = \sigma(F_o^2)/2F$

If $I_{net} < Q\ \sigma(I_{net})$ the reflection is regarded

as unobserved and I_{net} is replaced by $Q\ \sigma(I_{net})$.

Q represents the confidence probabilities and

its value 2.58 used throughout this work gives

99% probability that any measured count is

greater than the background.

Cards with reflection indices, F_o^2 and $\sigma(F_o)$ are

punched in X-ray-63 format.

"Unobserved"reflections are flagged as "less-thans".

ABSO -   An extension of SODI which also applies an

absorption correction to crystals of arbitrary

shape and calculates the $I_o\beta$ term for the

secondary extinction correction.

Program ICABS, written in FORTRAN IV for the IBM 7094,

was also used.

ICABS -   Processes 3- and 4-circle diffractometer,

precession camera and equi-inclination

Weissenberg data.   It makes $(LP)^{-1}$, absorption,

and extinction corrections.

The X-RAY-63 System

This is a completely homogenous system developed by Professor J.M. Stewart of the University of Maryland, U.S.A., from programs written by himself and others. It is available on the IBM 7094 computer of Imperial College, and has been slightly modified for ATLAS.

The system consists of a number of programs, mainly written in FORTRAN II and linked together such that output of one program can be fed into the next, thus performing several different types of calculations successively in one run.

The programs used by the author in this work are:-

DATRDN - The entry point to the system. Data fed in are such as: reflection list, atomic scattering factors, cell parameters, space group symmetry operations, etc.

Performed operations are:

$(LP)^{-1}$ correction (optional), scaling of the initial intensities to an approximately absolute scale, evaluating $F_{relative}$ value. The information from DATRDN is written up to magnetic tape for processing by the structure factor and other links.

FC - Calculates structure factors and a scale for each level of data (for A.E.D. there will be only one such scale factor). Since the least-squares routines also calculate structure factors, it can be dispensed with when these are used in a straight-forward way. If, however, only some atoms of the set are to be refined, the remaining atoms can be placed in FC first as

a "fixed atom contribution". It has an application for large structures, when the number of parameters exceeds the capacity of the available least-squares programs. For a small structure. atom parameters can be fixed in a least-squares refinement.FC always preceeds FOURR in the initial stages of finding the atoms.

FOURR - Calculates two- or three-dimensional Patterson and Fourier maps, for the latter using as input a set of observed structure amplitudes with phases calculated in FC link. The program is very flexible and a variety of modifications of the basic Fourier map can be produced, such as difference- and E-syntheses.

ORFLS - A full-matrix least-squares refinement program. It allows the simultaneous refinement of up to 180 variables such as: atomic positions, temperature factors, scale factors (of different levels), multiplicities and scattering factors. Temperature factors can be all isotropic, all anisotropic, or a mixture of the two. It also has an option of applying a dispersion correction.

BLOKLS - This is the block-diagonal least-squares approximation which must be used for large structures.

BONDLA - Calculates inter- & intra-molecular bond distances and angles, along with standard deviations. Symmetry and translation operations are allowed for. Hydrogen atom positions can also be generated from the positions of the

next neighbours, given whether the hydrogen is

tetrahedrally, trigonally, or linearly bonded.

LSQPL - Calculates the best plane through a given set

of atoms by least-squares methods, giving the

displacementsof the atoms from the plane, and

the displacements of any additional atoms

specified. The angle between planes and/or

lines can also be obtained.

LISTFC - Outputs structure factor lists in a format

suitable for reproduction in theses and papers.

Other Programs

ICEXT - Written in FORTRAN IV for the IBM 7094,

calculates the least-squares secondary

extinction coefficient $\underline{c}$ and applies the

extinction correction to all the data. It

can be used as the first link of the X-ray-63

system to enable application of the extinction

correction and further refinement in the same

run.

MOJO - Written in EXCHLF. This computes orthogonalised

Ångstrom co-ordinates and dihedral angles for

a given set of atoms.

ORTEP - Written by C.K. Johnson in FORTRAN IV, (see

Oak Ridge National Laboratory Technical Report

ORNL-3794). Adapted for CDC 6600 by G. Richards

and F. Stephens. It is the thermal-ellipsoid

plot program used for crystal-structure drawings.

The program can produce stereoscopic pairs of

illustrations on a Calcomp and similar incremental

plotters,and can calculate the principal axes
of thermal motion for each atom.

SECTION B

STRUCTURAL STUDIES

CHAPTER I

The Crystal Structure of

the Orthorhombic Form of

Hydridodicarbonylbis(triphenylphosphine)iridium(I)

$$IrH(CO)_2(PPh_3)_2$$
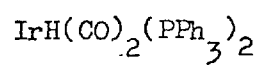
ABSTRACT

The crystal and molecular structure of the orthorhombic form of hydridodicarbonylbis(triphenylphosphine)iridium(I) has been determined from three-dimensional X-ray diffractometer data. The complex crystallises in space group Pna2$_1$ with four molecules in a unit cell of dimensions a = 17.759, b = 10.001, c = 18.389Å. The structure was refined by least-squares methods using all 2518 measured independent reflections to give R = 0.0187.

The complex is monomeric and the coordination about the iridium atom can best be described as a distorted trigonal bipyramid in which one of the phosphorus atoms and the hydride hydrogen occupy the axial positions. The Ir-P distances are nearly identical 2.375 and 2.370Å, but the phosphorus atoms are differently oriented with respect to the two carbonyl groups: P(1)-Ir-C ca. 95°, P(2)-Ir-C ca. 115°; mean Ir-C(carbonyl) distance is 1.850Å. The hydride hydrogen has been located and the estimated Ir-H distance is 1.64(5)Å.

INTRODUCTION

The complex hydridodicarbonylbis(triphenylphosphine)iridium(I) was prepared by Yagupsky and Wilkinson (1969) and found to have unusual spectroscopic behaviour indicating fluctional isomers in thermal equilibrium in solution. The iridium complex is the more thermally stable and chemically less reactive analogue of a rhodium complex, which appears to be the main catalytic species in the hydroformylation reaction of alkenes using $RhH(CO)(PPh_3)_3$ as catalyst (Evans et al., 1968).

A structural study of the iridium complex was undertaken in order to compare the spatial arrangement of the ligands in the solid state with those suggested by Yagupsky and Wilkinson for this complex in solution.

Since one of the ligands is a hydride hydrogen atom the determination of its position was important. In recent years hydride hydrogens have been located from X-ray data in second-row transition metal complexes (cf. La Placa and Ibers, 1965; Skapski and Troughton, 1968). This encouraged us to try to see whether this could be done for a complex of a third-row transition metal such as iridium (Z = 77).

A preliminary account of this work has already been published (Ciechanowicz et al., 1969).

EXPERIMENTAL

Hydridodicarbonylbis(triphenylphosphine)iridium(I) is obtained by the action of sodium borohydride on an ethanolic suspension of trans-chlorocarbonylbis(triphenylphosphine)iridium(I) saturated with carbon monoxide at atmospheric pressure. It can be recrystallized from toluene, cyclohexane or benzene, with or without addition of ethanol. Crystals were kindly provided by Professor G. Wilkinson and Dr. G. Yagupsky. Preliminary oscillation and Weissenberg photographs showed that from a single solution as many as three polymorphic forms could be obtained, the main details of which are given below.

Table 1

Form	Unit-cell dimensions					Space
	$\underline{a}$	$\underline{b}$	$\underline{c}$	$\underline{\beta}$	$\underline{V}$	Group
Orthorhombic	17.759(3)	10.001(3)	18.389(2)		3266.0	$\underline{Pna2}_1$
Monoclinic(I)	18.036(5)	10.075(2)	19.474(5)	$113°22(2)'$	3248.5	$\underline{P2_1/a}$
Monoclinic(II)	17.679(4)	10.205(3)	18.390(5)	$91°47(1)'$	3317.1	$\underline{P2_1/c}$

The orthorhombic form was the first of these to be examined structurally. Weissenberg photographs showed systematic absences of the type $0\underline{kl}:\underline{k} + \underline{l} = 2\underline{n} + 1$ and $\underline{h}0\underline{l}:\underline{h} = 2\underline{n} + 1$. These are consistent with space groups $\underline{Pna2}_1$ (No.33) and $\underline{Pnam}$ (No.62); the successful solution and refinement of the structure showed the former to be the correct one. Other crystal data are:

$\underline{D}_m$ (by flotation) $= 1.33$ g cm^{-3}, $\underline{D}_c = 1.341$ g cm^{-3} for $\underline{Z} = 4$, $\underline{F}(000) = 1528$, MW.$= 773.8$ for $IrP_2C_{38}H_{31}O_2$.

Intensity data were collected for a crystal of approximate size $0.65 \times 0.3 \times 0.3$ mm. The crystal was mounted about the longest morphological axis ($\underline{b}$ axis) on a Siemens off-line automatic four-circle diffractometer. Cu-$\underline{K}\alpha$ radiation at a take-off angle of $4.5°$, a Niβ filter and a Na(Tl)I scintillation counter were used. The Θ - 2Θ scan technique was employed using a "five-value" measuring procedure (Skapski and Troughton, 1970). 2518 independent reflections were measured to $\Theta = 60°$, of which 55 were judged insignificant as the net count was below 2.58 times the standard deviation (i.e. below the 99% confidence limit) and were assigned a count equal to this value. The 0 0 10 reflection was used as a reference every 20 reflections: the net count of this reflection did not change significantly over the period of data collection (approximately 5 days). The data were adjusted to a common arbitrary scale using the reference reflection, and Lorentz and polarisation corrections were applied.

SOLUTION AND REFINEMENT OF THE STRUCTURE

A three-dimensional Patterson gave a straightforward solution for the position of the iridium atom. At this stage it was consistent with being placed in a general position in space group $\underline{Pna2_1}$ or on a mirror in space group $\underline{Pnam}$. The $\underline{z}$ coordinate was therefore fixed at $\underline{z} = \frac{1}{4}$ and three cycles of least-squares refinement reduced the standard agreement factor $\underline{R}(=\Sigma ||\underline{F}_{\underline{o}}|-|\underline{F}_{\underline{c}}||/\Sigma|\underline{F}_{\underline{o}}|)$ to 0.23. A difference Fourier revealed one of the phosphorus atoms essentially on the "mirror" and another one in a completely general position with peaks of half weight on either side of the mirror. This suggested that the true space group was $\underline{Pna2_1}$, or $\underline{Pnam}$ with disorder. The first was thought more probable and it was assumed that one half-weight peak was a true phosphorus position, while the other was its mirror image. Least-squares refinement in the non-centrosymmetric space group including the two phosphorus atoms went smoothly and reduced $\underline{R}$ to 0.163.

Although the pseudo-mirror persisted to a large extent in difference Fouriers it proved possible to unscramble the carbons of the phenyl rings from their mirror images and locate the carbonyl groups. Least-squares refinement with the iridium atom anisotropic and all non-hydrogen atoms isotropic gave $\underline{R} = 0.074$.

At this stage an absorption correction was applied, as the crystal was quite large and the linear absorption coefficient $\mu = 89.8$ cm^{-1}. The correction was made using the Gaussian integration method, with an 8 x 8 x 8 grid, described by Busing and Levy (1957) with crystal pathlengths determined by the vector analysis procedure of Coppens et al. (1965). This correction reduced $\underline{R}$ to 0.051.

Inclusion of all phenyl hydrogen atoms gave $\underline{R} = 0.045$. All non-hydrogen atoms were now refined anisotropically, a dispersion correction for Ir and P was applied and four reflections were removed for suspected extinction to reduce $\underline{R}$ to 0.028.

Since extinction was still visibly affecting the other strong reflections it was decided to apply an extinction correction to all measured reflections using the formula of Zachariasen (1963). The procedure of getting the approximate value of the c parameter was that described by Åsbrink and Werner (1966). Least-squares refinement on extinction-corrected data, with shifts damped to 0.5, brought R to 0.0206.

A weighting scheme of the type described by Hughes (1941) and a dispersion correction for oxygen and carbon were now applied. The weighting scheme was $\sqrt{w} = 1$ if $F_o \leqslant F^*$ and $\sqrt{w} = F^*/F_o$ if $F_o > F^*$, with $F^* = 100$ found to be optimum. Application of the weighting scheme reduced the standard deviations by $\underline{ca}$. 10%. To allow for the effect of the weighting scheme the extinction parameter c was slightly readjusted several times to its final value of 8.1×10^{-5}, and refinement was terminated at $R = 0.0187$.

The atomic scattering factors used were those tabulated by Cromer and Waber (1965) and the values for the real and the imaginary parts of the dispersion correction for Ir and P atoms were those given by Cromer (1965), and for O and C atoms by Hope et al. (1969).

The solution and refinement of the structure were carried out using the Crystal-Structure Calculations System, X-Ray '63 (described by J.H. Stewart in the University of Maryland Technical Report TR-64-6). The calculations were carried out on either the Imperial College IBM 7094 or the University of London Atlas computers.

Table 2 lists the final coordinates of the non-hydrogen atoms and Table 3 the coefficients for the anisotropic temperature factors $\exp[-(\beta_{11}h^2 + \beta_{22}k^2 + \beta_{33}l^2 + 2\beta_{12}hk + 2\beta_{13}hl + 2\beta_{23}kl)]$. In these tables the standard deviations have been estimated from block-diagonal matrix refinement and are, therefore, a slight underestimate of the true deviations. The coordinates of the hydrogen atoms are given in Table 4. Table 5 lists the observed structure amplitudes and the calculated structure factors.

DETERMINATION OF THE HYDRIDE HYDROGEN POSITION.

The first attempt at localizing the hydride hydrogen was undertaken when $\underline{R}$ reached a value of 0.028. A difference Fourier for reflections with sin $\Theta/\lambda < 0.25$ was calculated revealing an unambiguous peak at the expected Ir-H distance and in a stereochemically sensible position. From this stage on the hydride hydrogen atom was included in structure factor calculations but was not refined in least squares until $\underline{R}$ was 0.0197.

After the refinement of the structure was terminated at $\underline{R} = 0.0187$ the procedure described by Ibers and Cromer (1958) was used to determine the hydride hydrogen position more exactly. These authors have pointed out that in principle there is an optimum number of data to use in the location of light atoms in the presence of heavy atoms. Thus, in a Fourier series, the ratio of the peak height of an atom to the standard deviation of the electron density should go through a maximum as a function of scattering angle. This maximum can be determined experimentally by varying the number of terms in the Fourier series.

Difference Fourier maps were therefore calculated for different cut-offs in sin Θ/λ and the results are summarised in Table 6. Among other information the table includes the observed height of the hydrogen peak $(\rho^o{}_H)$, the calculated peak height $(\rho^c{}_H)$ of a hydrogen atom with B of $3\AA^2$, the estimated standard deviation of electron density σ_ρ calculated according to Cruickshank's (1950) formula for a non-centrosymmetric structure $\sigma_\rho = 2\underline{V}^{-1}(\Sigma(\underline{F}_o - \underline{F}_c)^2)^{\frac{1}{2}}$, and the signal-to-noise ratios $(\rho^o{}_H/\sigma_\rho$, $\rho^c{}_H/\sigma_\rho)$ for this and two other instances where the analogous procedure was carried out i.e. for $RhH(CO)(PPh_3)_3$ (La Place and Ibers, 1965a) and $RuClH(PPh_3)_3$ (Skapski and Troughton, 1968).

While examining the Fourier maps calculated for different numbers of terms one should bear in mind that their reliability can be affected

by factors such as ripples from termination of the Fourier series, residual perturbations around the heavy atom due to the inadequacy in the description of its scattering form factors or its thermal motion, etc. In the present work, however, none of the four difference Fourier maps appeared to be markedly inferior on this score.

As the observed signal-to-noise ratios gave no clear cut best value, and the ratios themselves were fairly similar it seemed most reasonable to take Ir-H as the average of all four distances, 1.64Å. (This is identical to the distance from the Fourier having the best <u>calculated</u> signal-to-noise ratio.)

It is encouraging to note that it proved possible to refine the hydride hydrogen to give an Ir-H distance of 1.604Å ($\sigma = 0.048$). We believe, however, that the hydrogen position estimated from the series of Fourier maps is more realistic because the least-squares procedure does not give really reliable values of the parameter shifts for such a light atom as hydrogen, when it is refined together with a very heavy atom. The hydrogen temperature factor, $\underline{B} = 0.9\text{Å}^2$($\sigma = 1.2$), obtained in least-squares refinement, although low, is not significantly different from that characterising thermal vibrations of the Ir atom, i.e. $\underline{B} = 2.6\text{Å}^2$. As all values of Ir-H distances found from the Fouriers lie within the range of one least-squares estimated standard deviation, its value seems a reasonable one to adopt.

The successful location of hydride hydrogen in the vicinity of an atom as heavy as iridium ($Z = 77$) was possible only because the following factors were present together: good quality of the diffractometer data, no disorder in the structure, easily describable crystal shape allowing accurate absorption correction, and good iridium scattering from factors.

It is interesting to consider at what value of $\sin \theta / \lambda$ the maximum in calculated signal-to-noise ratio is likely to occur. In order to do that

the function of the hydrogen atom peak height vs. sin Θ/λ was calculated according to the formula

$$\rho_H^c = \frac{1}{2\pi^2} \cdot \int_0^{S_0} (1 + a^2 s^2/4)^{-2} \exp(-Bs^2/16\pi^2) s^2 ds$$

(where $s = 4\pi\lambda^{-1} \sin\Theta$, a is the Bohr radius (0.5292Å) and the result is illustrated in Fig 1.

As can be seen the function rises quite steeply and then flattens out to a plateau, but its exact shape depends markedly on the temperature factor B of the hydrogen atom. If σ_ρ were a linear function of $\sin\Theta/\lambda \equiv S$, the optimum signal-to-noise ratio would occur at $S = 0.478$ for $B = 1Å^2$, 0.409 for $3Å^2$ and 0.354 for $6Å^2$, as shown in Fig 2. These values are very similar, but not identical to those corresponding to the "maximum of curvature" as indicated by the second differential of the function ρ which has a minimum at $S = 0.449$, 0.398 and 0.350 respectively. In reality (see Table 6) $\sigma_\rho(S)$ is not proportional to S. The values of

$$\frac{\sigma_\rho(S_2) - \sigma_\rho(S_1)}{S_2 - S_1}$$

for successive points S_n tend to fall off with increasing S. This has the effect of shifting the observed maximum in ρ/σ_ρ to a higher value of $\sin\Theta/\lambda$.

In general, the higher the thermal vibration of the hydrogen atom, the smaller will be the optimum number of data to use in a difference Fourier. Secondly, if any distinction can be drawn between visual and diffractometer data, it is that for visual data, where accuracy of individual measurements tends to deteriorate more at higher angles (α_1, α_2 separation etc.), σ_ρ as a function of $\sin\Theta/\lambda$ may show more of an "upswing". This would tend to shift the optimum ρ/σ_ρ to a lower value of $\sin\Theta/\lambda$ compared to diffractometer data.
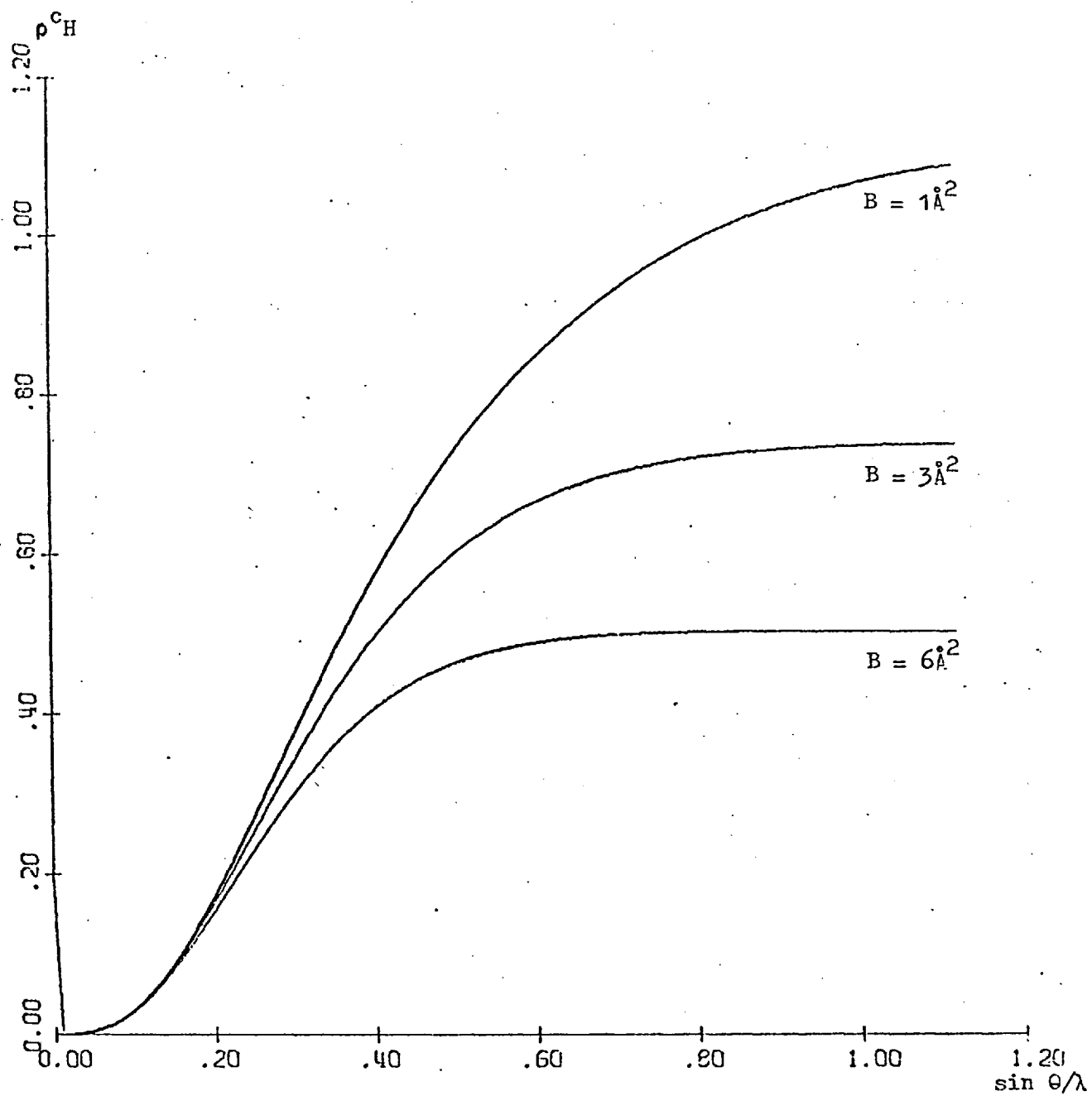
Fig. 1

Electron density function calculated for a hydrogen atom with three different temperature factors

Figure 2 — graph with vertical axis labeled ${}_0{}^C H\lambda/\sin\theta$ (values 0.00, .40, .80, 1.20, 1.60) and horizontal axis labeled $\sin\theta/\lambda$ (0.00, .20, .40, .60, .80, 1.00, 1.20), showing three curves labeled $B = 1\text{Å}^2$, $B = 3\text{Å}^2$, $B = 6\text{Å}^2$.
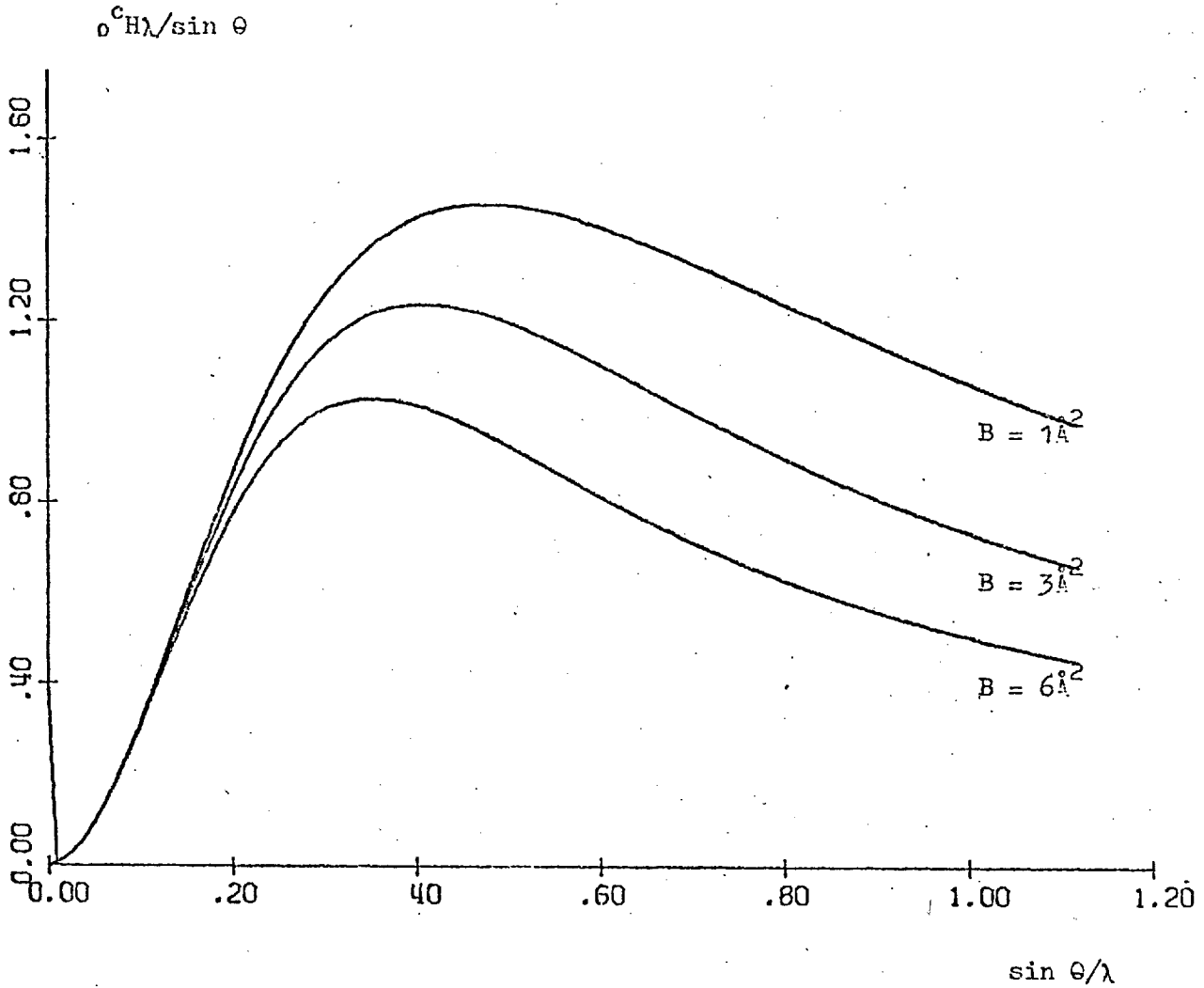
<p style="text-align:center">Fig. 2</p>

Signal-to-noise ratio calculated assuming σ_ρ to be a linear function of $\sin\theta/\lambda$ i.e. $\sigma_\rho = C \sin\theta/\lambda$

Table 6

ρ^c_H	$\sin\theta/\lambda$	Number of terms	IrH(CO)$_2$(PPh$_3$)$_2$						RuClH(PPh$_3$)$_3$,C$_6$H$_6$			RhH(CO)(PPh$_3$)$_3$		
			Ir-H(Å)	ρ^o_H(e/Å^3)	σ_ρ	ρ^o_H/σ_ρ	ρ^c_H/σ_ρ		σ_ρ	ρ^o_H/σ_ρ	ρ^c_H/σ_ρ	σ_ρ	ρ^o_H/σ_ρ	ρ^c_H/σ_ρ
0.162	0.20								0.025	11.9	6.5	0.025	6.3	6.5
0.254	0.25	230	1.674	0.27	0.028	9.6	9.1		0.029	15.0	8.8	0.033	8.1	7.7
0.342	0.30								0.032	15.1	10.7	0.043	7.9	8.0
0.423	0.35	619	1.673	0.45	0.036	12.5	11.8		0.036	16.8	11.8	0.052	9.9	8.1
0.515	0.417								0.041	16.4	12.6	0.061	8.7	8.5
0.553	0.45	1287	1.639	0.60	0.043	13.9	12.9							
0.643	0.56	2469	1.590	0.73	0.051	14.3	12.6							

DESCRIPTION OF STRUCTURE AND DISCUSSION

Figure 3, obtained using the program ORTEP (Johnson, 1965), shows

the molecular structure of the complex and the thermal vibrations of

the atoms. The more interesting bond lengths and angles are quoted in

Table 7. The coordination about the iridium atom is a distorted one,

but can best be described as trigonal bipyrimidal with one of the phosphorus

atoms P(1) and the hydride hydrogen in axial positions, and the other

phosphorus P(2) and the two carbonyl groups in equatorial positions. The

atoms in the equatorial plane are bent away from the phosphorus towards

the hydrogen atom, such that P(1)-Ir-P(2) is 101.4° and P-Ir-carbonyl

ca. 95°. This distortion can readily be understood in terms of the steric

hinderance of the bulky triphenylphosphine ligands and the small size of

the hydride hydrogen in the opposite positions.

Although the two phosphorus atoms are differently oriented with respect

to the carbonyl groups, with angles P(1)-Ir-carbonyl of ca. 95°,and

P(2)-Ir-carbonyl of ca. 115°, the Ir-P distances are not significantly

different (2.375 and 2.370Å respectively). These distances fall in the

middle of the range of those found in other structures, e.g., 2.38(1)

and 2.36(1)Å found for $IrO_2Cl(CO)(PPh_3)_2$ (La Placa and Ibers, 1965),

2.339(3)Å in $[Ir(NO)_2(PPh_3)_2]ClO_4$, (Mingos and Ibers, 1970) and 2.407

and 2.408Å in $[IrCl(CO)(NO)(PPh_3)_2]BF_4$ (Hodgson et al., 1968).

We believe the two Ir-C distances, which are unexceptional, are

probably the same although they apparently differ by about 5σ. This is

because in the least-squares refinement the atom C(2) is slightly pulled

in towards the metal atom by the presence of a small iridium "ripple"

visible in the final difference Fourier directly on the line Ir-C(2)

and just short of the carbon atom. A more realistic pointer to equivalence

of the two carbonyls is the Ir....O distance which is virtually the same
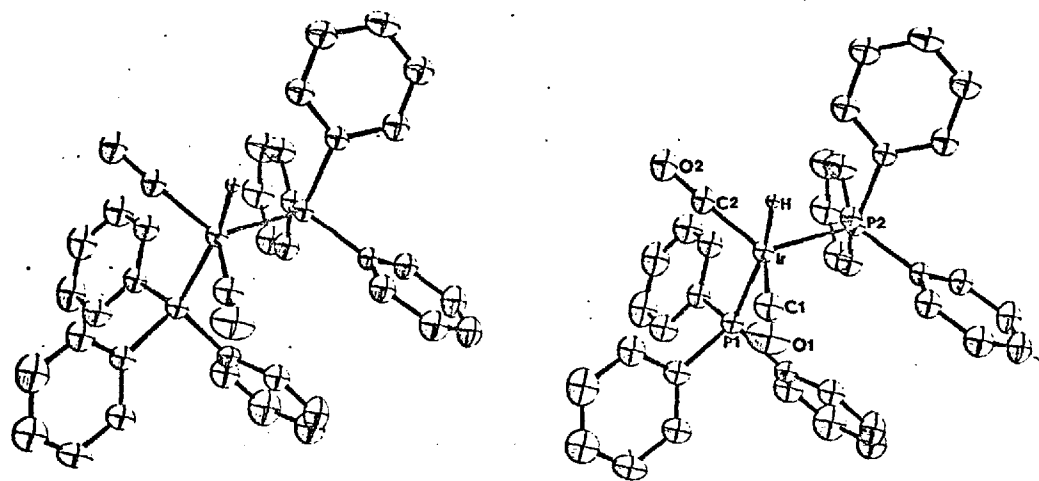
Fig. 3

Molecular structure of the orthorhombic form of $IrH(CO)_2(PPh_3)_2$. A stereoscopic drawing with thermal ellipsoid vibrations scaled to enclose 40% probability.

for both carbonyl groups, 3.023 and 3.029(6)Å.

The position of the hydride hydrogen atom has been located and the Ir-H distance is estimated to be 1.64(5)Å. The nature of the metal-hydrogen bond in transition-metal hydride complexes has been of interest since 1955 when the first compound of this type $(\pi\text{-}(C_5H_5)_2ReH)$ was obtained by Wilkinson and Birmingham (1955). A summary of the existing theories, based among others on the results of the only two structural studies known at that time, viz. $RhH(CO)(PPh_3)_3$ and K_2ReH_9, was given by Ibers (1965). He discussed the alternative concepts of a hydrogen being buried in the metal orbitals or of hydrogen being situated at a normal covalent distance from the metal and thus exerting a profound influence on the stereochemistry. Ibers regarded the latter theory as more probable. Table 8 summarises the recent structural determinations of metal-hydrogen distances. The results support Ibers' conclusion, but it is noteworthy that in every case the observed Me-H distances are longer than the sum of Pauling's covalent radii. (This is true even in the case of the more reliable neutron diffraction studies.)

Table 8

Complex	Method	Bond length	Sum of * Coval-ent radii Me-H	Reference
K_2ReH_9	neutron	1.61-1.72; average 1.68(1)	1.58	Abrahams et al. (1964)
$RhH(CO)(PPh_3)_3$	X-ray	1.60(12)	1.55	La Placa and Ibers (1965)
$RuH(C_{10}H_7)\text{-}(Me_2P.CH_2.CH_2.PMe_2)_2$	X-ray	1.7	1.55	Ibekwe et al. (1969)
$RuHCl(PPh_3)_3$	X-ray	1.68(7)	1.55	Skapski and Troughton(1968)
$\beta\text{-}HMn(CO)_5$	neutron	1.601(16)	1.47	La Placa et al. (1969)
$CoH(N_2)(PPh_3)_3$	X-ray	1.64(11) and 1.67(12)	1.46	Davis et al. (1969)
$IrH(CO)_2(PPh_3)_2$	X-ray	1.64(5)	1.57	this work

* Ref. Pauling (1960)

Figure 4 shows a stereoscopic view of the packing of molecules in the structure while Table 9 lists some of the shorter intermolecular distances.

Table 10 shows that the phenyl rings are satisfactorily planar. The main point of interest here, however, is that the phosphorus atoms are in some cases a considerable distance out of the least-squares plane of the phenyl rings (phosphorus atom not included in plane calculation). While it has seemed likely that due to steric strain some bending can occur at the C(ml) atom it has been difficult to demonstrate this conclusively as in most structure determinations the standard deviations at the phenyl rings tend to be relatively high, and the effect is a small one. Distortions of this type are most likely in structures when the packing of the molecules in the crystal is mainly determined by the phenyl rings of triphenylphosphine (or similar) ligands; one structure where a genuine distortion seems to occur is $RhMeI_2(PPh_3)_2$ (Troughton and Skapski, 1968) where P-C(1)-C(4) angles down to 175.7° ($\sigma = 0.24$) were found. Table 10 shows that in this iridium complex significant bending occurs for five of the six rings. The most striking example is P(2), which is 0.32Å out of the plane of ring C(5n) involving a P(2)-C(51)-C(54) angle of ca. 170°. A priori one would expect that serious distortion at C(ml) is most likely to be caused by steric pressure at C(m4) (or more strictly on the hydrogen atom attached to C(m4)), since pressure on C(m2, 3, 5 or 6) can more conveniently be eased by a twist of the ring about the P-C(ml) axis. It may be significant that the two shortest contacts between phenyl hydrogens, H(54)....H(46) (2.33Å) and H(64)....H(23) (2.31Å), involve the Hm4 hydrogens in the two rings showing the largest distortion.

Pentacoordinate structures are known to be potentially non-rigid in a stereochemical sense (Muetterties and Schunn, 1966; Holmes et al., 1969). The two extremes of geometrical configuration encountered in these structures
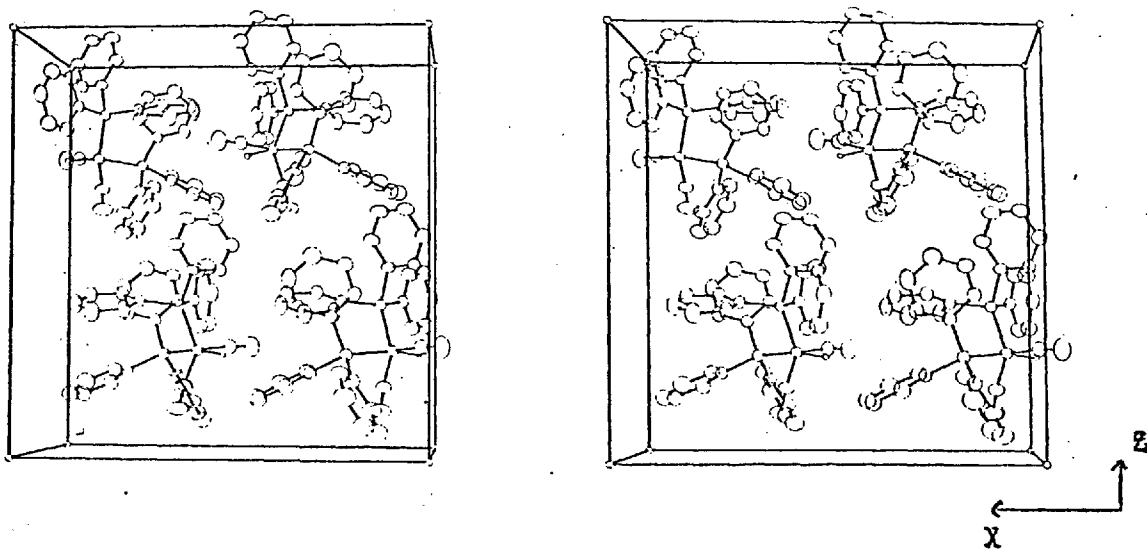
Fig. 4

Crystal structure of the orthorhombic form of $IrH(CO)_2(PPh_3)_2$

can be idealised as a trigonal bipyramid (TBP) and square pyramid (SP), although in real molecules considerable distortion can be expected. In some compounds the difference in energy levels for the two configurations may be small with respect to such factors as lattice energy, and packing forces, or in solution, solvation and association energies. This fact explains the existance of isomers in both the liquid and the solid state. For structures of the type $MLL_2'L_2''$ with three different kinds of ligands there are five possible geometrical isomers for TBP and six for SP.

Two different isomeric forms of $IrH(CO)_2(PPh_3)_2$ have been found by Yagupsky and Wilkinson (1969) to exist in thermal equilibrium in solution and to undergo rapid interchange. They considered the possible configurations for the two isomers and concluded that, although no decision could be made between TBP and SP, one isomer has $\underline{C_s}$ and the other $\underline{C_{2v}}$ symmetry. In our molecular structure of the orthorhombic form the coordination about iridium has approximately $\underline{C_s}$ symmetry if one ignores the phenyl rings, although it is different from those found in solution. This is not particularly surprising in view of the known lability of five-coordinate species.

In a recent paper Wilkinson and his coworkers have discussed the different reactivity of $IrH(CO)_2(PPh_3)_2$ and $IrH(CO)(PPh_3)_3$ towards ethylene and the isomerisation of alk-1-enes. They do so in terms of the relatively easy approach of ethylene towards the metal which can be visualised in this structure, and which is likely to be true of the species existing in solution (Yagupsky et al., 1970).

Table 2

Fractional coordinates, $\underline{x}$, $\underline{y}$, $\underline{z}$, with estimated standard deviations in parentheses.

Atom	$\underline{x}$	$\underline{y}$	$\underline{z}$
Ir	0.08919(1)	0.07000(1)	0.25000
P(1)	0.19156(8)	-0.08196(14)	0.24134(14)
P(2)	0.11982(8)	0.18736(15)	0.35796(8)
O(1)	-0.0319(3)	-0.1418(5)	0.2592(6)
O(2)	0.1218(4)	0.2214(6)	0.1109(3)
C(1)	0.0174(4)	-0.0653(6)	0.2594(7)
C(2)	0.1118(4)	0.1606(7)	0.1662(4)
C(11)	0.2787(4)	-0.0179(7)	0.1996(4)
C(12)	0.2944(4)	0.1168(8)	0.2021(4)
C(13)	0.3614(6)	0.1631(10)	0.1731(5)
C(14)	0.4132(5)	0.0798(10)	0.1424(5)
C(15)	0.3976(5)	-0.0555(11)	0.1399(5)
C(16)	0.3311(5)	-0.1045(8)	0.1679(5)
C(21)	0.2224(4)	-0.1611(6)	0.3257(4)
C(22)	0.2973(4)	-0.1871(8)	0.3437(5)
C(23)	0.3158(5)	-0.2456(11)	0.4097(6)
C(24)	0.2602(5)	-0.2788(10)	0.4588(5)
C(25)	0.1859(5)	-0.2544(9)	0.4411(4)
C(26)	0.1673(4)	-0.1953(7)	0.3769(4)
C(31)	0.1687(4)	-0.2266(7)	0.1834(4)
C(32)	0.1265(5)	-0.2072(8)	0.1210(4)
C(33)	0.1116(6)	-0.3106(11)	0.0735(5)
C(34)	0.1370(6)	-0.4361(9)	0.0897(6)
C(35)	0.1769(6)	-0.4584(8)	0.1520(5)

Table 2 ctd

Atom	x	y	z
C(36)	0.1924(5)	-0.3542(8)	0.2000(4)
C(41)	0.0987(4)	0.1044(6)	0.4445(3)
C(42)	0.1398(4)	0.1211(7)	0.5076(4)
C(43)	0.1192(5)	0.0598(9)	0.5720(4)
C(44)	0.0555(5)	-0.0201(9)	0.5735(4)
C(45)	0.0131(5)	-0.0375(8)	0.5115(5)
C(46)	0.0358(4)	0.0242(7)	0.4478(4)
C(51)	0.2177(3)	0.2396(6)	0.3675(4)
C(52)	0.2417(4)	0.3662(8)	0.3445(3)
C(53)	0.3176(5)	0.3962(9)	0.3392(5)
C(54)	0.3701(4)	0.2999(9)	0.3584(6)
C(55)	0.3490(4)	0.1783(9)	0.3825(6)
C(56)	0.2728(4)	0.1466(8)	0.3867(5)
C(61)	0.0702(3)	0.3487(6)	0.3683(4)
C(62)	0.0566(5)	0.4038(8)	0.4358(4)
C(63)	0.0235(5)	0.5286(8)	0.4414(5)
C(64)	0.0060(4)	0.6010(7)	0.3796(5)
C(65)	0.0193(5)	0.5467(8)	0.3116(5)
C(66)	0.0496(4)	0.4202(7)	0.3064(4)

Carbon atoms are numbered C(mn) where m is the ring no. and n is the atom no. in the ring. n is such that C(m1) is attached to P and other atoms are numbered in succession such that C(m4) is para to C(m1).

Table 3

Anisotropic thermal parameters

Atom	β_{11}	β_{22}	β_{33}	β_{12}	β_{13}	β_{23}
Ir	0.00216(1)	0.00669(2)	0.00176(1)	-0.00016(1)	-0.00019(1)	0.00000(2)
P(1)	0.00238(4)	0.0068(1)	0.0021(7)	-0.0002(6)	0.00008(6)	-0.0003(1)
P(2)	0.00197(5)	0.0065(15)	0.00174(4)	-0.00017(7)	-0.00010(4)	-0.00008(7)
O(1)	0.0039(2)	0.0122(6)	0.0066(3)	-0.0027(3)	0.0000(3)	0.0014(5)
O(2)	0.0074(3)	0.0133(7)	0.0026(2)	-0.0023(4)	0.0004(2)	0.0022(3)
C(1)	0.0027(2)	0.0094(5)	0.0031(4)	0.0007(3)	0.0000(3)	0.0006(4)
C(2)	0.0038(3)	0.0098(8)	0.0020(2)	-0.0007(4)	0.0003(2)	0.0000(4)
C(11)	0.0024(2)	0.0097(8)	0.0023(2)	-0.0009(3)	0.0004(2)	-0.00003(34)
C(12)	0.0035(3)	0.0111(9)	0.0028(2)	-0.0016(4)	0.0003(2)	-0.0002(4)
C(13)	0.0054(4)	0.0155(12)	0.0041(3)	-0.0043(6)	0.0018(3)	0.0003(5)
C(14)	0.0040(3)	0.0203(15)	0.0036(3)	-0.0031(6)	0.0016(3)	-0.0016(6)
C(15)	0.0033(3)	0.0219(15)	0.0037(3)	-0.0006(5)	0.0015(3)	-0.0012(6)
C(16)	0.0036(3)	0.0114(9)	0.0036(3)	-0.0009(4)	0.0010(2)	-0.0012(4)
C(21)	0.0025(2)	0.0063(6)	0.0025(2)	0.0004(3)	-0.0002(2)	0.0001(3)
C(22)	0.0026(3)	0.0128(9)	0.0039(3)	0.0001(4)	-0.0002(2)	0.0013(5)
C(23)	0.0031(3)	0.0202(15)	0.0053(4)	0.0001(6)	-0.0013(3)	0.0036(7)
C(24)	0.0048(4)	0.0155(12)	0.0039(3)	-0.0002(5)	-0.0010(3)	0.0030(5)
C(25)	0.0037(3)	0.0172(12)	0.0025(2)	-0.0010(5)	0.0002(2)	0.0021(5)
C(26)	0.0026(2)	0.0093(8)	0.0029(2)	-0.0004(4)	-0.0002(2)	0.0005(4)
C(31)	0.0027(2)	0.0077(7)	0.0028(2)	-0.0004(3)	0.0004(2)	-0.0013(3)
C(32)	0.0051(4)	0.0114(9)	0.0028(3)	-0.0004(5)	-0.0004(3)	-0.0016(4)
C(33)	0.0061(4)	0.0180(14)	0.0037(3)	0.0010(7)	-0.0011(3)	-0.0030(6)
C(34)	0.0056(4)	0.0139(12)	0.0042(6)	-0.0005(6)	0.0000(3)	-0.0033(5)
C(35)	0.0064(4)	0.0074(8)	0.0046(4)	-0.0007(5)	0.0004(3)	-0.0013(5)
C(36)	0.0045(3)	0.0083(8)	0.0034(3)	-0.0007(4)	-0.0005(3)	-0.0012(4)

Table 3 ctd

Atom	β_{11}	β_{22}	β_{33}	β_{12}	β_{13}	β_{23}
C(41)	0.0028(2)	0.0070(7)	0.0017(2)	0.0001(3)	0.0002(2)	0.0001(3)
C(42)	0.0039(3)	0.0096(8)	0.0023(2)	-0.0010(4)	-0.00008(21)	0.0001(4)
C(43)	0.0050(4)	0.0149(11)	0.0023(2)	0.0007(5)	-0.0006(2)	0.0008(4)
C(44)	0.0045(3)	0.0129(9)	0.0022(2)	0.0014(5)	0.0008(2)	0.0012(4)
C(45)	0.0036(3)	0.0119(11)	0.0032(3)	-0.0009(5)	0.0007(2)	0.0008(4)
C(46)	0.0023(2)	0.0103(8)	0.0027(2)	0.0002(4)	0.0002(2)	0.0003(4)
C(51)	0.0021(2)	0.0080(7)	0.0022(2)	0.0001(3)	0.0001(2)	-0.0004(3)
C(52)	0.0023(2)	0.0099(8)	0.0048(3)	-0.0010(4)	0.0001(2)	0.0000(5)
C(53)	0.0037(3)	0.0143(11)	0.0060(4)	-0.0025(5)	0.0004(3)	0.0002(6)
C(54)	0.0024(3)	0.0163(12)	0.0056(4)	-0.0016(5)	0.0000(3)	-0.0021(6)
C(55)	0.0027(3)	0.0143(11)	0.0039(3)	0.0003(4)	-0.0007(2)	-0.0018(5)
C(56)	0.0024(2)	0.0119(9)	0.0030(2)	0.0005(4)	-0.0006(2)	-0.0017(4)
C(61)	0.0019(2)	0.0069(6)	0.0024(2)	0.0000(3)	0.0000(2)	-0.0005(3)
C(62)	0.0038(3)	0.0099(8)	0.0028(2)	0.0003(4)	0.0004(2)	-0.0004(4)
C(63)	0.0046(3)	0.0104(9)	0.0038(3)	0.0013(5)	0.0008(3)	-0.0020(4)
C(64)	0.0029(3)	0.0074(7)	0.0049(3)	0.0004(4)	0.0002(2)	-0.0009(4)
C(65)	0.0043(3)	0.0097(9)	0.0037(3)	0.0013(4)	-0.0008(3)	0.0003(4)
C(66)	0.0034(3)	0.0089(8)	0.0031(2)	0.0005(4)	-0.0004(2)	0.0002(4)

Table 4

Fractional coordinates of the hydrogen atoms

Atom	x	y	z
H(1)	0.019	0.176	0.248
H(12)	0.251	0.172	0.230
H(13)	0.373	0.245	0.182
H(14)	0.459	0.118	0.127
H(15)	0.438	-0.113	0.123
H(16)	0.323	-0.187	0.175
H(22)	0.341	-0.181	0.294
H(23)	0.358	-0.256	0.433
H(24)	0.275	-0.324	0.499
H(25)	0.151	-0.257	0.474
H(26)	0.115	-0.152	0.365
H(32)	0.131	-0.124	0.107
H(33)	0.080	-0.289	0.027
H(34)	0.136	-0.536	0.061
H(35)	0.172	-0.533	0.180
H(36)	0.218	-0.367	0.245
H(42)	0.175	0.167	0.500
H(43)	0.152	0.081	0.615
H(44)	0.034	-0.057	0.618
H(45)	-0.038	-0.089	0.515
H(46)	0.001	0.013	0.411
H(52)	0.204	0.436	0.327
H(53)	0.339	0.493	0.321
H(54)	0.430	0.319	0.357
H(55)	0.382	0.115	0.410
H(56)	0.248	0.052	0.411
H(62)	0.075	0.352	0.474
H(63)	0.009	0.566	0.491
H(64)	-0.026	0.695	0.386
H(65)	0.010	0.593	0.248
H(66)	0.058	0.376	0.252

For phenyl hydrogens the numbers correspond to those of the carbon atoms to which they are bonded.

Table 5

Final observed and calculated

structure factors

The format of the table is

h	k	l
1	$10|F_o|$	$10|F_c|$

* Reflections of intensities not significantly greater than the background ("less-thans") are marked:*

Table 7

Selected bond lengths (Å) and angles (°) with standard deviations in parentheses.

Ir - P(1)	2.375(2)	C(1) - O(1)	1.163(8)
Ir - P(2)	2.370(2)	C(2) - O(2)	1.199(9)
Ir - C(1)	1.867(6)	Ir....O(1)	3.023(5)
Ir - C(2)	1.833(7)	Ir....O(2)	3.029(6)

Ir - H(1)   1.64

P(1) - C(11)	1.843(7)	P(2) - C(41)	1.833(7)
P(1) - C(21)	1.826(7)	P(2) - C(51)	1.824(6)
P(1) - C(31)	1.842(7)	P(2) - C(61)	1.848(6)

mean C-C

ring C(1n)	1.380(12)	ring C(4n)	1.382(10)
C(2n)	1.383(10)	C(5n)	1.384(10)
C(3n)	1.378(12)	C(6n)	1.384(10)

P(1) - Ir - P(2)	101.38(7)	P(2) - Ir - C(1)	116.0(4)
P(1) - Ir - C(1)	93.8(2)	P(2) - Ir - C(2)	114.2(2)
P(1) - Ir - C(2)	95.3(2)	C(1) - Ir - C(2)	125.9(4)

P(1) - Ir - H(1)   175

Ir - P(1) - C(11)	116.7(2)	C(11) - P(1) - C(21)	104.7(3)
Ir - P(1) - C(21)	116.7(2)	C(11) - P(1) - C(31)	102.4(3)
Ir - P(1) - C(31)	112.0(2)	C(21) - P(1) - C(31)	102.5(3)
Ir - P(2) - C(41)	117.1(2)	C(41) - P(2) - C(51)	104.0(3)
Ir - P(2) - C(51)	116.2(2)	C(41) - P(2) - C(61)	102.1(3)
Ir - P(2) - C(61)	114.1(2)	C(51) - P(2) - C(61)	101.2(3)

Table 9

Some selected non-bonded distances

$C(64) - C(23)^I$	3.715		$H(64) - H(23)^I$	2.31
$C(54) - C(46)^{II}$	3.802		$H(54) - H(46)^{II}$	2.33
$C(55) - C(33)^{III}$	3.582		$H(55) - H(33)^{III}$	2.46
$C(52) - C(36)^{IV}$	3.956		$H(52) - H(36)^{IV}$	2.49
$C(65) - C(15)^I$	3.827		$H(65) - H(15)^I$	2.51
$C(43) - C(16)^{III}$	3.894		$H(43) - H(16)^{III}$	2.57
$C(63) - C(14)^{III}$	3.897		$H(63) - H(14)^{III}$	2.61
$C(26) - C(64)^V$	3.516		$H(26) - H(64)^V$	2.97
$C(63) - C(25)^{IV}$	3.609		$H(63) - H(25)^{IV}$	3.09

$H(1) - H(66)$ 2.12 (intramolecular)

Superscripts refer to atoms in the following positions:

I $x - \frac{1}{2}, \frac{1}{2} - y, z$ II $\frac{1}{2} + x, \frac{1}{2} - y, z$ III $\frac{1}{2} - x, \frac{1}{2} + y, \frac{1}{2} + z$

IV $x, 1 + y, z$ V $x, y - 1, z$

Table 10

Planarity of Phenyl rings

Ring	Mean deviation (Å)	Maximum deviation (Å)	Distance of phosphorus atom from least-squares plane
$C(1n)$	0.002	0.003	0.078(2)
$C(2n)$	0.004	0.009	0.024(6)
$C(3n)$	0.007	0.020	0.101(12)
$C(4n)$	0.003	0.006	0.076(4)
$C(5n)$	0.007	0.011	0.319(8)
$C(6n)$	0.012	0.019	0.151(14)

97

References

1. S.C. Abrahams, A.P. Ginsberg, and K. Knox, Inorg. Chem., 3 558, (1964).

2. S. Åsbrink and P.E. Werner, Acta Cryst., 20, 407, (1966).

3. W.R. Busing and H.A. Levy, Acta Cryst., 10, 180, (1957).

4. M. Ciechanowicz, A.C. Skapski, and P.G.H. Troughton, Acta Cryst., A25, s 172, (1969).

5. P. Coppens, L. Leiserowitz, and D. Rabinovich, Acta Cryst., 18, 1035, (1965).

6. D.T. Cromer and J.T. Waber, Acta Cryst., 18, 104, (1965).

7. D.T. Cromer, Acta Cryst., 18, 17, (1965).

8. D.W.J. Cruickshank, Acta Cryst., 3, 72, (1950).

9. B.R. Davis, C. Payne, and J.A. Ibers, Inorg. Chem., 8, 2719, (1969)

10. D. Evans, J.A. Osborn, and G. Wilkinson, J. Chem. Soc. (A), 3133, (1968).

11. D.J. Hodgson, N.C. Payne, J.A. McGinnety, R.G. Pearson, and J.A. Ibers, J. Amer. Chem. Soc., 90, 4486, (1968).

12. R.R. Holmes, R.M. Deiters, and J.A. Golen, Inorg. Chem., 8, 2612, (1969).

13. H. Hope, U. de la Camp, and W.E. Thiessen, Acta Cryst., A25, s 78, (1969).

14. E.W. Hughes, J. Amer. Chem. Soc., 63, 1737, (1941).

15. S.D. Ibekwe, B.T. Kilbourn, U.A. Raeburn, and D.R. Russell, Chem. Comm., 433 (1969).

16. J.A. Ibers and D.T. Cromer, Acta Cryst., 11, 794, (1958).

17. J.A. Ibers, Ann. Rev. Phys. Chem., 16, 375, (1965).

18. C.K. Johnson, ORTEP thermal ellipsoid plotting program, Oak Ridge National Laboratory Report, 1965, ORNL-3794.

19. S.J. La Placa and J.A. Ibers, Acta Cryst., 18, 511, (1965a).

20. S.J. La Placa and J.A. Ibers, J. Amer. Chem. Soc., 87, 2581, (1965).

21. S.J. La Placa, W.C. Hamilton, J.A. Ibers and A. Davison, Inorg. Chem., 8, 1928, (1969).

22. D.M.P. Mingos and J.A. Ibers, Inorg. Chem., 9, 1105, (1970).

23. E.L. Muetterties and R.A. Schunn, Quart. Rev., 20, 245, (1966).

24. L. Pauling, "The Nature of the Chemical Bond", Third Edition, Cornell University Press, Ithaca, 1960, p.256.

25. A.C. Skapski and P.G.H. Troughton, Chem. Comm., 1230, (1968); J. Chem. Soc. (A), in the press.

26. A.C. Skapski and P.G.H. Troughton, Acta Cryst., B26, 716 (1970).

27. P.G.H. Troughton and A.C. Skapksi, Chem. Comm., 575 (1968); A.C. Skapski and P.G.H. Troughton, J. Chem. Soc. (A), in the press.

28. G. Wilkinson and J.M. Birmingham, J. Amer. Chem. Soc., 77, 3421, (1955).

29. G. Yagupsky and G. Wilkinson, J. Chem. Soc. (A), 725, (1969).

30. G. Yagupsky, C.K. Brown and G. Wilkinson, J. Chem. Soc. (A), 1392,(1970).

31. W.H. Zachariasen, Acta Cryst., 16, 1139, (1963).

CHAPTER II

The Crystal Structure of

the Monoclinic(I) Form of

Hydridodicarbonylbis(triphenylphosphine)iridium(I)

$$IrH(CO)_2(PPh_3)_2$$
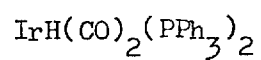
ABSTRACT

The crystal and molecular structure of the monoclinic(I) form of
hydridodicarbonylbis(triphenylphosphine)iridium(I) has been determined
from three-dimensional X-ray diffractometer data. The compound crystallises
in space group $P2_1/a$ with four molecules in a unit cell of dimensions
$a = 18.036$, $b = 10.075$, $c = 19.474Å$, $\beta = 113.365°$. The structure was
refined by least-squares methods using 3248 measured independent reflections
to give $R = 0.028$.

Of the five iridium ligands two are triphenylphosphine groups in
a cis configuration, with a P(1) - Ir - P(2) angle of $102.17°$ and Ir - P
distances of 2.357 and $2.359Å$. Two other ligands - the carbonyl groups,
are disordered and under these circumstances location of the hydride
hydrogen atom has proved impossible. It appears from the arrangement
of the disordered carbonyl groups that two different molecular forms
coexist in the crystal in ratio ca. 2:1.

INTRODUCTION

The significance of the hydridodicarbonylbis(triphenylphosphine)
iridium(I) complex, as an analogue of a rhodium complex, was mentioned
in a previous chapter. The main crystallographic details of the
three polymorphic forms of the iridium complex, all obtained in one
batch of crystals were also given in this chapter.

The co-crystallization of three polymorphs suggests minimal free
energy differences between them, and this is in general agreement with
the conclusion of Yagupsky and Wilkinson (1969) that there are different
conformers coexisting in solution. It was thought interesting to
determine the molecular structure for each of the three polymorphic
forms in a solid state, and the present work is concerned with the
first of the two monoclinic forms, refered to as monoclinic(I).

EXPERIMENTAL

The monoclinic(I) form of hydridodicarbonylbis(triphenylphosphine) iridium(I) was obtained by the reaction in solution of $IrCl(CO)(PPh_3)_2$ with $NaBH_4$ in the presence of carbon monoxide. Crystals were kindly provided by Professor G. Wilkinson and Dr. G. Yagupsky. Preliminary oscillation and Weissenberg photographs showed the crystals to be monoclinic with systematic absences given by $0k0:k = 2n + 1$ and $h0l:h = 2n +1$. These absences are consistent with the space group $P2_1/a$ (No. 14).

Intensity data were collected for a crystal of a platelike shape of approximate dimensions 0.3 x 0.3 x 0.1 mm, mounted about the b axis on a Siemens off-line automatic four-circle diffractometer. Cu-Kα radiation at a take-off angle of 4.5°, a Niβ filter and a Na(Tl)I scintillation counter were used. The $\Theta - 2\Theta$ scan technique was employed using a "five-value" measuring procedure (Skapski and Troughton, 1970). 3248 independent reflections (to $\Theta = 50^\circ$) were measured, of which 235 were judged insignificant as the net count was below 2.58 times the standard deviation (i.e. below the 99% confidence limit) and were assigned a count equal to this value. The 8 0 0 reflection was used as a reference every 25 reflections and there were no appreciable changes in the counts for this reflection over the data collection period (5 days). The data were scaled using the reference reflection and Lorentz and polarisation corrections were applied.

The unit-cell dimensions and their estimated probable errors, measured on the Siemens diffractometer at $20^\circ C$ are: $a = 18.036(5)$, $b = 10.075(2)$, $c = 19.474(5)$, $\beta = 113.365(10)$; D_m (by flotation) $= 1.60$ gcm^{-3}, $D_c = 1.582$ gcm^{-3} for $Z = 4$; M.W. $= 773.8$ for $IrP_2C_{38}H_{31}O_2$, $F(000) = 1528$.

SOLUTION AND REFINEMENT OF THE STRUCTURE

The solution and refinement of the structure were carried out using the Crystal Structure Calculations System X-Ray-63 described by J.M. Stewart in the University of Maryland Technical Report TR-64-6. The calculations were carried out on the Imperial College IBM 7094 computer.

A three dimensional Patterson gave a straightforward solution for the iridium atoms which are in a set of general positions. Refinement of this position gave a value for the standard agreement factor R (= $\Sigma |\,|F_o|$ $-|F_c|\,|/|F_o|$) of 0.33. The two phosphorus atoms were located from the resultant difference Fourier. Further refinement including these positions reduced R to 0.26, and the next difference Fourier revealed the positions of all six phenyl rings and one carbonyl group. Refinement of all these atoms brought R to 0.152 and the next difference Fourier showed what could be a second carbonyl group. Location of the carbonyl groups, and especially the second one, was difficult due to the "smeared out" appearance of the peaks and much lower height than one would expect for these groups. Refinement of all the located atoms, treating the iridium and both phosphorus atoms anisotropically, gave R = 0.129.

The hydrogen-atom positions in the phenyl rings were calculated using the carbon positions and assuming a C-H distance of 1.08Å; all hydrogen atoms were assigned an isotropic temperature factor of 3.0Å^2. Two more cycles of anisotropic refinement of all atoms using a fixed hydrogen contribution gave R = 0.112.

At this stage an absorption correction was made (μ = 90.31 cm^{-1}) using a program which combines the Gaussian integration method, described by Busing and Levy (1957) with the crystal path lengths determined by the vector analysis procedure of Coppens et al. (1965). In this particular case the crystal volume was sampled at 8 x 8 x 8 points. The next four

cycles of anisotropic refinement with fixed hydrogens for all phenyl rings reduced $\underline{R}$ to 0.068.

To define the new, better, positions of the carbonyl groups a difference Fourier was calculated (Figure 1). This showed that both carbonyl groups are disordered, and the two alternative positions for the carbonyl group (2 and 2*) with greater separation of atoms were found. In the subsequent refinement they were assigned occupancies of 0.6 and 0.4 respectively. The separation of the alternative positions of the other carbonyl group (1 and 1*) is much smaller and the identification of these positions was done in two stages: first the oxygen was split on the basis of the difference Fourier, calculated at $\underline{R}$ = 0.052 while the disorder of the corresponding carbon atom (C1) was not defined until after the dispersion correction had been applied. Further attempts to refine the disordered atoms as two separate carbonyl groups led to an estimated occupancy ratio of 0.63 to 0.37, and were eventually successful in giving two distinct orientations of each of the carbonyl groups.

At this stage two reflections, strongly affected by extinction, were removed, and a dispersion correction for the Ir and P atoms was applied.

These adjustments brought the $\underline{R}$ factor from 0.040 to 0.032. New positions of the hydrogens in the phenyl rings were then generated and were used with an assigned B of $3.0\text{\AA}^2$ as fixed atom contributions.

Up to this point unit weights were given to the reflections in the refinement because of the approximately constant counting statistics arising from the method of measurement of the data. Inspection of the $\Delta\underline{F}$'s suggested that secondary extinction was present. However, in view of the inadequacy of the atomic model arising from disorder it was felt that the labour involved in applying a correction was not justified. In these circumstances only a weighting scheme of the type suggested by Hughes (1941), which would partly compensate for lack of this correction, was used, with
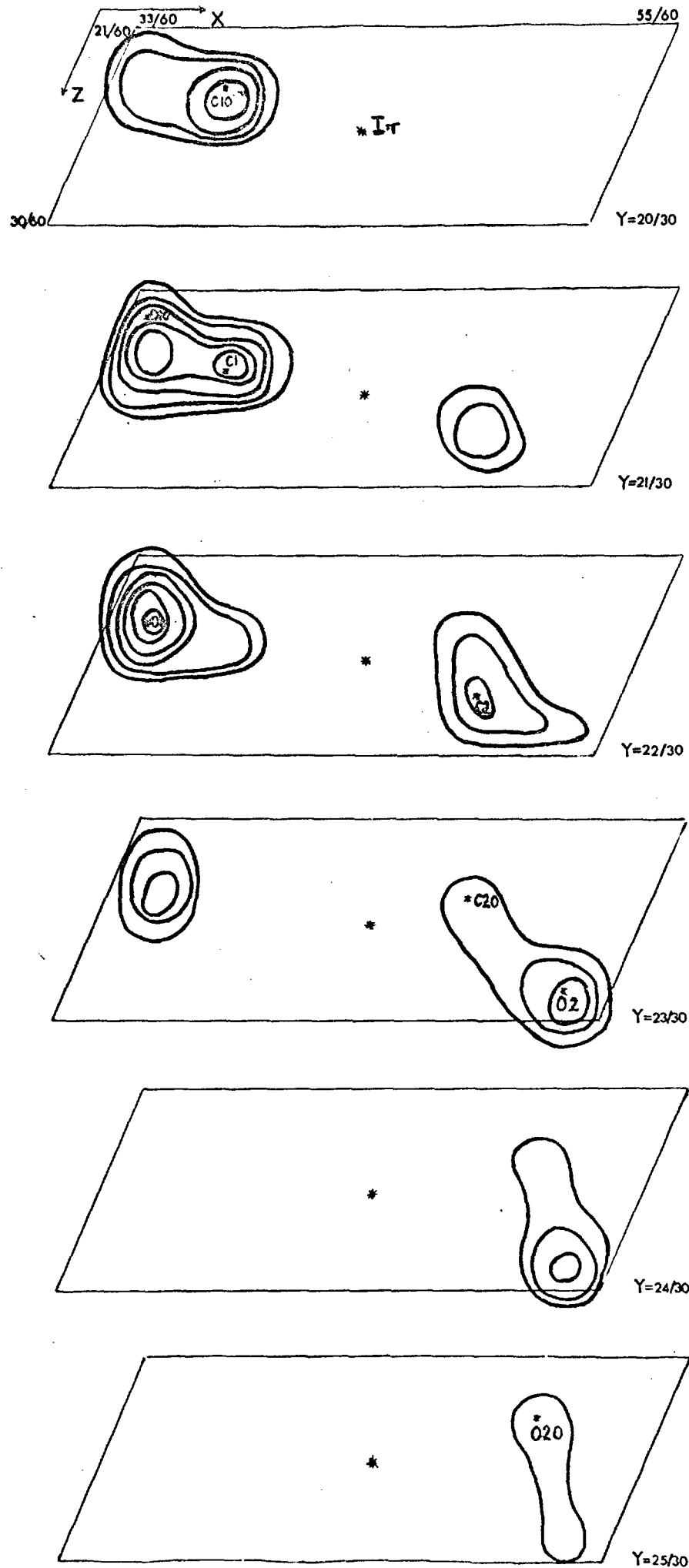
Fig. 1. Electron density difference maps. Contours at intervals of $0.5e/Å^3$ (lowest contour at $0.8e/Å^3$)

$\sqrt{w} = 1$ if $\underline{F}_o \leqslant \underline{F}^*$ and $\sqrt{w} = \underline{F}^*/\underline{F}_o$ if $\underline{F}_o > \underline{F}^*$, and $\underline{F}^* = 100$. This reduced $\underline{R}$ from 0.028 to 0.027.

Bond-length calculations showed that some Ir-C distances were on the short side (especially for $C(1^*)$), whereas the Ir....O distances were more normal. This suggested that in the least-squares refinement the carbon atoms were being "pulled in" towards the iridium. The carbon atoms were therefore relocated at the geometrically calculated positions, and their coordinates were kept fixed during the last few cycles of refinement which brought the $\underline{R}$ value to 0.028. The final average ratio of shift to standard deviation was 0.05 and the maximum ratio was 0.30.

In the refinement, the usual least-squares function, $\Sigma\underline{w}(\underline{F}_o - \underline{F}_c)^2$, was minimised. The atomic scattering factors used were those tabulated by Cromer and Waber (1965) and the values for the real (f') and imaginary (f") parts of the dispersion correction were those given by Cromer (1965). The anomalous dispersion was treated as follows: the new values of the atomic scattering factors were calculated as a resultant $f_{corr} = [(f + f')^2 + (f")^2]^{\frac{1}{2}}$ and used from then on in place of values not corrected for dispersion. The unobserved reflections were included throughout the refinement of the structure but are omitted from all estimates of the agreement factor $\underline{R}$.

A final difference Fourier showed a maximum electron-density peak of $0.8e/\text{Å}^3$ and nine other peaks of an electron-density range $0.3e/\text{Å}^3 - 0.5e/\text{Å}^3$. All those peaks were in the vicinity of an iridium atom and the Ir-peak distances were calculated for each of them. Only three occurred at the expected Ir-hydrogen distance of about 1.7Å, and of those only one was in a geometrically sensible position.

Table 1 lists the final coordinates of the non-hydrogen atoms and Table 2 the coefficients for the anisotropic temperature factors $\exp[-(\beta_{11}\underline{h}^2 + \beta_{22}\underline{k}^2 + \beta_{33}\underline{l}^2 + 2\beta_{12}\underline{hk} + 2\beta_{13}\underline{hl} + 2\beta_{23}\underline{kl})]$. In these tables the standard deviations have been estimated from block-diagonal matrix refinement and are, therefore, a slight underestimate of the true deviations.

The coordinates of the hydrogen atoms are given in Table 3. Table 4
lists the observed structure amplitudes and the calculated structure
factors.

DESCRIPTION OF STRUCTURE AND DISCUSSION

A steroscopic drawing (Johnson 1965) of an asymmetric unit of the
$IrH(CO)_2(PPh_3)_2$ structure found in monoclinic(I) form is shown in
Figure 2. It can be seen that the carbonyl groups are disordered,
whereas the triphenylphosphine groups are not. The position(s) of the
hydride ligand were not found. The disordered carbonyls do not occupy
the alternative positions with equal probability, but are present in
a ratio of ca. 2:1. The major form is marked as (CO) and the minor
form as (CO*). While it is fairly unusual to find such unequal occupancy,
it has been encountered in other structures, for instance in $Pt_2S(CO)(PPh_3)_3$
(Skapski and Troughton, 1969) or $RuH(naphthyl)(dmpe)_2$ (Gregory et al.,
1971).

The triphenylphosphine groups are in a cis configuration with a
P(1)-Ir-P(2) angle of $102.17(5)^{\circ}$, very similar to that found in the
orthorhombic form (101.4°). The two Ir-P distances are identical to
within one standard deviation, 2.357(2) and 2.359(2). These are shorter
than those found in the orthorhombic form by ca. 0.015Å, possibly a
significant difference. Comparison with Ir-P distances found in other
structures was made in the previous chapter.

The existence of disorder among the carbonyl groups, with unequal
occupancy, suggests a number of possibilities. Firstly, one could
envisage that only one molecular form, which may or may not be the same
as that in the orthorhombic form (Form A), fits into the packing scheme
in two orientations, such that P(1) takes the place of P(2) and vice
versa (see below)
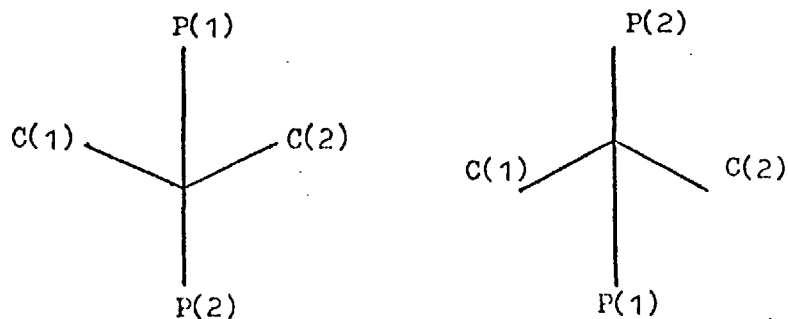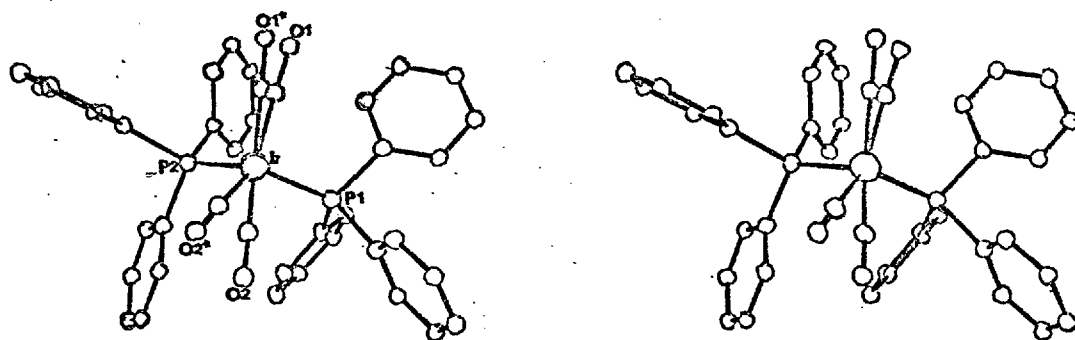
Fig. 2

Molecular structure of the monoclinic(I) form of $IrH(CO)_2(PPh_3)_2$, showing disorder of the two carbonyl groups.

This would be possible if one assumed that during crystal growth the phenyl rings rotate to find the best fit onto the crystal surface. A second possibility is that two forms, one of which is form A, coexist in the crystal.
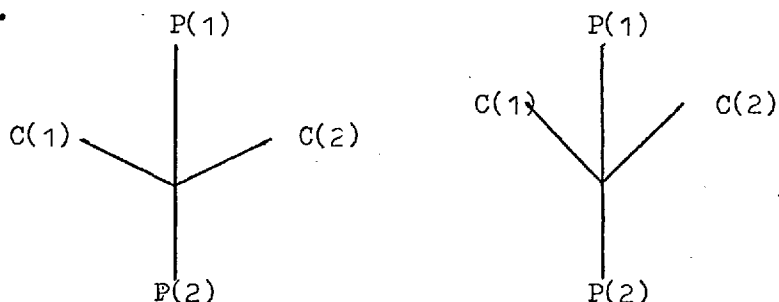
Thirdly the two forms present could be different from each other and from form A, and finally there might be the possibility of dynamic disorder. This last is rather unlikely in view of the fairly large separation between CO(1) and CO(1)*.

Figures 3(a) and 3(b) show separately the molecular structures of the major and minor forms. The thermal vibrations of the atoms are shown, and the orientation of the ellipsoids of the carbon atoms of the disordered carbonyl groups confirms what was observed during least-squares refinement, namely that these atoms were being "pulled" in towards the iridium atom.

Selected bond lengths and angles relevent to both the major and the minor form are given in Table 5. In a separate table (6), a comparison is made of the spatial arrangement of ligands in these two forms with that in form A. While the presence of disorder has led to somewhat limited accuracy as regards the carbonyl groups, it would appear that all three forms are different from each other.

While the configuration of form A could be described with some confidence as a distorted trigonal bipyramid(TBP), a description of the major and the minor forms in terms of TBP or SP is much more difficult.
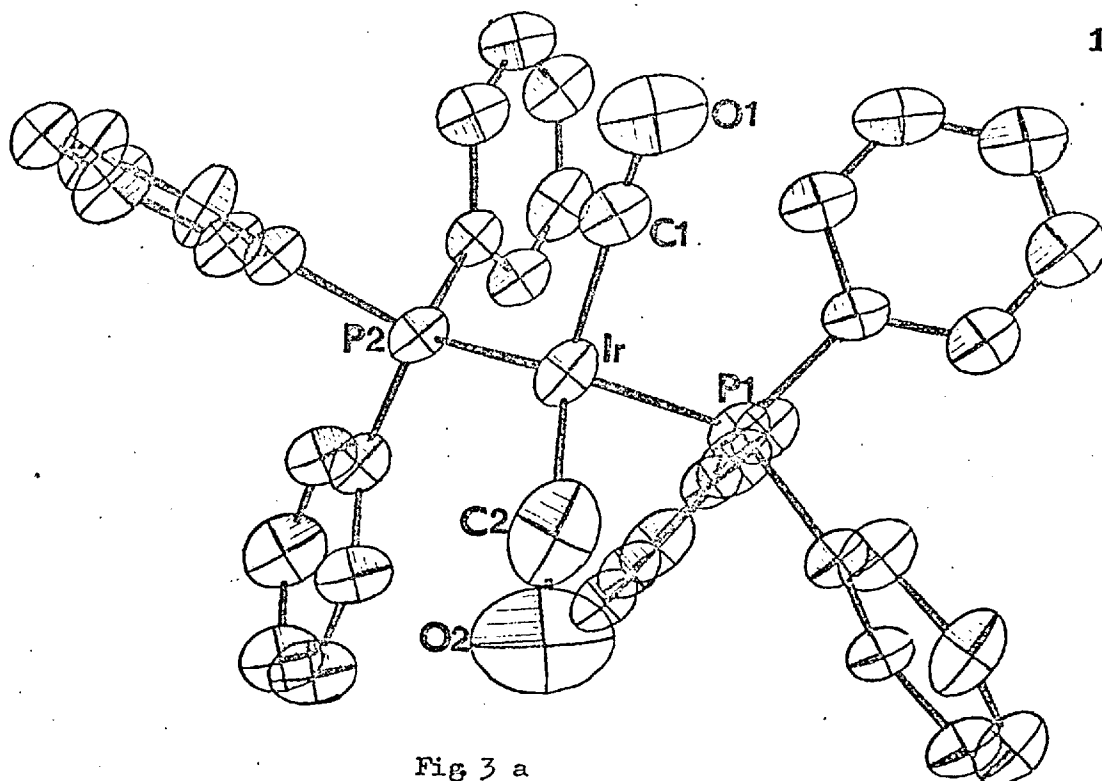
Fig 3 a

Molecular structure of the major form in monoclinic(I) $IrH(CO)_2(PPh_3)_2$
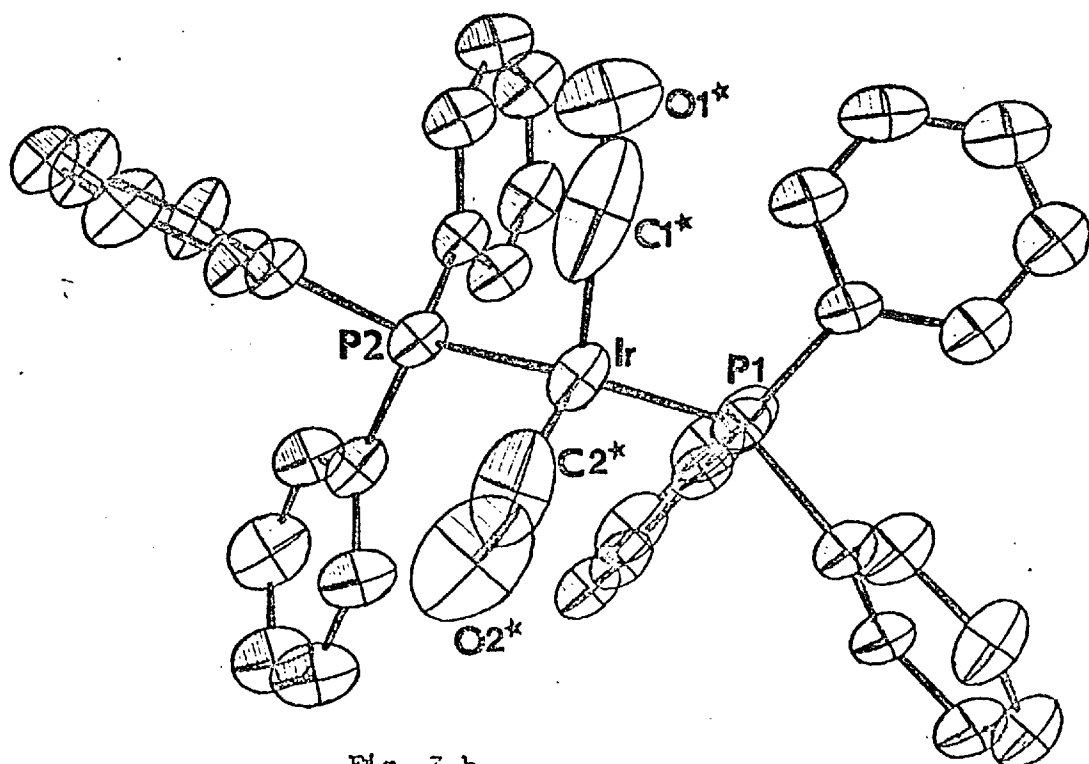
Fig. 3 b

Molecular structure of the minor form in monoclinic(I) $IrH(CO)_2(PPh_3)_2$.
Thermal ellipsoid vibrations were scaled to enclose 40% probability.

This is because of the five ligands one, the hydride hydrogen, was not located, and two others are known with limited accuracy. The major form is probably closer to SP, with P(2) at the apex and four atoms of the base bent away from it at average angles of $107°$. The minor form is, if anything, nearer TBP, with arrangement of ligands similar to that in form A.

While discussing the configuration of ligands around the iridium atom in the orthorhombic form of the complex the conclusion was reached that it is different from those suggested by Yagupsky and Wilkinson (1969) for the two isomers existing in thermal equilibrium in solution. It seems likely that the two forms in the monoclinic(I) polymorph are also different from those in solution.

Calculations were carried out to check the planarity of the phenyl rings and the results are summarised in Table 7. All the rings are satisfactorily planar. In this structure also some bending is found to occur at the C($\underline{m}$1) atoms; thus P(1) (not included in the plane calculation) is 0.143Å away from the plane of ring C(2$\underline{n}$) and 0.147Å from plane of ring C(3$\underline{n}$). This corresponds to P(1)-C($\underline{m}$1)-C($\underline{m}$4) angles of ca. $175°$. The bending is almost certainly due to steric pressure. As in the orthorhombic form, the shortest intermolecular contact between phenyl hydrogen atoms involves H$\underline{m}$4 hydrogen (H(34); and indeed, all four shortest contacts are between hydrogens of rings C(2$\underline{n}$) and C(3$\underline{n}$), as shown in Table 8.

The P-C($\underline{m}$1) distances are very similar to those found in the orthorhombic form (1.838 and 1.836Å respectively). The same applies to the C-C distances in the phenyl rings, which would lengthen a little if a libration correction were applied.

Figure 4 shows a stereoscopic view of the packing of molecules in the unit cell. It may be noted that monoclinic(I) has the smallest
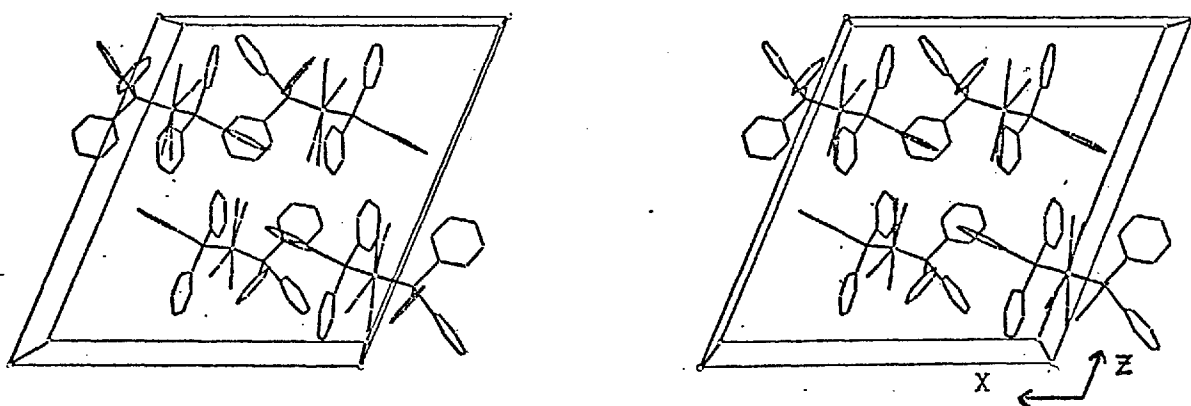
Fig. 4

Crystal structure of the monoclinic(I) form of $IrH(CO)_2(PPh_3)_2$.

unit-cell volume of the three polymorphs of $IrH(CO)_2(PPh_3)_2$ as shown

in Table 1 of the previous chapter. It may be that slightly more

efficient packing is a consequence of the disorder present. Hopefully,

the structure of monoclinic(II), which has yet to be determined and

which has the highest unit-cell volume, will be free of such disorder.

Table 1

Fractional coordinates, x, y, z, with estimated standard deviations in parentheses.

Atom	x	y	z
Ir	0.42979(2)	0.64219(3)	0.73383(2)
P(1)	0.55377(9)	0.52821(15)	0.77153(8)
P(2)	0.33731(9)	0.46734(15)	0.71731(8)
O(1)	0.4094(6)	0.7313(10)	0.5808(5)
O(2)	0.4774(9)	0.7840(12)	0.8832(7)
O(1*)	0.3723(10)	0.6957(15)	0.5651(8)
O(2*)	0.3933(13)	0.8345(20)	0.8270(13)
C(1)	0.417	0.698	0.637
C(2)	0.460	0.732	0.828
C(1*)	0.394	0.676	0.628
C(2*)	0.407	0.763	0.793
C(11)	0.5941(4)	0.5017(6)	0.6992(3)
C(12)	0.5444(4)	0.4517(7)	0.6302(4)
C(13)	0.5727(5)	0.4232(7)	0.5768(4)
C(14)	0.6532(5)	0.4480(7)	0.5905(4)
C(15)	0.7029(4)	0.4996(7)	0.6571(4)
C(16)	0.6749(4)	0.5253(6)	0.7135(4)
C(21)	0.5628(3)	0.3595(6)	0.8106(3)
C(22)	0.5900(4)	0.2524(6)	0.7821(4)
C(23)	0.5892(5)	0.1270(7)	0.8091(4)
C(24)	0.5633(4)	0.1057(7)	0.8655(4)
C(25)	0.5378(4)	0.2115(8)	0.8965(4)
C(26)	0.5373(4)	0.3400(6)	0.8684(4)
C(31)	0.6380(3)	0.6161(6)	0.8435(3)
C(32)	0.6474(4)	0.7484(6)	0.8338(4)
C(33)	0.7146(4)	0.8177(7)	0.8843(4)
C(34)	0.7708(4)	0.7538(7)	0.9435(4)
C(35)	0.7606(4)	0.6207(7)	0.9546(4)
C(36)	0.6947(4)	0.5526(6)	0.9047(3)
C(41)	0.3470(3)	0.3339(6)	0.6577(3)
C(42)	0.3117(4)	0.3547(7)	0.5797(4)
C(43)	0.3201(5)	0.2611(8)	0.5308(4)
C(44)	0.3618(4)	0.1463(7)	0.5587(4)
C(45)	0.3973(4)	0.1265(7)	0.6361(4)
C(46)	0.3899(4)	0.2190(6)	0.6842(3)
C(51)	0.2294(3)	0.5078(6)	0.6703(3)
C(52)	0.1728(4)	0.4067(7)	0.6420(4)
C(53)	0.0905(4)	0.4361(7)	0.6092(4)
C(54)	0.0638(4)	0.5644(7)	0.6018(4)
C(55)	0.1200(4)	0.6612(6)	0.6291(4)
C(56)	0.2013(4)	0.6353(6)	0.6628(4)
C(61)	0.3390(4)	0.3841(6)	0.8021(3)
C(62)	0.3636(4)	0.4566(7)	0.8677(4)
C(63)	0.3666(5)	0.3963(8)	0.9330(4)
C(64)	0.3459(5)	0.2672(9)	0.9342(4)
C(65)	0.3189(5)	0.1966(8)	0.8686(5)
C(66)	0.3145(4)	0.2545(7)	0.8028(4)

Phenyl carbon atoms are numbered C(mn) where m is the ring no. and n is the atom no. in the ring. n is such that C(m1) is attached to P and other atoms are numbered in succession such that C(m4) is para to C(m1).

115

Table 2

Anisotropic thermal parameters

Atom	β_{11}	β_{22}	β_{33}	β_{12}	β_{13}	β_{23}
Ir	0.00317(1)	0.00804(2)	0.00425(1)	-0.00025(1)	0.00107(1)	-0.00064(2)
P(1)	0.00334(6)	0.0081(2)	0.00311(5)	-0.00036(8)	0.00109(5)	-0.00011(8)
P(2)	0.00334(6)	0.0085(2)	0.00326(6)	0.00015(8)	0.00121(5)	-0.00030(8)
O(1)	0.0104(6)	0.0213(14)	0.0056(4)	-0.0034(8)	0.0034(4)	0.0025(6)
O(1*)	0.0100(10)	0.0177(21)	0.0054(6)	-0.0054(6)	-0.0021(6)	0.0015(9)
O(2)	0.0182(11)	0.0267(19)	0.0090(6)	-0.0071(12)	0.0081(7)	-0.0071(9)
O(2*)	0.0108(13)	0.0288(34)	0.0129(13)	0.0028(16)	0.0033(11)	-0.0117(18)
C(1)	0.0044(5)	0.0126(13)	0.0036(4)	0.0028(6)	0.0017(3)	0.0039(6)
C(1*)	0.0052(12)	0.0278(49)	0.0226(31)	0.0009(19)	-0.0059(16)	-0.0221(35)
C(2)	0.0073(7)	0.0212(22)	0.0102(8)	0.0016(11)	0.0060(7)	0.0036(11)
C(2*)	0.0061(10)	0.0138 27)	0.0121(15)	-0.0052(14)	0.0064(11)	-0.0107(17)
C(11)	0.0043(3)	0.0085(7)	0.0028(2)	0.0009(4)	0.0015(2)	0.0004(3)
C(12)	0.0057(3)	0.0112(8)	0.0037(3)	0.0016(4)	0.0016(2)	-0.0003(4)
C(13)	0.0083(4)	0.0129(9)	0.0033(3)	0.0030(5)	0.0022(3)	-0.0001(4)
C(14)	0.0081(4)	0.0140(1)	0.0048(3)	0.0037(5)	0.0036(3)	0.0016(4)
C(15)	0.0061(4)	0.0121(9)	0.0057(3)	0.0023(5)	0.0036(3)	0.0021(4)
C(16)	0.0050(3)	0.0089(7)	0.0044(3)	0.0007(4)	0.0023(2)	0.0009(4)
C(21)	0.0035(3)	0.0085(7)	0.0031(2)	-0.0004(3)	0.0006(2)	0.0002(3)
C(22)	0.0044(3)	0.0084(7)	0.0047(3)	0.0004(4)	0.0012(2)	0.0005(4)
C(23)	0.0057(4)	0.0108(9)	0.0057(3)	0.0008(4)	0.0011(3)	0.0012(4)
C(24)	0.0052(3)	0.0089(8)	0.0064(4)	0.0001(4)	0.0002(3)	0.0027(4)
C(25)	0.0041(3)	0.0175(11)	0.0044(3)	-0.0015(5)	0.0005(2)	0.0032(5)
C(26)	0.0037(3)	0.0116(8)	0.0037(2)	-0.0002(4)	0.0003(2)	0.0014(4)
C(31)	0.0034(3)	0.0086(7)	0.0032(2)	-0.0000(3)	0.0013(2)	-0.0006(3)
C(32)	0.0046(3)	0.0104(8)	0.0047(3)	-0.0003(4)	0.0012(2)	-0.0006(4)
C(33)	0.0039(3)	0.0118(9)	0.0064(4)	-0.0019(4)	0.0009(3)	-0.0024(5)
C(34)	0.0039(3)	0.0153(10)	0.0047(3)	-0.0006(4)	0.0007(2)	-0.0027(4)
C(35)	0.0045(3)	0.0150(9)	0.0034(3)	0.0001(4)	0.0003(2)	-0.0011(4)
C(36)	0.0039(3)	0.0117(8)	0.0028(2)	-0.0003(4)	0.0011(2)	-0.0003(3)
C(41)	0.0032(2)	0.0094(7)	0.0034(2)	-0.0008(3)	0.0017(2)	-0.0014(3)
C(42)	0.0053(3)	0.0129(9)	0.0040(3)	0.0001(4)	0.0022(2)	-0.0003(4)
C(43)	0.0064(4)	0.0171(10)	0.0037(3)	-0.0001(5)	0.0020(3)	-0.0014(4)
C(44)	0.0055(4)	0.0154(10)	0.0053(3)	-0.0009(5)	0.0026(3)	-0.0035(5)

Table 2 ctd

C(45)	0.0043(3)	0.0121(9)	0.0063(3)	0.0011(4)	0.0022(3)	-0.0014(4)
C(46)	0.0042(3)	0.0083(7)	0.0038(2)	0.0003(4)	0.0016(2)	-0.0009(3)
C(51)	0.0033(2)	0.0095(7)	0.0033(2)	0.0004(3)	0.0015(2)	0.0001(3)
C(52)	0.0031(3)	0.0098(8)	0.0068(3)	0.0000(4)	0.0013(2)	-0.0001(4)
C(53)	0.0040(3)	0.0118(9)	0.0063(3)	-0.0016(4)	0.0012(3)	0.0004(4)
C(54)	0.0037(3)	0.0125(8)	0.0041(3)	0.0002(4)	0.0014(2)	0.0007(4)
C(55)	0.0049(3)	0.0091(8)	0.0054(3)	0.0013(4)	0.0012(3)	-0.0014(4)
C(56)	0.0039(3)	0.0097(7)	0.0039(3)	0.0000(4)	0.0009(2)	-0.0006(4)
C(61)	0.0035(3)	0.0104(8)	0.0039(2)	0.0002(4)	0.0015(2)	0.0003(3)
C(62)	0.0058(3)	0.0137(9)	0.0035(3)	0.0013(5)	0.0019(2)	0.0003(4)
C(63)	0.0079(5)	0.0189(12)	0.0042(3)	0.0013(6)	0.0028(3)	-0.0018(5)
C(64)	0.0074(4)	0.0217(13)	0.0046(3)	0.0007(6)	0.0033(3)	0.0016(5)
C(65)	0.0077(4)	0.0153(10)	0.0063(4)	-0.0022(6)	0.0037(3)	0.0022(5)
C(66)	0.0053(3)	0.0149(9)	0.0037(6)	-0.0016(5)	0.0019(2)	0.0000(4)

Table 3

Fractional coordinates of the hydrogen atoms

Atom	x	y	z
H(12)	0.488	0.434	0.620
H(13)	0.539	0.384	0.524
H(14)	0.661	0.421	0.549
H(15)	0.759	0.521	0.668
H(16)	0.715	0.559	0.759
H(22)	0.618	0.270	0.747
H(23)	0.613	0.051	0.788
H(24)	0.568	0.012	0.882
H(25)	0.524	0.216	0.944
H(26)	0.515	0.430	0.887
H(32)	0.614	0.790	0.786
H(33)	0.729	0.904	0.883
H(34)	0.832	0.791	0.983
H(35)	0.800	0.583	1.000
H(36)	0.688	0.460	0.915
H(42)	0.267	0.438	0.560
H(43)	0.284	0.281	0.475
H(44)	0.373	0.082	0.530
H(45)	0.430	0.052	0.654
H(46)	0.416	0.201	0.740
H(52)	0.200	0.325	0.641
H(53)	0.055	0.369	0.589
H(54)	0.002	0.580	0.573
H(55)	0.101	0.745	0.623
H(56)	0.246	0.708	0.694
H(62)	0.386	0.555	0.872
H(63)	0.391	0.448	0.983
H(64)	0.366	0.247	0.996
H(65)	0.320	0.112	0.869
H(66)	0.297	0.213	0.760

The number of each hydrogen atom is the same as that of the carbon to which it is bonded.

Table 4

Final observed and calculated

structure factors

The format of the table is

h	k	l
l	$10|F_o|$	$10|F_c|$

Reflections of intensities not significantly greater than the background ("less-thans") are marked: *

Table 5

Selected bond lengths (Å) and angles (°) with standard deviations in parentheses.

	Ir - P(1)	2.357(2)	
	Ir - P(2)	2.359(2)	
Ir - C(1)	1.886	Ir - C(1*)	1.938
Ir - C(2)	1.916	Ir - C(2*)	1.829
Ir....O(1)	2.994(10)	Ir...O(1*)	3.076(15)
Ir...O(2)	3.042(12)	Ir...O(2*)	2.902(25)
	O(1)....O(1*)	0.714(19)	
	O(2)....O(2*)	1.562(22)	
P(1) - C(11)	1.842(7)	P(2) - C(41)	1.829(6)
P(1) - C(21)	1.843(6)	P(2) - C(51)	1.838(6)
P(1) - C(31)	1.836(5)	P(2) - C(61)	1.841(7)

mean C - C

ring C($1n$)	1.380	ring C($4n$)	1.385
C($2n$)	1.385	C($5n$)	1.375
C($3n$)	1.379	C($6n$)	1.377

P(1) - Ir - P(2) 102.17(5)

P(1) - Ir - C(1)	100.5	P(1) - Ir - C(1*)	107.1
P(1) - Ir - C(2)	93.3	P(1) - Ir - C(2*)	123.6
P(2) - Ir - C(1)	106.7	P(2) - Ir - C(1*)	93.7
P(2) - Ir - C(2)	113.4	P(2) - Ir - C(2*)	105.1
C(1) - Ir - C(2)	133.5	C(1*) - Ir - C(2*)	119.1

Ir - P(1) - C(11)	116.5(2)	C(11) - P(1) - C(21)	100.6(3)
Ir - P(1) - C(21)	119.7(2)	C(11) - P(1) - C(31)	101.3(3)
Ir - P(1) - C(31)	113.5(2)	C(21) - P(1) - C(31)	102.7(2)
Ir - P(2) - C(41)	113.3(2)	C(41) - P(2) - C(51)	101.3(3)
Ir - P(2) - C(51)	117.0(2)	C(41) - P(2) - C(61)	105.2(3)
Ir - P(2) - C(61)	117.3(2)	C(51) - P(2) - C(61)	100.7(3)

Table 6

Selected angles for three forms of $IrH(CO)_2(PPh_3)_2$

	Orthorhombic form	Monoclinic(I) Major form	Minor form
P(1) - Ir - P(2)	101.38(7)	102.17(5)	
P(1) - Ir....O(1)	95.7(1)	100.5(2)	107.1(4)
P(1) - Ir....O(2)	96.7(1)	93.3(3)	123.6(4)
P(2) - Ir....O(1)	117.6(2)	106.7(2)	93.7(3)
P(2) - Ir....O(2)	114.6(1)	113.4(3)	105.1(5)
O(1)....Ir....O(2)	122.2(2)	133.5(3)	119.1(5)

Since the carbonyl carbon atoms in monoclinic(I) were placed in calculated positions, angles involving the oxygen atoms are quoted.

Table 7

Planarity of phenyl rings

Ring	Mean deviation (Å)	Maximum deviation (Å)	Distance of phosphorus atom from least-squares plane
C(1n)	0.008	0.013	0.084(10)
C(2n)	0.007	0.011	0.143(8)
C(3n)	0.006	0.009	0.147(7)
C(4n)	0.005	0.009	0.078(6)
C(5n)	0.005	0.010	0.058(7)
C(6n)	0.012	0.020	0.045(14)

Table 8

Some selected non-bonded distances.

C(34) - C(25)^I	3.643	H(34) - H(25)^I	2.540
C(33) - C(23)^{II}	3.787	H(33) - H(23)^{II}	2.621
C(32) - C(23)^{II}	3.934	H(32) - H(23)^{II}	2.630
C(35) - C(24)^I	3.682	H(35) - H(24)^I	2.663
C(44) - C(54)^{III}	4.007	H(44) - H(54)^{III}	2.680
C(13) - C(13)^{IV}	3.463	H(13) - H(13)^{IV}	2.703
O(1) - C(54)^V	3.354	O(1) - H(54)^V	2.573
O(1*) - C(14)^{IV}	3.134	O(1*) - H(14)^{IV}	2.374
C(1*) - C(14)^{IV}	3.223	C(1*) - H(14)^{IV}	3.327

Superscripts refer to atoms in the following positions:

I $1\frac{1}{2} - x, \frac{1}{2} + y, 2 - z$ II $x, 1 + y, z$ III $\frac{1}{2} + x, \frac{1}{2} - y, z$

IV $1 - x, 1 - y, 1 - z$ V $\frac{1}{2} + x, 1\frac{1}{2} - y, z$

REFERENCES

1. W.R. Busing and H.A. Levy, Acta Cryst., 10, 180, (1957).

2. P. Coppens, L. Leiserowitz and D. Rabinovich, Acta Cryst., 18, 1035, (1965).

3. D.T. Cromer and J.T. Waber, Acta Cryst., 18, 104, (1965).

4. D.T. Cromer, Acta Cryst., 18, 17, (1965).

5. U.A. Gregory, S.D. Ibekwe, B.T. Kilbourn and D.R. Russell, J. Chem. Soc., (A), 1118, 1971.

6. E.W. Hughes, J. Amer. Chem. Soc., 63, 1737, (1941).

7. C.K. Johnson, ORTEP thermal ellipsoid plotting program, Oak Ridge National Laboratory Report, 1965, ORNL-3794.

8. A.C. Skapski and P.G.H. Troughton, J. Chem. Soc.,(A), 2772(1969).

9. A.C. Skapski and P.G.H. Troughton, Acta Cryst., B26, 716 (1970).

10. G. Yagupsky and G. Wilkinson, J. Chem. Soc. (A), 725, (1969).

CHAPTER III

The Crystal Structure of

Potassium μ-Nitrido-bis[tetrachloroaquoruthenate(IV)]

$$K_3[Ru_2NCl_8(H_2O)_2]$$

There has been much recent interest in transition-metal μ-nitrido

complexes, although only a few are known.   They include $[Os_2N(NH_3)_8X_2]X_3$

(X = Cℓ, Br or I) [1], and the heterometallic compound $[(PEt_2Ph)_3C\ell_2ReN$

$PtC\ell_2(PEt_3)]$.[2]   Recently Cleare and Griffith[3] showed, on the basis of

spectroscopic data, that the compounds $K_3[Ru_2NX_8(H_2O)_2]$ (X = Cℓ or Br)

belong to this category.   As no structural information existed about

this type of compound we have determined the structure of $K_3[Ru_2NC\ell_8(H_2O)_2]$

by $\underline{X}$-ray single-crystal methods.   The structure determination has

confirmed Cleare and Griffith's conception and shows that the Ru-N-Ru

bridge has multiple bonding with very short Ru-N distances of 1.720Å.

A preliminary account of this work has appeared[4].

In the final stages of the refinement of this structure we became

aware that Gee and Powell had independently determined the structure of

the ammonium analogue of the title compound[5].   A comparison of the two

shows them to be isostructural.

EXPERIMENTAL

Potassium μ-nitrido-bis[tetrachloroaquoruthenate(IV)] crystallises

from dilute hydrochloric acid as deep red plates.   They were examined

by single-crystal oscillation and Weissenberg methods with Cu-Kα

radiation (λ = 1.5418Å).

<u>Crystal Data</u>. $K_3[Ru_2NC\ell_8(H_2O)_2]$, $\underline{M}_W$ = 653.2, Monoclinic,

$\underline{a}$ = 15.89, $\underline{b}$ = 7.34, $\underline{c}$ = 8.16, β = 120.4°, $\underline{U}$ = 820.9Å^3, $\underline{D}_m$ = 2.64, $\underline{Z}$ = 2,

$\underline{D}$ = 2.64g cm^{-3}, $\underline{F}(000)$ = 616.   Space group $\underline{C}2/\underline{m}$ (No.12).

A crystal of approximate size 0.12 x 0.15 x 0.025 mm^3 was selected

and equi-inclination Weissenberg photographs were taken about [010] to

give $\underline{ho\ell}$ - $\underline{h6\ell}$ reflections.   Intensities were estimated visually from

multiple-film exposures.   A total of 703 observable independent

reflections were measured.   The Lorentz-polarisation correction was

applied, as was also an absorption correction (μ = 340.8 cm^{-1}). This

correction was made using the Gaussian integration method with an

8 x 8 x 8 grid, described by Busing and Levy[6] with crystal path lengths

determined by the vector analysis procedure of Coppens et al[7].

SOLUTION AND REFINEMENT OF THE STRUCTURE

The structure was solved by standard Patterson and Fourier methods.

Computation was carried out on the Imperial College IBM7094 computer

using the Crystal Structure Calculation System X-ray -63 described by

J.M. Stewart in the University of Maryland Technical Report TR-64-6.

The atomic scattering factors used were those tabulated by Cromer and

Waber[8], a correction for anomalous dispersion was applied and the values

of the real and imaginary parts of dispersion correction were those

given by Cromer[9].

The first round of isotropic least-squares refinement using all

measured reflections gave $\underline{R}$ = 0.15. The absorption correction was

applied, and the $\underline{R}$ fell to 0.104. At this stage it was obvious that

the strongest reflections suffered from extinction, and 6 of them were

removed. Isotropic refinement was used to fix the inter-layer scale

factors and gave $\underline{R}$ = 0.096. Anisotropic refinement reduced $\underline{R}$ to 0.085.

At the final stage a weighting scheme of the type suggested by Hughes[10]

was applied, where $\underline{\omega}$ = 1 for $\underline{F} < \underline{F}^*$, $\sqrt{\underline{\omega}} = \underline{F}^*/\underline{F}$ for $\underline{F} \geqslant \underline{F}^*$. Various

values of $\underline{F}^*$ were tried, the most satisfactory being $\underline{F}^* = 17.0$. Although

the $\underline{R}$ factor rose to 0.088, the standard deviations were approximately

25% lower compared to unweighted refinement.

The final fractional coordinates and their standard deviations are

listed in Table 1, as are the orthogonal coordinates. Table 2 shows

the coefficients in the expression for the anisotropic temperature factors

$\exp[-(\beta_{11}h^2 + \beta_{22}k^2 + \beta_{33}\ell^2 + 2\beta_{12}hk + 2\beta_{13}h\ell + 2\beta_{23}k\ell)]$ and also the

isotropic temperature factors $\underline{B}$.

Observed structure amplitudes and calculated structure factors are listed in Table 3. Structure factors were also calculated for those reflections too weak to be observed. None of these in a position to be recorded were calculated to be greater than twice the minimum locally observable $|F_o|$. The positions of the water hydrogen atoms could not be confidently located from the final difference Fourier.

DESCRIPTION OF THE STRUCTURE AND DISCUSSION

The determination of the crystal structure has shown that the title compound contains the complex ion $[Ru_2NCl_8(H_2O)_2]^{3-}$ and potassium ions. The nitrido-bridged complex ion is shown in Figure 1a and the more important interatomic distances and angles are in Table 4. The anions have $2/\underline{m}$ crystallographic symmetry, with the bridging nitrogen atom lying on a centre of symmetry. The ruthenium atoms lie on mirror planes as do the water molecules which are _trans_ to the nitrogen. Four chlorine atoms complete the distorted octahedral coordination about each metal atom. The main feature of the distorted coordination is that all chlorines are bent away from the nitrogen and towards the water molecule. Two such octahedra share a common corner (N) to give a linear O-Ru-N-Ru-O system. A further important feature is that the orientation of the chlorines in the two octahedra is such that they are _eclipsed_, as found in the $Re_2Cl_8^{2-}$ ion.[11]

The structure of the complex ion is mainly determined by two factors:

a) the strong metal-nitrogen bond

b) repulsion forces between the chlorine atoms and nitrogen.

The Ru-N distances are very short, 1.720Å, indicating multiple bonding with a considerable amount of π-character[2,12]. Thus the _eclipsed_ configuration of the chlorine atoms is almost certainly a result of the
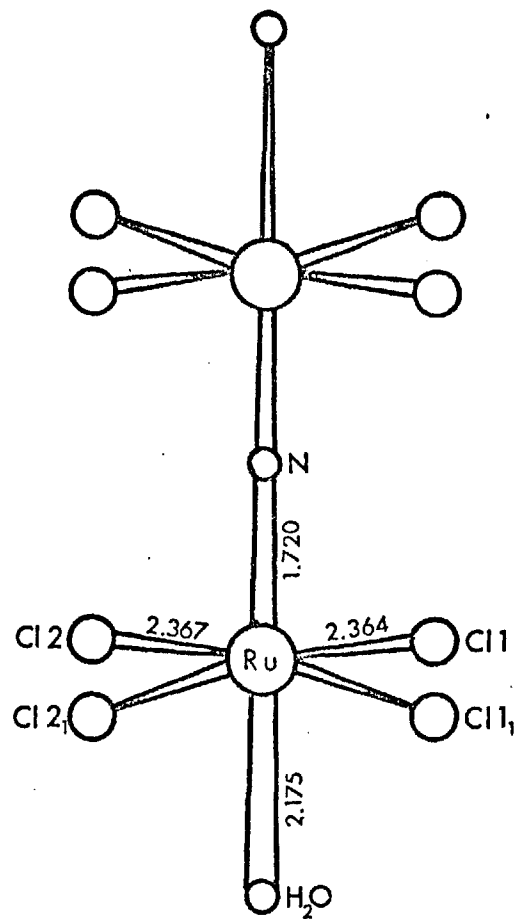
Fig. 1.a.

Schematic drawing of the
$[Ru_2NCl_8(H_2O)_2]^{3-}$ anion.
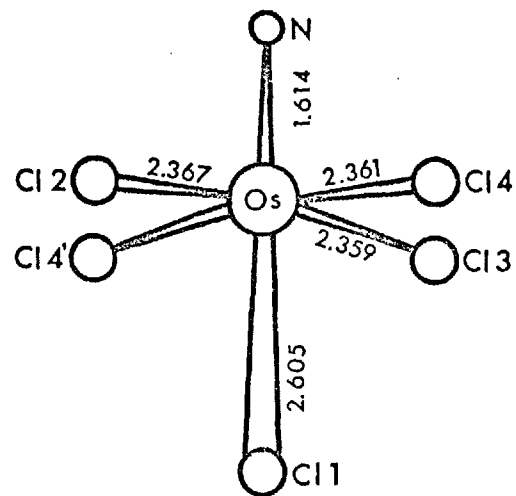
Fig. 1.b.

Schematic drawing of the
$OsNCl_5{}^{2-}$ anion. (Ref. 16).

rigidity of the central Ru-N-Ru bridge.   The short Ru-N distance may

be compared with bridging Ru-O distances of 1.80Å found in

$[Ru_2OCl_{10}]^{4-}$(Ref.13) and Re-O distances of 1.86Å in $[Re_2OCl_{10}]^{4-}$(Ref.14)

and 1.91Å in $Re_2O_3(S_2CNEt_2)_4$ (Ref. 15).

The repulsion between nitrogen and chlorine atoms is best discussed

by comparison with the structure of the $OsCl_5N^{2-}$ anion[16] shown in Fig.1b.

This ion is similar in having a short metal-nitrogen bond with all four

cis chlorines bent away from the nitrogen.   The Os-N bond is a triple one

and shorter than the title compound, nevertheless the N-Cl distances are

very similar, average of 3.04Å in the ruthenium complex and 3.00Å in the

osmium complex.   This is possible because the angular distortion in the

osmium complex is greater, with an average N-Os-cisCl angle of $96.2°$ as

against an average N-Ru-cisCl angle of $94.7°$.   Thus the amount of

angular distortion seems to be dictated by the requirement that a minimum

N-cisCl distance of ca 3.0Å be achieved.

In both complex ions the bond length trans to the nitrogen is rather

long (Ru-O(water) of 2.175Å).   Although a trans-influence is a possible

reason the more likely explanation is that the trans atoms are pushed

away by the cis chlorines.   The Ru-O(water) distance may be compared to

2.10Å found in $Cs_2RuCl_5(H_2O)$ [17] and an average of 2.12Å in $(C_6H_5)_4AsRuCl_4$

$(H_2O)_2 \cdot H_2O$ [18].   The Ru-Cl distances are normal, only slightly longer

than the average Ru-Cl distance of 2.34Å found in the last two compounds.

A comparison of the bondlengths and angles in the complex ion with those

obtained in the parallel and independent study of the ammonium salt[5]

shows very good agreement.

There are two crystallographically independent potassium ions in the

structure, both of which are co-ordinated to eight chlorine atoms placed

at the corners of a distorted cube at normal distances in the range

3.20 - 3.36Å.   The next nearest neighbours are in one case two nitrogen

atoms at 3.67Å (Fig. 2a), and in the other an oxygen at 3.42Å and a nitrogen at 3.75Å (Fig. 2b). These stick out of opposite faces of the cube, but are too far away to be considered as coordinated. The spatial relationship of the complex ions and the potassium ions is shown in Figure 3.

The water molecule also has four chlorine neighbours from two adjacent complex ions. Two of these are at a distance of 3.25Å which might be consistent with a weak O-H...Cl hydrogen bond. However, it is difficult to say whether any such interaction occurs as the water hydrogen atoms could not be located.
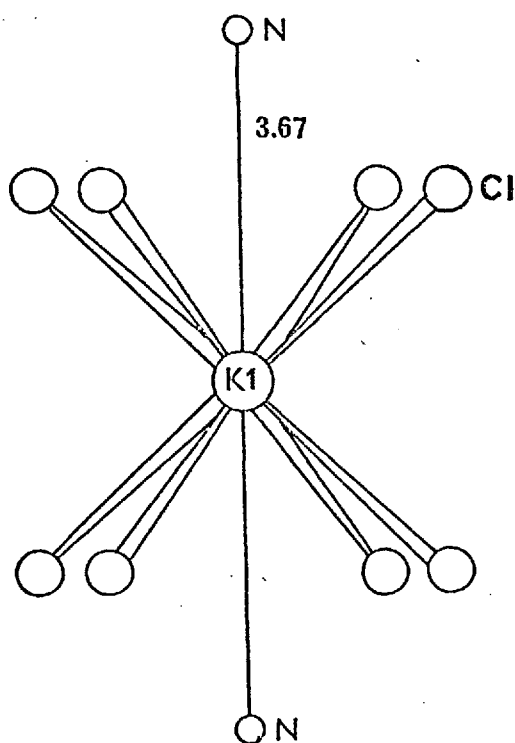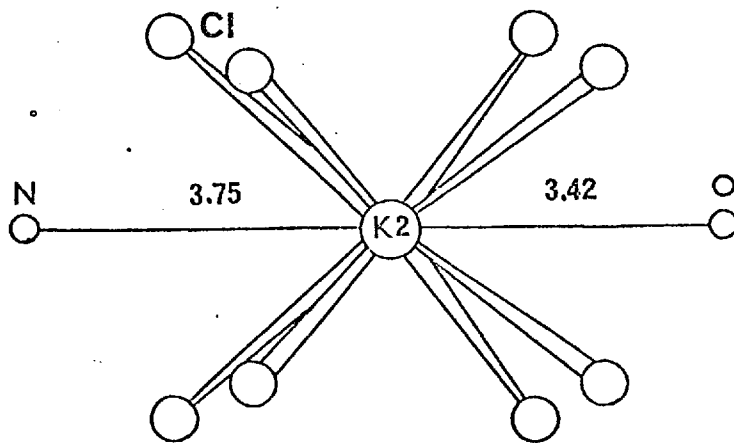
Fig. 2.a.   Fig. 2.b.

Schematic drawings of the coordination round the two crystallographicaly independent potassium atoms.
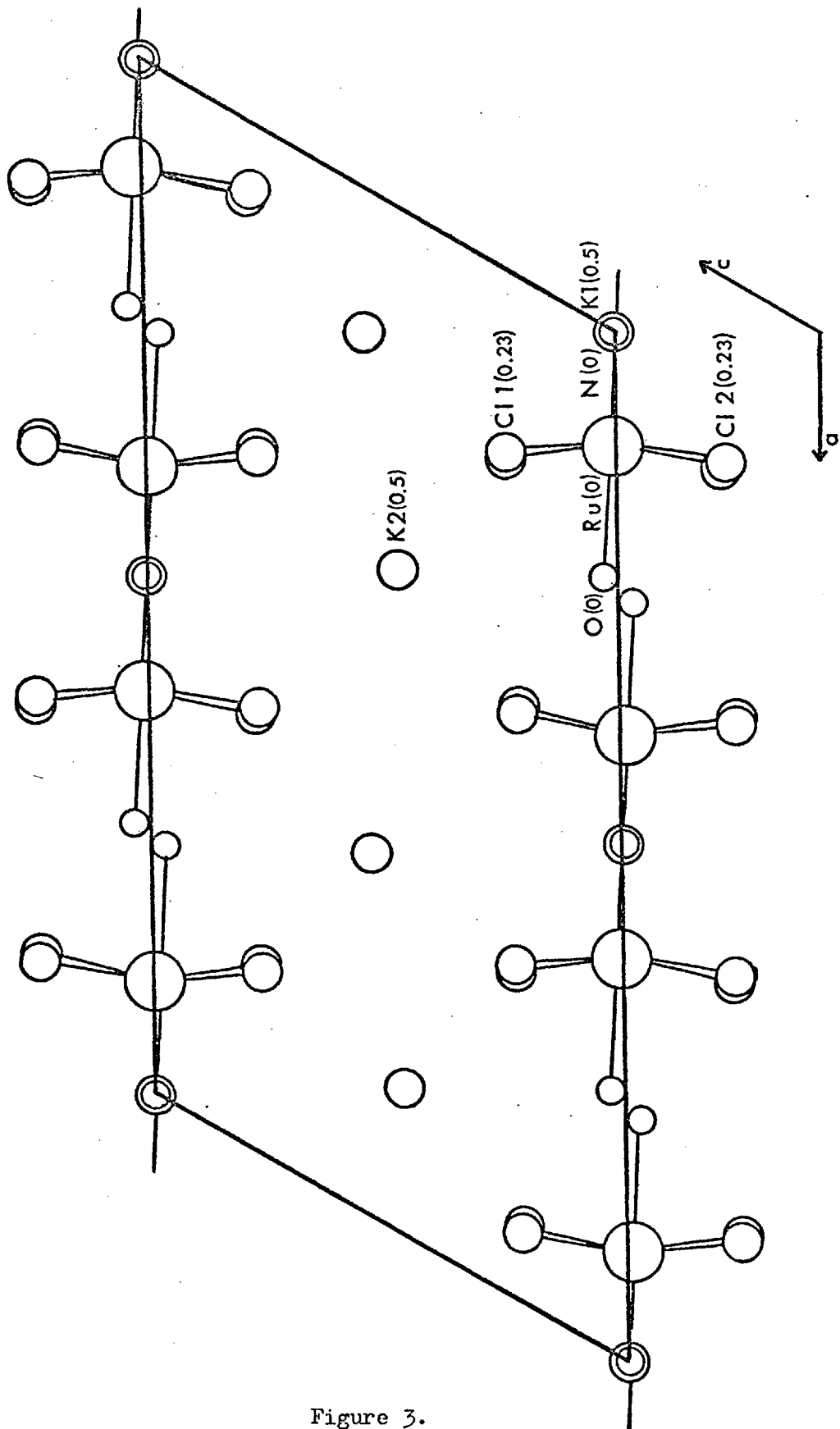
Figure 3.

The [010] projection of the structure of $K_3[Ru_2NCl_8(H_2O)_2]$.

The figures in parentheses indicate the height of atoms. For sake of clarity the chlorine atoms related by a mirror perpendicular to b have been slightly offset.

TABLE 1. $K_3[Ru_2NCl_8(H_2O)_2]$: fractional co-ordinates $\underline{x}$, $\underline{y}$, $\underline{z}$ with estimated standard deviations in parenthesis; orthogonal co-ordinates $\underline{X}$, $\underline{Y}$, $\underline{Z}'$, in Å. $\underline{X}$ is parallel to $\underline{a}$, $\underline{Y}$ is parallel to $\underline{b}$, and $\underline{Z}'$ is perpendicular to both, in a right-handed system.

	$\underline{x}$	$\underline{y}$	$\underline{z}$	$\underline{X}$	$\underline{Y}$	$\underline{Z}'$
Ru	0.11018(9)	0	0.00754(16)	1.7196	0.0	0.0531
K(1)	0	$\frac{1}{2}$	0	0.0	3.670	0.0
K(2)	0.3606(4)	$\frac{1}{2}$	0.4675(7)	3.799	3.670	3.290
Cl(1)	0.1799(3)	0.2270(6)	0.2450(5)	1.847	1.666	1.724
Cl(2)	0.0649(3)	0.2259(6)	-0.2297(5)	1.980	1.658	-1.617
N	0	0	0	0	0	0
O	0.2496(9)	0	0.0177(21)	3.893	0.0	0.124

TABLE 2. $K_3[Ru_2NCl_8(H_2O)_2]$: anisotropic thermal parameters and isotropic temperature factors($\underline{B}$).

	β_{11}	β_{22}	β_{33}	β_{12}	β_{13}	β_{23}	$\underline{B}(\text{Å}^2)$
Ru	0.0020	0.0070	0.0073	0	0.0021	0	1.13(5)
K(1)	0.0055	0.0090	0.0219	0	0.0061	0	3.00(19)
K(2)	0.0042	0.0172	0.0168	0	0.0052	0	2.74(13)
Cl(1)	0.0039	0.0158	0.0140	-0.0019	0.0035	-0.0041	2.61(10)
Cl(2)	0.0045	0.0131	0.0125	0.0001	0.0045	0.0015	2.32(9)
N	0.0048	0.0053	0.0051	0	0.0026	0	2.1(6)
O	0.0018	0.0129	0.0171	0	0.0037	0	2.4(4)

TABLE 3. $K_3[Ru_2NCl_8(H_2O)_2]$: observed structure amplitudes and calculated structure factors. The 6 reflections marked with an asterisk were omitted from least-squares refinement because of extinction.

h	k	l	$\lvert F_o \rvert$	F_c
-2	0	0	44.16	42.51
-4	0	0	127.77	-152.56
-6	0	0	23.41	-25.15
-8	0	0	31.36	24.04
-10	0	0	49.05	43.30
-12	0	0	47.49	-52.24
-16	0	0	54.92	45.99
-2	0	1	59.04	70.19
-2	0	2	57.33	50.71
-2	0	4	96.70	97.80
-2	0	5	67.10	55.34
-2	0	6	61.50	57.11
-2	0	8	59.70	56.29
-2	0	9	46.48	41.47
-4	0	1*	193.44	-235.47
-4	0	2	121.94	-133.65
-4	0	3	154.64	164.05
-4	0	4	66.03	-70.50
-4	0	5	120.64	-140.97
-4	0	6	95.43	-97.98
-4	0	7	37.16	30.46
-4	0	9	67.75	-61.01
-6	0	1	96.49	-103.80
-6	0	2	89.06	-88.68
-6	0	3	42.61	-40.76
-6	0	4	54.93	-50.03
-6	0	5	72.67	-75.20
-6	0	6	103.57	-106.27
-6	0	7	19.24	-19.29
-6	0	8	31.32	-33.74
-6	0	9	41.94	-40.97
-6	0	10	63.00	-63.95
-8	0	1	105.52	111.55
-8	0	2*	253.41	300.15
-8	0	3	78.91	73.31
-8	0	4	27.90	16.47
-8	0	5	46.18	37.56
-8	0	6	149.36	175.39
-8	0	7	67.38	61.34
-8	0	10	64.87	51.97
-10	0	1	83.51	90.53
-10	0	2	101.21	99.17
-10	0	3	114.63	127.42
-10	0	4	66.10	65.56
-10	0	5	54.94	61.93
-10	0	6	113.15	120.11
-10	0	7	45.32	47.25
-10	0	8	61.21	61.22
-10	0	9	20.66	25.54
-10	0	10	72.55	73.18
-14	0	1	53.60	-65.21
-14	0	2	41.84	-43.78
-14	0	3	45.32	-114.57
-14	0	4	79.65	-77.84
-14	0	5	46.32	-51.31
-14	0	6	47.80	-43.93
-14	0	7	79.28	-81.22
-14	0	8	66.24	-83.36
-14	0	9	21.22	-25.10
-14	0	10	22.39	-28.81
-16	0	2	24.42	-23.41
-16	0	3	16.56	12.76
-16	0	4	56.68	67.58
-16	0	5	17.01	-16.00
-16	0	6	39.03	-30.67
-16	0	7	25.67	-22.87
-16	0	8	42.39	40.07
-18	0	2	26.36	25.96
-18	0	3	44.17	50.75
-18	0	4	61.40	58.55
-18	0	5	71.38	71.22
-18	0	6	29.12	27.73
-18	0	7	36.32	36.00
-18	0	8	61.65	62.52
0	0	2	66.34	56.33
0	0	3	100.42	99.44
0	0	4*	225.21	247.77
0	0	5	127.73	138.94
0	0	6	31.14	29.52
0	0	7	42.06	38.61
0	0	8	92.93	91.31
2	0	1	60.41	58.08
2	0	3	44.63	35.43
2	0	4	39.82	-32.13
2	0	5	39.57	28.82
2	0	8	35.24	-26.76
4	0	1	134.01	142.76
4	0	2	68.54	-60.84
4	0	3	157.76	-158.94
4	0	4	119.63	-110.65
4	0	6	22.00	-14.73
4	0	7	79.12	-76.27
6	0	1	69.57	-70.10
6	0	2	21.57	-16.55
6	0	3	54.21	-46.52
6	0	5	42.41	-37.29
8	0	1	64.71	57.46
8	0	2	167.48	178.87
8	0	3	157.73	165.32
8	0	4	14.18	18.52
8	0	5	33.87	30.03
8	0	6	65.45	67.80
10	0	1	95.00	90.08
10	0	2	54.10	41.94
10	0	3	57.15	55.48
10	0	4	37.94	24.03
10	0	5	41.35	38.25
12	0	1	71.21	-65.26

h	k	l	$\lvert F_o \rvert$	F_c
12	0	2	54.91	-46.17
12	0	3	14.55	11.54
14	0	1	75.68	-69.60
14	0	2	33.92	-32.17
16	0	1	38.76	31.42
-12	0	1	68.89	75.69
-12	0	2	44.90	-43.60
-12	0	3	61.32	-62.55
-12	0	4	26.57	-19.94
-12	0	5	47.47	102.88
-12	0	7	36.84	-34.63
-12	0	8	26.89	-22.96
-12	0	9	51.96	52.63
-12	0	10	21.60	17.41
-3	1	0	149.51	-155.94
-5	1	0	133.95	-154.57
-7	1	0	33.35	28.44
-9	1	0	65.48	76.05
-11	1	0	57.73	-60.23
15	1	0	24.46	-21.92
-3	1	1	66.83	-60.63
-3	1	2	98.77	-113.61
-3	1	3	40.17	-34.82
-3	1	4	65.31	-66.60
-3	1	5	50.18	-47.17
-3	1	6	26.40	-24.94
-3	1	7	23.54	-22.32
-3	1	9	17.43	-14.35
-5	1	1	128.93	-143.98
-5	1	2*	153.68	-192.04
-5	1	3	75.69	-79.50
-5	1	4	137.64	-151.24
-5	1	5	86.31	-88.92
-5	1	6	106.39	-121.96
-5	1	7	53.44	-47.70
-5	1	8	72.85	-70.95
-5	1	9	52.29	-48.97
-7	1	1	37.49	-39.42
-7	1	2	39.26	36.00
-7	1	3	54.55	-54.99
-7	1	4	13.90	-17.07
-7	1	5	37.97	-36.90
-7	1	6	16.98	-15.51
-7	1	7	24.54	-23.77
-7	1	8	26.65	-27.27
-7	1	9	15.26	-16.15
-7	1	10	21.05	-22.33
-9	1	1	84.69	96.01
-9	1	2	104.99	126.66
-9	1	3	61.68	55.71
-9	1	4	92.73	105.72
-9	1	5	62.16	59.29
-9	1	6	111.96	114.31
-9	1	7	59.01	55.72
-9	1	8	66.82	69.29
-9	1	9	35.39	34.91
-9	1	10	54.30	56.16
-11	1	1	47.16	46.97
-11	1	2	12.44	-11.93
-11	1	3	46.02	40.83
-11	1	5	51.52	49.95
-11	1	6	20.11	16.63
-11	1	7	37.60	33.64
-11	1	8	27.68	27.43
-11	1	9	28.12	30.25
-11	1	10	33.11	31.64
-13	1	1	64.30	-64.77
-13	1	2	67.81	-69.24
-13	1	3	76.65	-75.33
-13	1	4	85.36	-80.15
-13	1	5	42.34	-40.68
-13	1	6	63.14	-67.51
-13	1	7	45.98	-42.63
-13	1	8	56.27	-59.67
-13	1	9	17.13	-16.94
-13	1	10	31.79	-24.99
-15	1	1	48.72	-57.17
-15	1	2	35.24	-36.59
-15	1	3	56.58	-69.36
-15	1	4	36.57	-37.14
-15	1	5	72.94	-76.90
-15	1	6	50.98	-49.20
-15	1	7	73.15	-67.54
-15	1	8	42.29	-45.76
-15	1	9	50.61	-51.92
-17	1	2	21.05	22.81
-17	1	3	29.65	32.39
-17	1	4	32.73	37.94
-17	1	5	29.75	27.50
-17	1	6	26.80	26.95
-17	1	7	12.83	13.63
-17	1	8	34.33	34.84
-19	1	3	40.20	48.33
-19	1	4	27.16	27.94
-19	1	5	41.50	49.65
-19	1	6	29.15	31.05
-19	1	7	42.31	51.11
-1	1	2	123.76	140.74
-1	1	3	58.41	49.22
-1	1	4	135.03	145.52
-1	1	5	69.42	64.30
-1	1	6	80.64	82.02
-1	1	7	41.94	44.24
-1	1	8	61.14	67.11
-1	1	9	40.43	44.92
1	1	1	62.50	57.60
1	1	2	56.59	76.15
1	1	3	67.18	63.47

h	k	l	$\lvert F_o \rvert$	F_c
1	1	4	54.21	56.99
1	1	5	51.82	49.48
1	1	6	19.67	22.84
1	1	7	35.41	35.06
1	1	8	15.75	15.74
3	1	1	20.00	-19.26
3	1	2	99.89	-113.67
3	1	3	56.97	-50.69
3	1	4	87.25	-92.39
3	1	5	29.65	-29.62
3	1	6	52.50	-50.09
3	1	7	40.97	-37.64
5	1	1	112.28	-109.66
5	1	2	113.24	-111.91
5	1	3	112.19	-129.32
5	1	4	66.84	-66.87
5	1	5	68.01	-66.96
5	1	6	44.27	-41.64
5	1	7	45.63	-47.90
7	1	1	27.50	-28.54
7	1	2	55.67	48.95
7	1	4	29.52	25.62
7	1	6	29.31	27.36
9	1	1	92.25	86.31
9	1	2	72.12	68.54
9	1	3	73.64	69.31
9	1	4	44.08	39.46
9	1	5	58.92	51.59
11	1	1	20.83	19.64
11	1	2	10.49	-9.32
11	1	3	17.09	15.53
13	1	1	79.63	-71.92
13	1	2	51.01	-44.99
15	1	1	35.36	-31.79
-2	2	0	30.80	24.06
-4	2	0	101.06	-94.42
-6	2	0	56.10	-42.10
-8	2	0*	174.79	226.27
-10	2	0	73.19	64.54
-12	2	0	50.73	-45.09
-14	2	0	39.97	-37.47
16	2	0	16.25	-13.37
-2	2	1	38.35	34.45
-2	2	2	73.33	79.58
-2	2	3	54.27	55.64
-2	2	4	54.75	55.93
-2	2	6	64.33	72.22
-2	2	7	45.93	45.73
-2	2	8	44.82	39.54
-4	2	1	133.01	155.45
-4	2	2	99.93	-139.69
-4	2	3	144.61	-166.54
-4	2	4	159.29	-116.33
-4	2	5	73.52	64.39
-4	2	6	34.97	-31.47
-4	2	7	83.10	-67.97
-4	2	8	69.93	-63.64
-6	2	1	64.02	-57.91
-6	2	2	46.94	-45.13
-6	2	3	82.22	-87.06
-6	2	4	93.64	-99.54
-6	2	5	30.42	-25.31
-6	2	6	44.13	-43.43
-6	2	7	52.80	-51.62
-6	2	8	82.96	-80.62
-8	2	1	70.28	61.44
-8	2	2	51.39	28.73
-8	2	3	76.21	70.11
-8	2	4	208.59	227.07
-8	2	5	73.91	66.37
-8	2	6	85.02	93.18
-8	2	9	43.44	45.19
-10	2	1	108.87	107.72
-10	2	2	57.77	52.67
-10	2	3	86.11	79.41
-10	2	4	112.86	112.35
-10	2	5	106.69	108.65
-10	2	6	72.05	65.82
-10	2	7	42.55	40.02
-10	2	8	84.93	93.42
-10	2	9	77.71	71.55
-10	2	10	47.01	48.19
-12	2	1	71.72	-61.23
-12	2	3	92.50	89.07
-12	2	4	31.63	-26.24
-12	2	5	48.17	-43.02
-12	2	6	33.82	-24.06
-12	2	7	69.39	71.61
-14	2	1	85.56	-86.78
-14	2	2	66.75	-63.17
-14	2	3	53.64	-60.29
-14	2	4	48.87	-44.72
-14	2	5	96.66	-97.66
-14	2	6	86.74	-81.81
-14	2	7	57.25	-35.71
-14	2	8	41.21	-36.42
-14	2	9	65.07	-56.72
-16	2	1	25.39	25.04
-16	2	2	57.03	54.64
-16	2	4	14.74	-24.29
-16	2	6	66.14	52.67
-16	2	8	74.42	-26.45
-16	2	9	37.84	-27.95
-18	2	3	71.12	64.70
-18	2	4	57.34	20.34
-18	2	5	46.44	45.95
-18	2	6	[illegible]	[illegible]
-18	2	7	44.24	[illegible]

h	k	l	$\lvert F_o \rvert$	F_c
-18	2	8	21.75	23.34
0	2	1	122.47	141.34
0	2	2*	229.77	[illegible]
0	2	3	143.46	162.62
0	2	4	49.94	65.44
0	2	5	51.43	58.82
0	2	6	118.35	151.22
0	2	7	82.34	95.74
2	2	1	47.36	45.65
2	2	3	43.06	46.41
2	2	6	31.18	-23.13
4	2	1	135.04	-177.59
4	2	2	109.39	-124.95
4	2	3	37.58	42.64
4	2	4	52.63	-32.47
4	2	5	91.41	-104.64
4	2	6	65.43	-75.77
6	2	1	72.61	-77.24
6	2	3	43.01	-50.19
6	2	5	21.43	-20.36
8	2	1	111.78	110.63
8	2	3	34.75	38.44
8	2	4	95.18	104.23
8	2	5	63.92	78.22
10	2	1	68.49	77.41
10	2	2	26.57	33.84
10	2	3	59.64	58.23
10	2	4	34.10	25.86
12	2	1	37.95	33.34
12	2	3	51.35	-48.45
14	2	1	45.61	-52.92
14	2	2	34.62	-34.10
-1	3	0	58.90	65.85
-3	3	0	93.28	-93.42
-5	3	0	118.57	-142.73
-7	3	0	57.33	59.78
-9	3	0	96.86	102.85
11	3	0	18.62	-17.24
13	3	0	49.93	-50.67
15	3	0	38.15	-31.74
-3	3	2	96.75	-103.46
-3	3	3	64.50	-73.97
-3	3	4	48.23	-48.82
-3	3	5	18.96	-16.59
-3	3	6	27.18	-22.51
-3	3	7	40.50	-31.14
-5	3	1	66.69	-61.34
-5	3	2	124.93	-133.27
-5	3	3	122.37	-135.92
-5	3	4	142.93	-151.75
-5	3	5	37.04	-34.93
-5	3	6	72.50	-59.54
-5	3	7	77.75	-76.05
-5	3	8	79.46	-97.06
-5	3	9	22.93	-21.15
-7	3	1	47.55	-47.46
-7	3	2	14.09	-17.35
-7	3	3	34.47	-31.14
-7	3	4	22.45	17.35
-7	3	5	39.96	-39.42
-7	3	6	34.69	-24.55
-7	3	7	14.55	-21.43
-7	3	8	27.12	-16.77
-7	3	9	8.36	[illegible]
-9	3	1	82.73	86.75
-9	3	2	69.81	63.06
-9	3	3	68.51	59.67
-9	3	4	119.76	135.13
-9	3	5	75.61	72.15
-9	3	6	55.81	61.64
-9	3	7	36.77	33.40
-9	3	8	76.48	87.90
-9	3	9	41.85	47.56
-11	3	1	20.56	17.03
-11	3	3	63.41	56.85
-11	3	5	33.07	26.26
-11	3	6	22.29	17.65
-11	3	7	45.14	-40.73
-11	3	8	31.07	27.52
-11	3	9	27.15	23.54
-13	3	1	76.44	-84.18
-13	3	2	64.55	-69.22
-13	3	3	49.01	-38.09
-13	3	4	41.78	-60.98
-13	3	5	65.65	-76.10
-13	3	6	65.44	-72.36
-13	3	8	41.92	-41.06
-13	3	9	41.71	-37.10
-15	3	1	44.43	-41.97
-15	3	2	45.62	-71.41
-15	3	3	62.57	-68.12
-15	3	4	44.59	-46.69
-15	3	5	46.59	-64.37
-15	3	6	45.52	-35.77
-15	3	7	67.52	-69.43
-15	3	8	44.15	-47.44
-15	3	9	41.49	-49.63
-17	3	2	34.86	37.42
-17	3	3	37.33	33.54
-17	3	4	13.97	13.66
-17	3	5	22.51	15.14
-17	3	6	44.73	45.36
-17	3	7	23.54	20.34
-19	3	4	14.52	31.57
-19	3	5	43.13	50.45
-19	3	6	23.10	27.70
-1	3	1	51.92	34.24
-1	3	2	153.46	172.67

TABLE 4. $K_3[Ru_2NCl_8(H_2O)_2]$: interatomic distances [Å] and bond angles (°).   The standard deviations also take into account the uncertainty in the unit-cell dimensions.

Ru - Cl1	2.364(6)
Ru - Cl2	2.367(6)
Ru - N	1.720(4)
Ru - O	2.175(17)

K1 - Cl1	3.225(7)		N - Cl1	3.027(6)
K1 - Cl2	3.253(7)		N - Cl2	3.046(7)
K1 - N	3.67(1)			
			Cl1 - Cl2	3.34(1)
K2 - Cl1	3.206(8)		$Cl1 - Cl1_1$	3.33(1)
$K2 - Cl1_4$	3.197(9)		$Cl2 - Cl2_1$	3.32(1)
$K2 - Cl2_3$	3.201(9)		$Cl1 - Cl2_2$	3.83(1)
$K2 - Cl2_5$	3.358(8)			
$K2 - O_3$	3.42 (2)		O - Cl1	3.09(2)
$K2 - N_4$	3.75 (1)		O - Cl2	3.07(1)

N - Ru - Cl1	94.3(2)		Cl1 - Ru - Cl2	90.0(3)
N - Ru - Cl2	95.1(2)		$Cl1 - Ru - Cl1_1$	89.7(3)
O - Ru - Cl1	85.6(3)		$Cl2 - Ru - Cl2_1$	88.9(3)
O - Ru - Cl2	85.0(3)		N - Ru - O	179.9(4)

Subscripts refer to atoms in the following positions : 1 $\underline{x},\underline{-y},\underline{z}$;
2 $\underline{-x},\underline{y},\underline{-z}$; 3 $\frac{1}{2}\underline{-x},\frac{1}{2}\underline{+y},\underline{-z}$; 4 $\frac{1}{2}\underline{-x},\frac{1}{2}\underline{+y},\underline{1-z}$; 5 $\frac{1}{2}\underline{+x},\frac{1}{2}\underline{-y},\underline{1+z}$.

REFERENCES

1. F.P. Dwyer and J.W. Hogarth, J.Proc.Roy.Soc. New South Wales, 1950, 84, 117.

2. J. Chatt and B.T. Heaton, Chem.Comm., 1968, 274.

3. M.J. Cleare and W.P. Griffith, Chem.Comm., 1968, 1302;

    J.Chem.Soc.(A), 1970, 1117.

4. M. Ciechanowicz and A.C. Skapski, Chem.Comm., 1969, 574.

5. R.J.D. Gee and H.M. Powell, personal communication.

6. W.R. Busing and H.A. Levy, Acta Cryst., 1957, 10, 180.

7. P. Coppens, L. Leiserowitz and D. Rabinovich, Acta Cryst., 1965, 18, 1035.

8. D.T. Cromer and J.T. Waber, Acta Cryst., 1965, 18, 104.

9. D.T. Cromer, Acta Cryst., 1965, 18, 17.

10. E.W. Hughes, J.Amer.Chem.Soc., 1941, 63, 1737.

11. F.A. Cotton and C.B. Harris, Inorg.Chem., 1965, 4, 330.

12. D.J. Hewkin and W.P. Griffith, J.Chem.Soc.(A), 1966, 472.

13. A.M. Mathieson, D.P. Mellor and N.C. Stephenson, Acta Cryst., 1952, 5, 185.

14. J.C. Morrow, Acta Cryst., 1962, 15, 851.

15. S.R. Fletcher and A.C. Skapski, to be published.

16. D. Bright and J.A. Ibers, Inorg. Chem., 1969, 8, 709.

17. T.E. Hopkins, A. Zalkin, D.H. Templeton and M.G. Adamson, Inorg.Chem., 1966, 5, 1431.

18. T.E. Hopkins, A. Zalkin, D.H. Templeton and M.G. Adamson, Inorg.Chem., 1966, 5, 1427.

CHAPTER IV

The Structure of the

μ-Nitrido-hexasulphatotriaquotri-iridate(IV, IV, III) ion

$$[\text{Ir}_3\text{N}(\text{SO}_4)_6(\text{H}_2\text{O})_3]^{-4}$$
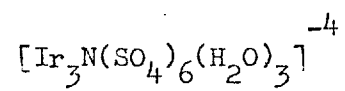
ABSTRACT

The crystal structure of ammonium μ-nitrido-hexasulphatotriaquotri-iridate(IV, IV, III) has been determined from three-dimensional X-ray diffractometer data. The compound forms cubic crystals for which $\underline{a}$ = 22.805Å, least-squares refinement in space group $I\overline{4}3\underline{d}$ using 565 independent reflections gave $\underline{R}$ = 0.032.

The structure contains the complex ion $[Ir_3N(SO_4)_6(H_2O)_3]^{4-}$. In it the central nitrogen atom, which lies on a threefold axis, is coordinated to three iridium atoms, and each pair of metal atoms is joined by double sulphate bridges. The octahedral coordination about iridium is completed by water molecules trans to the nitrogen. The arrangement of the nitrogen, iridium atoms and water molecules is essentially planar. The Ir-N distances are 1.918Å, Ir-H_2O, 2.058Å, and Ir-O(sulphato) 2.006 - 2.059Å.

A clear-cut distinction could not be made between the ammonium cations and molecules of water of crystallisation which are also present in the lattice.

INTRODUCTION

Although a substantial number of polynuclear oxy-complexes are known, there are few examples in literature of polynuclear nitrido-species. The structures of two binuclear μ-nitrido complexes have recently been reported. They are those of $K_3[Ru_2NCl_8(H_2O)_2]$[1] and $(NH_4)_4[Ru_2NCl_8(H_2O)_2]$[2].

The structures of trinuclear μ-nitrido complexes have not been examined by X-ray methods until now, although some have been known for a long time[3]. A number of these compounds have, however, been examined by I.r. and Raman spectroscopy: $K_4[Ir_3N(SO_4)_6(H_2O)_3]$, $Cs_4[Ir_3N(SO_4)_6(H_2O)_3]$, $K_7[Ir_3N(SO_4)_6(OH)_3]$, and $Cs_4[Ir_3NCl_{12}(H_2O)_3]$[4]. Our original intention had been to examine the structure of the complex $K_4[Ir_3N(SO_4)_6(H_2O)_3]$. Unfortunately, the crystals were found to be unsuitable for data collection.

It proved possible, however, to find a good crystal of an ammonium salt, containing the same complex ion and given the formula $(NH_4)_4[Ir_3N(SO_4)_6(H_2O)_3]$. $3H_2O$. The presence of both NH_4^+ groups and molecules of water has led, as had been feared, to difficulties in distinguishing them. Nevertheless, the main point of interest i.e. the structure of the complex ion $[Ir_3N(SO_4)_6(H_2O)_3]^{-4}$ has been established with confidence.

EXPERIMENTAL

Ammonium µ-nitrido-hexasulphatotriaquotri-iridate(IV, IV, III) was prepared by Delépines method[5] and crystallised from sulphuric acid as very dark green crystals. They were kindly provided by Dr. M.J. Cleare and Dr. W.P. Griffith. The crystals were tetrahedral in shape and showed a tendency to twin, forming aggregates which, however, could be easily broken up to give separate crystals.

Preliminary oscillation and Weissenberg photographs showed that the crystals were cubic, with $m3m$ Laue symmetry. The systematic absences were hkl: $h + k + l = 2n + 1$ and hhl: $2h + l = 4n + 1$. These indicate uniquely the space group $I\bar{4}3d$ (No. 220).

Three-dimensional X-ray data were collected for a crystal of tetrahedral shape, with edge dimensions of ca. 0.15 mm. It was mounted about the [111] axis on a Siemens off-line automatic diffractometer, using Cu-K_α radiation at a take-off angle of $4.5°$, a Niβ filter and a Na(Tl)I scintillation counter. The $\Theta - 2\Theta$ scan technique was employed, using a "five-value" measuring procedure[6]. A total of 565 independent reflections were measured (to $\Theta = 50°$), of which 14 were judged to be unobserved as their net count was below 2.58 times the standard deviation (i.e. below the 99% confidence limit) and were assigned a count equal to this figure. The 12 0 0 reflection was used as a reference every 25 reflections; its count did not alter significantly during the period of data collection (ca. 2 days). The data were scaled using the reference reflection and the Lorentz-polarisation correction was applied.

The unit-cell dimensions measured on the Siemens diffractometer (Cu-K_{α_1} = 1.54051Å) at $20°C$ gave a = 22.805Å (σ = 0.005Å). V = 11860Å³, space group $I\bar{4}3d$, D_{obs} = 3.06 gcm⁻³, Z = 16, D_{calc} = 3.05 gcm⁻³ for a formula $(NH_4)_4[Ir_3N(SO_4)_6(H_2O)_3].3\frac{1}{2}H_2O$, M.W. = 1360.71, $F(000)$ = 10200.

SOLUTION AND REFINEMENT OF THE STRUCTURE

The solution and refinement of the structure were carried out

using the Crystal Structure Calculations System X-Ray-63 described

by J.M. Stewart in the University of Maryland Technical Report TR-64-6.

The Imperial College IBM 7094 computer was used for these calculations.

The space group I$\overline{4}$3d has 48-fold general positions. As this

coincided with the number of iridium atoms in the unit cell it seemed likely

that there was only one independent metal atom in a general position.

The predicted structure of the complex anion had a triangle of iridium

atoms held together by a central nitrogen. If this structure was

accepted as correct (as proved to be the case), one would have a triangle

of iridium atoms ca. 3Å apart. This gives rise to a regular planar

hexagon of peaks in the Patterson all~3Å from the origin. Although

several such peaks were present, no combination gave a planar hexagon. In

retrospect it can be seen that this difficulty was caused by the very high

symmetry, m3m, such that a total of eight hexagons are found about the

origin - in four pairs, which are perpendicular to the 3-fold axes, and the

two hexagons of each pair are related to each other by mirror planes.

This profusion of peaks produces overlaps in cases of some of them, giving

peaks whose maxima are in incorrect positions. It was only after it was

realized, that a planar hexagon can be built up only out of peaks whose

coordinates obey the following rule $|u| + |v| = |w|$, that it proved

possible to disentangle all the existing hexagons and show where the true

positions of peaks lay in the case of coalesced peaks. These hexagon

peaks, together with those of the type u, 0, w, were used to fix an iridium

position at X = -0.0125, y = 0.1000, z = 0.0750. Refinement of this

position gave a value for the standard agreement factor

R ($= \Sigma ||F_o| - |F_c|| / \Sigma |F_o|$) of 0.25. The two independent sulphur atoms

were located from a resultant difference Fourier. Further refinement
including these positions reduced $\underline{R}$ to 0.16. Next, all eight oxygen atoms of
the sulphate groups were located, and refinement reduced $\underline{R}$ to 0.090.
The two remaining anion atoms, the bridging nitrogen on a triad, and
the water oxygen were then located and gave $\underline{R}$ = 0.086. Four other peaks
were at this stage assigned bearing in mind required point symmetries,
as follows: a nitrogen on a triad, a nitrogen on $\overline{4}(NH_4^+)$, an oxygen on a
diad and an oxygen in a general position (H_2O). Refinement including
these atoms reduced $\underline{R}$ to 0.051.

Refinement was carried out by the least-squares procedure, minimising
the function $\Sigma \underline{w}(\underline{F}_o - \underline{F}_c)^2$. The full-matrix ORFLS program, which was used
throughout, has no facilities of refining atoms having two or three coordinates
equal, and therefore at this stage the atoms on the three fold axes were kept
fixed in their positions during the refinement.

Next the iridium and sulphur atoms were allowed to refine anisotropically,
but this gave only a fairly small improvement in $\underline{R}$, to 0.047. A correction
for anomalous dispersion was applied for the iridium atom: with the sign
of $\Delta f''$ one way $\underline{R}$ dropped to 0.045, while with the sign reversed $\underline{R}$ rose
to 0.060. A difference Fourier now revealed another atom in a general
position, but its low peak height and very elongated shape suggested the
presence of disorder. Further refinement including this atom, tentatively
as oxygen, with half-occupancy, reduced $\underline{R}$ to 0.038.

Although the crystal was regular in shape, it was decided to carry out
an absorption correction before proceeding with refinement, because the
absorption coefficient (μ = 301.6 cm^{-1}) was quite high. The correction
was made using the Gaussian integration method with a 10 x 10 x 10 grid,
described by Busing and Levy[7] with crystal path lengths determined by the
vector analysis procedure of Coprens et al. No significant positional
shifts occured, but the temperature factors rose, on average, by 25%. There
was no significant improvement in $\underline{R}$.

In order to be able to refine the two atoms lying on a triad the ORFLS program was "patched"[9] to keep $\underline{x} = \underline{y} = \underline{z}$. Refinement in this way reduced $\underline{R}$ to 0.035.

At this stage a difference Fourier was computed to try to find the hydrogen atoms. Although various peaks were observed, which could be hydrogens, it was felt that such positions would only be hopeful guesses. Inability to locate the hydrogens with confidence makes it very difficult to decide which of the atoms outside the complex anion is an ammonium ion, and which is a water molecule. Various refinements were carried out in which the labels were changed, but these gave only changes of $\underline{B}$ of $\sim 2\mathring{A}^2$ and insignificant change in $\underline{R}$. Even the point symmetry of some of the positions can not be a firm guide (i.e. NH_4^+ on $\overline{4}$ or 3) since disorder is known to exist for at least one atom in the structure. It must in honesty be stated that the naming of these five atoms (Table 1) is not certain, and probably could only be placed on a firm basis if a neutron-diffraction study of the compound were carried out.

The limited number of independent reflections does not allow all atoms to be refined anisotropically. Of the light atoms, only five were chosen for anisotropic refinement - four of the sulphate oxygen, which showed greater anisotropy than others in the complex ion, and the disorder oxygen. This gave R = 0.033.

At this stage a weighting scheme of the type described by Hughes[10] was applied where $\sqrt{\underline{w}} = 1$ if $\underline{F}_o < \underline{F}^*$, and $\sqrt{\underline{w}} = \underline{F}^*/\underline{F}_o$ if $\underline{F}_o > \underline{F}^*$, with $\underline{F}^* = 500$. This reduced the standard deviations by $\underline{ca}$. 20% and refinement was terminated at $\underline{R} = 0.032$.

A final difference Fourier showed the highest remaining peak to be $0.9e/\mathring{A}^3$ in the vicinity of the iridium atom. The atomic scattering factors used were those tabulated by Cromer and Weber[11] and the values for the real and imaginary parts of the dispersion correction those given by Cromer[12].

Table 1 lists the final coordinates of the atoms together with their isotropic temperature factors, and Table 2 the coefficients for the anisotropic temperature factors: $\exp^r-(a_{11}\underline{h}^2 + a_{22}\underline{k}^2 + a_{33}\underline{l}^2 + 2a_{12}\underline{hk} + 2a_{13}\underline{hl} + 2a_{23}\underline{kl})]$. The standard deviations quoted are from full-matrix refinement and are probably more realistic than those which would have been obtained from a block-diagonal refinement. Table 3 lists the observed structure amplitudes and the calculated structure factors.

DESCRIPTION OF THE STRUCTURE AND DISCUSSION

The major point of interest in the structure is the complex anion $[Ir_3N(SO_4)_6(H_2O)_3]^{4-}$, shown as a stereoscopic pair in Figure 1. The central nitrogen atom lies on a triad, and is bonded to three iridium atoms at a distance of $1.918\overset{\circ}{A}$ ($\sigma = 0.002\overset{\circ}{A}$). The iridium atoms, therefore, form an equilateral triangle of edge $3.322(2)\overset{\circ}{A}$; there is of course no metal-metal bonding. Each pair of metal atoms is joined by double sulphate bridges, and the distorted octahedral coordination about iridium is completed by a water molecule _trans_ to the nitrogen. The arrangement of the nitrogen atom, iridium atoms and water molecules is essentially planar, with a maximum deviation from the least-squares plane of $0.012\overset{\circ}{A}$. The structure of the complex ion has therefore confirmed the prediction of Jørgensen[13] and Orgel[14] and supports the results obtained from studies of the vibrational spectra of normal and ^{15}N-enriched salts[15].

The Ir-N bond length, $(1.918\overset{\circ}{A})$, may be compared with other known metal-triply bridging nitrogen distances in $(CH_3N)_2Fe_3(CO)_9$ of mean value $1.928(11)\overset{\circ}{A}$. This bond length is $0.14\overset{\circ}{A}$ shorter than the sum of the single-bond covalent radii, $1.32\overset{\circ}{A}$ (Ir(III), octahedral) and $0.74\overset{\circ}{A}(N)$[15]. This suggests that there is some π-bonding between the $2p_z$ orbital of the nitrogen atom (perpendicular to the Ir_3N triangle) and the suitably placed orbitals on the iridium atoms.

The distances Ir-O(sulphate) of 2.006 - 2.059 (σ = 0.03$\mathring{A}$) and Ir-O
(σ = 0.035$\mathring{A}$)
(water) of 2.058$\mathring{A}$ are normal. The differences observed in the S-O

distances in the sulphate tetrahedra are not significant; the average

S-O distance is 1.479$\mathring{A}$. The more interesting bond distances and angles

in the complex anion are quoted in Table 4.

In a recent study[16] of the ^{193}Ir Mössbauer spectrum of the

$K_4[NIr_3(SO_4)_6.3H_2O]$ at 4°K two peaks were observed, and this was interpreted

as showing iridium atoms in two different oxidation states (III and IV).

The X-ray evidence does not indicate any departure from symmetry about

the threefold axis of the molecule. However, even if some inequivalence

of the three iridium atoms were present it would not necessarily appear

in the crystallographic data because, in the first place the complex

ion might adopt three different orientations in the crystal with equal

probability, fulfilling in this way the requirements of three-fold symmetry.

Secondly, on the basis of X-ray data, the three iridium atoms might

appear to be equivalent due to a time-averaging effect, whereas the

very short time scale of Mössbauer measurements makes possible a distinction

between the iridium III and IV atoms. The third possibility is that the

situation at 4°K is not quite the same as at room temperature at which the

X-ray structure was determined.

It is worth pointing out that the standard deviation quoted for

the Ir-N distance 0.002$\mathring{A}$, assumes that the three-fold axis operates even

at the molecular level, in which case the uncertainty in this distance

depends mainly on the standard deviations of the iridium atom.coordinates.

If the three-fold axis is merely the result of averaging asymmetric

complex ions the "standard deviation" will be indeterminable, but the

variation in Ir-N distances will be much greater than implied by σ = 0.002$\mathring{A}$.

In view of the difficulty of distinguishing between a nitrogen and an

oxygen atom by x-ray methods the other evidence for the anion containing a

nitrogen and not an oxygen as the central bridging atom can be summarised as follows:

1. A complex of a green colour can be obtained only from the ammonium salt in the reaction[17]

$$(NH_4)_3[IrCl_6] + H_2SO_4 \rightarrow [Ir_3N(SO_4)_6(H_2O)_3]^{4-},$$ while an oxy-complex of a blue colour is obtained in the reaction[18]

$$K_3[IrCl_6] + H_2SO_4 \rightarrow [Ir_3\underline{O}(SO_4)_9]^{10-}$$

2. Analytical data for $K_4[Ir_3N(SO_4)_6(H_2O)_3]$, $Cs_4[Ir_3N(SO_4)_6(H_2O)_3]$, $K_7[Ir_3N(SO_4)_6(OH)_3]$ and $Cs_4[Ir_3NCl_{12}(H_2O)_3]$ all show presence of the nitrogen[15]

3. The infrared spectra of normal and ^{15}N substituted $Cs_4[Ir_3N(SO_4)_6(H_2O)_3]$, $K_7[Ir_3N(SO_4)_6(OH)_3]$ and $Cs_4[Ir_3NCl_{12}(H_2O)_3]$ are different. In each case one band near 780 cm^{-1} shifts downwards in frequency by ca. 20 cm^{-1} on ^{15}N substitution[15]. This band can not be attributed to NH_4^+ or NH_3 since such species do not show infrared bands in this region.

4. All the complexes quoted in (3) above are diamagnetic[19]; the corresponding oxy-complexes (e.g. $K_4[Ir_3O(SO_4)_6(H_2O)_3]$ are paramagnetic, since they contain an odd number of electrons.

The presence of a nitrogen atom at the centre of the anion also has crystallographic support - the temperature factor $\underline{B}$ of the nitrogen, 0.8 Å^2, is the same as that of the iridium atom. This is exactly what one would expect i.e. that the tightly bonded Ir_3N unit would vibrate in a very similar way. When, in the final stages of refinement an oxygen atom was substituted, at the centre of the anion, its temperature factor rose to 2.9 Å^2.

The formula used in a previous section of this chapter, $(NH_4)_4[Ir_3N(SO_4)_6(H_2O)_3].3\frac{3}{4}H_2O$, agrees reasonably well with the analytical data[20]

	Found	Calculated
NH_4^+	4.9%	5.3%
N(total)	4.8%	5.1%
S	14.4%	14.1%
O	36.0%	36.2%
Ir	41.2	36.2%
	mean 42.45	
	43.7	42.4%

As was pointed out when describing the refinement of the structure, the labelling of the atoms outside the complex anion is uncertain, and therefore detailed discussion of them is omitted. Intermolecular distances were, however, calculated for all those species, and some of the more interesting ones are quoted in Table 5. It is quite obvious from these distances that a considerable number of hydrogen bonds occur between the ammonium ions, water molecules and the outer atoms of the complex anion.

The structure of the complex ion $[Ir_3N(SO_4)_6(H_2O)_3]^{4-}$ is the first established example of a coplanar triangular M_3N unit, with the nitride nitrogen acting as a bridging atom. An analogous arrangement has been suggested by Jørgensen[13] for the Ir_3O unit in $[Ir_3O(SO_4)_9]^{10-}$ and his suggestion has received some support from studies of the vibrational spectra of oxy-complexes[4].

The coplanar (or nearly so) M_3O unit has been suggested for a number of complexes such as $[Ru_3O(OAc)_6](OAc).8H_2O$ and $[(MeHg)_3O]ClO_4$[17], investigated by Raman and I.r. methods, and for four others which had structures determined by X-ray methods. These four complexes are: $[Mn_3O(OAc)_6]OAc.HOAc$[21], $[Fe_3O(OAc)_6(H_2O)_3]Cl.6H_2O$, the chromium(III) analog[22] isomorphous to it and recently examined compound $[Ru_3O(OAc)_6(PPh_3)_3]$[23]. Since the accuracy of the determination of

the structure of the first two compounds is rather low, the selected

average interatomic distances are quoted below only for the Cr and Ru

compounds

	$[Cr_3O(OAc)_6(H_2O)_3]Cl.6H_2O$ [24]	$[Ru_3O(OAc)_6(PPh_3)_3]$ [23]
M-O (central)	1.89(1)	1.92(2)
M-O (acetate)	1.98(1)	2.06(2)
M....M	3.274(4)	3.329(3)
M-L	2.02(1) (L = H_2O)	2.414 (L = PPh_3)
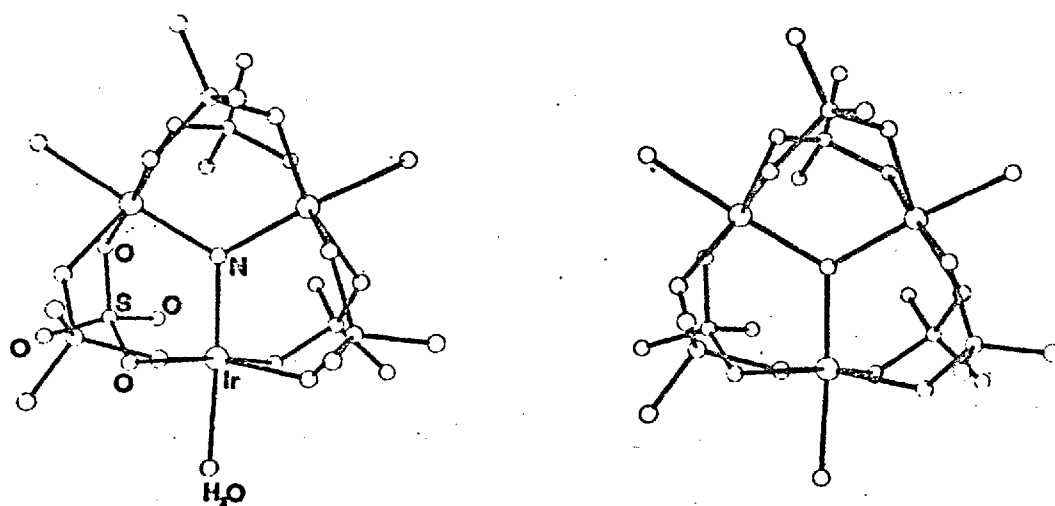
Fig. 1

Molecular structure of $[Ir_3N(SO_4)_6(H_2O)_3]^{-4}$ ion.

Table 1

Fractional coordinates, $\underline{x}$, $\underline{y}$, $\underline{z}$, with estimated standard deviations in parentheses, and isotropic temperature factors.

Atom	$\underline{x}$	$\underline{y}$	$\underline{z}$	$\underline{B}(\text{Å}^2)$
Ir	0.23706(8)	0.32403(8)	0.35079(8)	0.8(0.1)
N(1)	0.3042(14)	0.3042(14)	0.3042(14)	0.8(1.2)
S(1)	0.2208(6)	0.1861(5)	0.3406(6)	1.4(0.4)
S(2)	0.3280(6)	0.2834(5)	0.4519(5)	1.2(0.4)
O(11)	0.1946(16)	0.2455(14)	0.3381(16)	2.3(0.9)
O(12)	0.2839(15)	0.1910(15)	0.3599(15)	1.5(0.8)
O(13)	0.1890(14)	0.1536(15)	0.3836(15)	2.0(0.7)
O(14)	0.2160(16)	0.1628(17)	0.2825(18)	3.0(0.8)
O(21)	0.3283(15)	0.2300(14)	0.4866(15)	2.1(0.7)
O(22)	0.2663(15)	0.2932(14)	0.4278(14)	1.4(0.8)
O(23)	0.3458(16)	0.3348(15)	0.4855(15)	2.7(0.7)
O(24)	0.3714(14)	0.2789(15)	0.4001(14)	1.5(0.8)
O.(1)	0.1651(15)	0.3500(15)	0.3990(15)	2.4(0.6)
N(2)	0.1646(15)	0.1646(15)	0.1646(15)	0.5(1.2)
N(3)	0.0859(24)	0.2233(20)	0.4220(23)	5.8(1.1)
O(2)	0.1830(35)	0	$\frac{1}{4}$	5.3(2.3)
O(4)	0.2879(51)	0.0723(34)	0.2493(42)	5.9(3.0)
O(5)	$\frac{1}{8}$	$\frac{1}{2}$	$\frac{1}{4}$	4.6(1.9)

(The atom labels of the last five atoms are subject to uncertainty.)

Table 2

Anisotropic thermal parameters

Atom	β_{11}	β_{22}	β_{33}	β_{12}	β_{13}	β_{23}
Ir	0.00061(5)	0.00056(5)	0.00060(5)	0.00007(3)	0.0010(3)	0.00007(3)
S(1)	0.0008(3)	0.0005(3)	0.0007(3)	-0.0003(2)	-0.0001(2)	0.0002(2)
S(2)	0.0009(3)	0.0006(2)	0.0003(2)	-0.0001(2)	0.0000(2)	0.0001(2)
O(11)	0.0014(8)	0.0003(7)	0.0016(8)	-0.0001(6)	-0.0004(7)	-0.0000(7)
O(12)	0.0011(8)	0.0007(7)	0.0007(7)	-0.0004(6)	-0.0003(6)	-0.001(6)
O(22)	0.0005(7)	0.0015(8)	0.0005(6)	-0.0001(6)	0.0001(6)	-0.0001(6)
O(24)	0.0013(8)	0.0004(7)	0.0007(7)	-0.0001(6)	-0.0001(6)	0.0004(6)
O(4)	0.0067(41)	0.0003(15)	0.0026(27)	0.0023(21)	-0.0029(28)	-0.0014(17)

Table 3

Final observed and calculated

structure factors

The format of the table is

h	k	l
1	$10|F_o|$	$10|F_c|$

Reflections of intensities not
significantly greater than the
background ("less-thans") are
marked: *

Table 4

Selected bond lengths (Å) and angles(°) in the anion $[Ir_3N(SO_4)_6(H_2O)_3]^{4-}$

(Standard deviations are given in parentheses)

Octahedron around iridium atom

Ir - N(1)	1.918(.2)	Ir - O(12)	2.025(32)
Ir - O(1)	2.058(35)	Ir - O(22)	2.006(32)
Ir - O(11)	2.059(33)	Ir - O(24)	2.051(32)

N(1) - Ir - O(11)	95.1(1.1)	O(1) - Ir - O(11)	87.0(1.4)
N(1) - Ir - O(12)	95.0(1.1)	O(1) - Ir - O(12)	83.0(1.3)
N(1) - Ir - O(22)	98.0(1.1)	O(1) - Ir - O(22)	84.0(1.4)
N(1) - Ir - O(24)	87.9(1.0)	O(1) - Ir - O(24)	90.2(1.3)
O(11) - Ir - O(12)	90.0(1.4)	O(24) - Ir - O(22)	87.0(1.3)
O(12) - Ir - O(24)	94.0(1.3)	O(22) - Ir - O(11)	88.4(1.4)
O(11) - Ir - O(24)	175.0(1.4)	O(12) - Ir - O(22)	167.0(1.3)

N(1) - Ir - O(1)   177.1(1.0)

Tetrahedrons around sulphur atoms

S(1) - O(11)	1.482(34)	S(2) - O(21)	1.461(35)
S(1) - O(12)	1.510(36)	S(2) - O(22)	1.529(35)
S(1) - O(13)	1.426(35)	S(2) - O(23)	1.457(36)
S(1) - O(14)	1.433(42)	S(2) - O(24)	1.532(34)

O(11) - S(1) - O(12)	109.1(2.0)	O(22) - S(2) - O(24)	109.3(1.8)
O(11) - S(1) - O(13)	107.3(2.0)	O(22) - S(2) - O(21)	108.7(2.0)
O(11) - S(1) - O(14)	105.9(2.2)	O(22) - S(2) - O(23)	109.1(2.0)
O(12) - S(1) - O(13)	108.8(2.0)	O(24) - S(2) - O(21)	110.7(2.0)
O(12) - S(1) - O(14)	111.7(2.1)	O(24) - S(2) - O(23)	105.9(2.0)
O(13) - S(1) - O(14)	113.9(2.2)	O(21) - S(2) - O(23)	113.1(2.0)

Table 5

Some selected non bonded distances in $(NH_4)_4[Ir_3N(SO_4)_6(H_2O)_3] \cdot 3\frac{3}{4}H_2O$.

$N(2) - O(14)^{I}$	2.935	x3
$O(23) - N(2)^{II}$	2.896	x3
$N(3) - O(13)^{I}$	2.972	
$N(3) - O(4)^{III}$	2.409	
$O(13) - O(1)^{IV}$	2.680	
$O(2) - O(24)^{IV}$	3.093	x2
$O(2) - O(4)^{I}$	2.906	x2
$O(4) - O(14)^{I}$	2.746	
$O(4) - O(11)^{V}$	3.013	
$O(4) - N(3)^{V}$	3.131	
$O(4) - N(3)^{VI}$	3.114	
$O(13) - O(5)^{V}$	3.065	x4
$O(21) - O(5)^{V}$	2.995	x4

I x, y, z,   II $\frac{1}{4} + y$, $\frac{1}{4} + x$, $\frac{1}{4} + z$

III $z - \frac{1}{4}$, $\frac{1}{4} - y$, $\frac{3}{4} - x$ IV $y - \frac{1}{4}$, $\frac{1}{4} - x$, $\frac{3}{4} - z$

V z, x, y   VI $\frac{3}{4} - z$, $y - \frac{1}{4}$, $\frac{1}{4} - x$

Superscripts refer to atoms in the above positions.

REFERENCES

1. M. Ciechanowicz and A.C. Skapski, Chem. Comm., 1969, 574.

2. R.J.D. Gee and H.M. Powell, private communication; J. Chem. Soc. A in the press.

3. M. Delépine, Bull. Soc. Chim. Fr., 1909, 5, 359, 1084, 1126.

4. M.J. Cleare, W.P. Griffith, J. Chem. Soc.(A), 1970, 1117.

5. M. Delépine, Ann. Chim. (Paris), 1959, 1115; ibid, 1131.

6. A.C. Skapski and P.G.H. Troughton, Acta Cryst., B26, 1970, 716.

7. W.R. Busing and H.A. Levy, Acta Cryst., 1957, 10, 180.

8. P. Coppens, L. Leiserowitz and D. Rabinovich, Acta Cryst., 1965., 18, 1035.

9. W.R. Busing, K.O. Martin and H.A. Levy, ORFLS, Oak Ridge Technical Report, ORNI-TM-305, 1962.

10. E.W. Hughes, J. Amer. Chem. Soc., 1941, 63, 1737.

11. D.T. Cromer and J.T. Waber, Acta Cryst., 1965, 18, 104.

12. D.T. Cromer, Acta Cryst., 1965, 18, 17.

13. C.K. Jørgensen, Acta Chem. Scand., 1959, 13, 196.

14. L.E. Orgel, Nature, 1960, 187, 505.

15. Linus Pauling, "The Nature of the Chemical Bond", Third Edition, Cornell University Press, Ithaca, 1960,

16. D.R. Brown, M.B. Robin, J.D.E. McIntyre and W.F. Peck, Inorg. Chem.,1970, 9, 2315.

17. W.P. Griffith, J. Chem. Soc (A), 1969, 2270.

18. Lecoq de Boisbaudran, Compt. rend., 1883, 96, 1336, 1406.

19. W.P. Griffith "The Chemistry of the rarer platinum metals (Os, Ru, Ir and Rh)", Interscience Publishers, London, 1967.

20. W.P. Griffith and D. Pawson, private communication.

21. L.W. Hessel and C. Romers. Rec. Chim. Trav., 1969, $\underline{88}$, 545.

22. B.N. Figgis and G.B. Robertson, Nature, 1965, $\underline{205}$, 694.

23. F.A. Cotton and J.^{G}. Norman, Jr., in the press.

24. S.C. Chang and G.A. Jeffrey, Acta Cryst., 1970, $\underline{26B}$, 673.